THE UNIVERSITY OF MANITOBA

THE PERFORMANCE OF PROSTHETIC HEART VALVES AND ARTERIAL IMPLANTS

A THESIS BY

PAULINO JOSE LOZADA

SUBMITTED TO THE FACULTY OF GRADUATE STUDIES IN PARTIAL FULFILMENT OF THE REQUIREMENTS FOR THE DEGREE OF:

MASTER OF SCIENCE

DEPARTMENT OF MECHANICAL ENGINEERING
WINNIPEG MANITOBA

April, 1979

THE PERFORMANCE OF PROSTHETIC HEART VALVES AND ARTERIAL IMPLANTS

BY

PAULINO JOSE LOZADA

A dissertation submitted to the Faculty of Graduate Studies of the University of Manitoba in partial fulfillment of the requirements of the degree of

MASTER OF SCIENCE

I hereby declare that I am the sole author of this thesis. I authorize The University of Manitoba to lend it to other institutions or individuals for the purpose of scholarly research.

Paulino Jose Lozada

ABSTRACT

The commercially available arterial prostheses when implanted in the cardiovascular system produce reflected pulse pressure waves as a result of their inextensibility relative to the artery material. The result of these reflections could be higher non-physiological pressure waves that could damage the host organism. Turbulence and high shear stress in the blood flow induce thrombosis and hemolysis. Prosthetic heart valves that are not properly hydrodynamically designed can produce turbulence and high shear stress which is reflected as high energy losses in the blood flow when passing through the valves.

A mechanical model that simulates the human circulation in the left ventricle and ascending aorta was developed in order to reproduce and measure the reflected wave phenomenon and to evaluate a possible means of reduction of the reflected wave. One such means consisted of placing an elliptical insertion in the artery instead of the inextensible round insertion. The mechanical model was also used for evaluating the energy losses in prosthetic heart valves when physiological flow is induced.

The performance of the simulated heart-valve-artery system was satisfactory in efficiency, durability, frequency control, flow generation, valve behaviour and in data reading and data recording aspects. Some unwanted wave reflection was always present, and some viscoelastic parameters of the tubes were not known. These factors were constant, however, thus the results' comparative behaviour are valid. Round insertions in the elastic tube produced refected waves, thus modifying the pressure pattern, causing higher pressure peaks. The elliptic insertion did not produce as high pressure peaks as did the round rigid insertions.

Reflection factors due to rigid insertions were measured and the results showed some disagreement with the predictions based on the available idealized theory.

It was found that the Bjork-Shiley prosthetic heart valve was hydrodynamically superior to the Starr-Edwards. Fourier techniques proved to be valuable for analysing pressure pulse waves.

Experimentation with this model proved to be an inexpensive guide to the determination of variables which should be recorded and controlled. The results appear to make experimentation with animals regarding the variables measured here appear worthwhile.

ACKNOWLEDGEMENTS

The author would like to thank his supervisor, Professor A.B. Thoronton-Trump for his guidance and financial assistance through NRC Grant 8920 during the course of this research. He would also like to thank The University of Manitoba for its support and facilities.

The author thanks Professors K. McLachlan, J. Tinkler and E. Shwedyk for their help and advice. Finally, the author extends his warmest thanks to Jim Sewell for technical support and to all the other students with whom he shared work and enjoyment.

TABLE OF CONTENTS

LIST OF FIGURES

LIST OF TABLES

NOMENCLATURE

A	pressure gradient, real or complex.
A', A_1', A_2'	pressure - gradient modulus.
a	damping constant.
a_1	inner radius.
a_2	outer radius.
b	phase constant.
B	$E/(1 - \sigma^2)$ relation of the elastic constants.
c	complex wave velocity. Real part represents phase velocity and imaginary part represents wave attenuation.
c_o	$c_o = (Eh/2\,\rho_c\,a_1)^{1/2}$ phase velocity for the perfect fluid.
c_1, c_2, c_3, ...etc.	phase velocity, general.
D_1	arbitrary constant.
E	Young's modulus of elasticity.
E_1	arbitrary constant.
F	function of.
F_{10}	$F_{10} = \dfrac{2\,J_1\,(\alpha\,i^{3/2})}{\alpha\,i^{3/2}\,J_o\,(\alpha\,i^{3/2})} = 1 - M_{10}'\,e^{i\,E_{10}'}$ variable related to the complex wave velocity.
f	rotational frequency in revolutions per unit time.
H_1, H_2	total energy in a fluid.
H_{1-2}	total energy losses due to friction in a fluid.
h_{10}	$h_{10} = \dfrac{2M_1}{\alpha M_o}$ constant related to the modulus of Bessel functions.
h	$h = a_2 - a_1$ wall thickness.

I_v	$I_v = \dfrac{(1 - i)\ x'\ J_0\ \{(1 - i)\ x'\}}{J_1\ \{(1 - i)\ x'\}}$ variable related to the complex wave number in visco-elastic tubes. This function is tabulated in reference (19) for values of x' from 0.1 to 110. I_v approaches infinity if μ approaches zero.
I_o	$I_o = \dfrac{i\ Ka_1\ J_o\ (i\ Ka_1)}{J_1 (i\ Ka_1)} \approx 2$ variable related to the complex wave number in visco-elastic tubes.
I_1	real part of I_v.
I_2	imaginary part of I_v.
i	$i = \sqrt{-1}$.
J_o ( )	Bessel function of zero order.
J_1 ( )	Bessel function of first order.
K	$K = ia + b$ complex wave number.
k	$k \simeq h/a_1$ constant that relates wall thickness to inner radius.
L	physical constant related to damping.
M'_{10}	$M'_{10} = \sqrt{1 + h_{10}^2 + a\ h_{10} \cos \delta_{10}}$ constant related to modulus of Bessel functions.
M''_{10}	$M''_{10} = \lvert 1 + \eta\ F_{10} \rvert$ constant related to modulus of Bessel functions.
M_o	modulus of the Bessel functions of the zero order.
M_1	modulus of the Bessel functions of the first order.
N	$N = \dfrac{(I_v - I_o)\ \rho}{\rho_o} + I_o\ I_v\ (\tau + 1 + \sigma) + \tau\ (1 = 2\ I_o \sigma)$ variable related to the complex wave number in visco-elastic tubes.
N'	$N' = I_o\ (1 + \sigma)\ (\tau + \dfrac{I_v\ \rho}{\rho_o})\ \{1 + \tau\ (1 - \sigma)\}$ variable related to the complex wave number in visco-elastic tubes.

n — $n = 2\pi f$ angular velocity in radians per unit time.

p — pressure, real or complex.

p_0, p_1, p_2 — modulus of complex pressure.

r — radial axis in cylindrical coordinates, or position along the radial axis.

t — time.

u — fluid velocity component in the radial direction, real or complex.

u_1 — radial complex - velocity modulus of the fluid.

$\overline{V}$ (r, z, t) — displacement vector.

w — fluid velocity component in the axial direction, real or complex.

w_1 — axial complex-velocity modulus of the fluid.

x — $x = R\,(1 - \sigma_2)$ variable related to fluid velocity in thin walled elastic tubes.

x' — $x' = a_1 \left(\frac{\rho_o n}{2\mu}\right)^{1/2}$ non-dimensional constant that relates some properties of tube and fluid.

y — $y = r/a_1$, relation between radial position and inner radius.

z — axial axis in cylindrical coordinates, or position along the axial axis.

Z — any real variable.

α — $\alpha = a_1 \left(\frac{n}{\nu}\right)^{1/2}$ non-dimensional constant that relates some properties of tube and fluid.

γ — the propagation constant.

γ' — $n\,\mu_{vi}/\mu_s$ relation of some viscoelastic constant (Voigt solid).

∇ — vector differential operator.

ζ — inner wall displacement in the z - direction.

λ — wavelength.

λ_s — $\lambda_s = E\,\sigma/[(1 + \sigma)\,(1 - 2\sigma)]$ Lame's elasticity parameter.

μ	dynamic coefficient of viscosity of the fluid.
μ_{vi}	viscous constant of the wall material (Voigt solid).
μ_s	$\mu_s = E/[2(1+\sigma)]$ Lame's elasticity parameter.
υ	kinematic coefficient of viscosity of the fluid.
ξ	tube inner wall displacement in the r direction.
ρ	wall density.
ρ_o	fluid density.
σ	Poisson's ratio
τ	$\dfrac{2a_1/a_2}{a_2/a_1 - a_1/a_2}$ constant that relates inner and outer radii.
E'_{10}	$E'_{10} = \arctan\left(\dfrac{h_{10}\sin\sigma_{10}}{1 + h_{10}\cos\sigma_{10}}\right)$, constant related to the phase of Bessel functions.
E''_{10}	E''_{10} = phase of $(1 + F_{10})$, constant related to the phase of Bessel functions.
σ_{10}	$\sigma_{10} = \dfrac{3\pi}{4} - \theta_1 + \theta_0$, constant related to the phase of Bessel functions.

CHAPTER I INTRODUCTION

From theory and experience it is known that prosthetic arteries and heart valves produce alterations in the hydrodynamic characteristics of the blood flow when implanted in the cardiovascular system [8, 16, 20, 27, 35] as well as other side effects. Since the mortality figures for the users of the Bjork-Shiley and the Starr-Edwards prosthetic heart valves appear significantly different [11, 13, 18], measurements of the alterations of the pulse pressure waves caused by each type of valve and comparison of pressure patterns produced by the Bjork-Shiley tilting-disc and Starr-Edwards ball-and-cage prosthetic heart valves should be made to determine whether basic hydrodynamic differences could possibly contribute to the decreased life of the users of the one prosthetic valve. The design of the Bjork-Shiley tilting-disc heart valve has hydrodynamic characteristics closer to those known to be the best for the blood, heart and arteries than does the Starr-Edwards ball-and-cage heart valve [8, 27]. Confirmation, evaluation and quantization of such improvements is necessary.

Alterations of pulse pressure are also caused by an arterial prosthesis as a result of its rigidity relative to the artery itself. The extensibility of most knitted prostheses is only about 10% of that of the host vessel [16, 35]. Reflected pressure waves from a prosthesis may be added to the incident waves from the heart, thus producing higher non-physiological pressure pulses on the artery itself and on the heart valves if the insertion is in the aorta, close enough to the heart valves so the refected waves are not significantly damped before reaching the valves.

In order to investigate the pressure wave characteristics, the development of a heart-valve-artery model is necessary since "in vivo" measurements are beyond the scope of this work. The model must be designed to reproduce as closely as possible the flow characteristics of the human circulation in the aorta, which may be simulated by an elastic tube. It is possible to insert inextensible sections into the elastic tube which play the role of the inextensible prosthesis and, with pressure-transducers, to measure their effect on the pulse pressure wave. A possible method to reduce the magnitude of the reflected wave is to place in the test circuit an insertion with elliptic cross-section, instead of the round inextensible cross-section often used. In response to the pressure the elliptic insertion would approach a circular configuration, allowing greater flow cross-section thus reducing the pressure peak. The magnitude of this pressure wave reduction depends on the characteristics of the ellipse and the range over which the pressure excursions take place.

The equipment necessary to allow measurement of the pressure wave characteristics of the prosthetic arterial implants can be easily adapted to measure the effects of the prosthetic heart valves on the simulated arterial flow. The results of such investigations may be related to the characteristics known to be best for the cardiovascular system.

CHAPTER II REVIEW OF LITERATURE

The significance of changes in the hydrodynamics of blood flow as a result of implanted prostheses lies in the possible disruption of the ability of the blood to perform its functions. The disruption of the blood flow characteristics may also have an adverse effect on the functions of other physiological materials such as high pressures on heart valves or restriction of arterial movement. The importance of these aspects of blood flow can be appreciated through a review of the literature.

II.1 Principles of human circulation

The blood circulation duty is to maintain the constancy of the internal environment of the organism. In doing so, it must: bring oxygen to the tissues, exchange it for the metabolic CO_2, carry this gas back to the lungs, release it to the atmosphere and replace it with oxygen; at the same time the blood picks up nutrients from the digestive tract, brings them to be processed and stored in the appropriate organs and performs the final distribution of nutrients and transport of the waste products to the organs of excretion. It also plays an important role in the regulation and coordination of the body by distributing the hormones of the endocrine glands. It participates in the regulation of water and electrolytes as well as regulation of body temperature. Another duty is the production and distribution of antibodies for protection against foreign particles [5, 10].

The circulation from the heart to the lungs and back to the heart is called Pulmonary Circulation. The circulation from the heart to the body and back to the heart is called Systemic Circulation. In order to pump the blood through both systems the heart has a set of conveniently located valves. Figure II.1 is a schematic diagram of the double circulation and the heart with its valves [10].

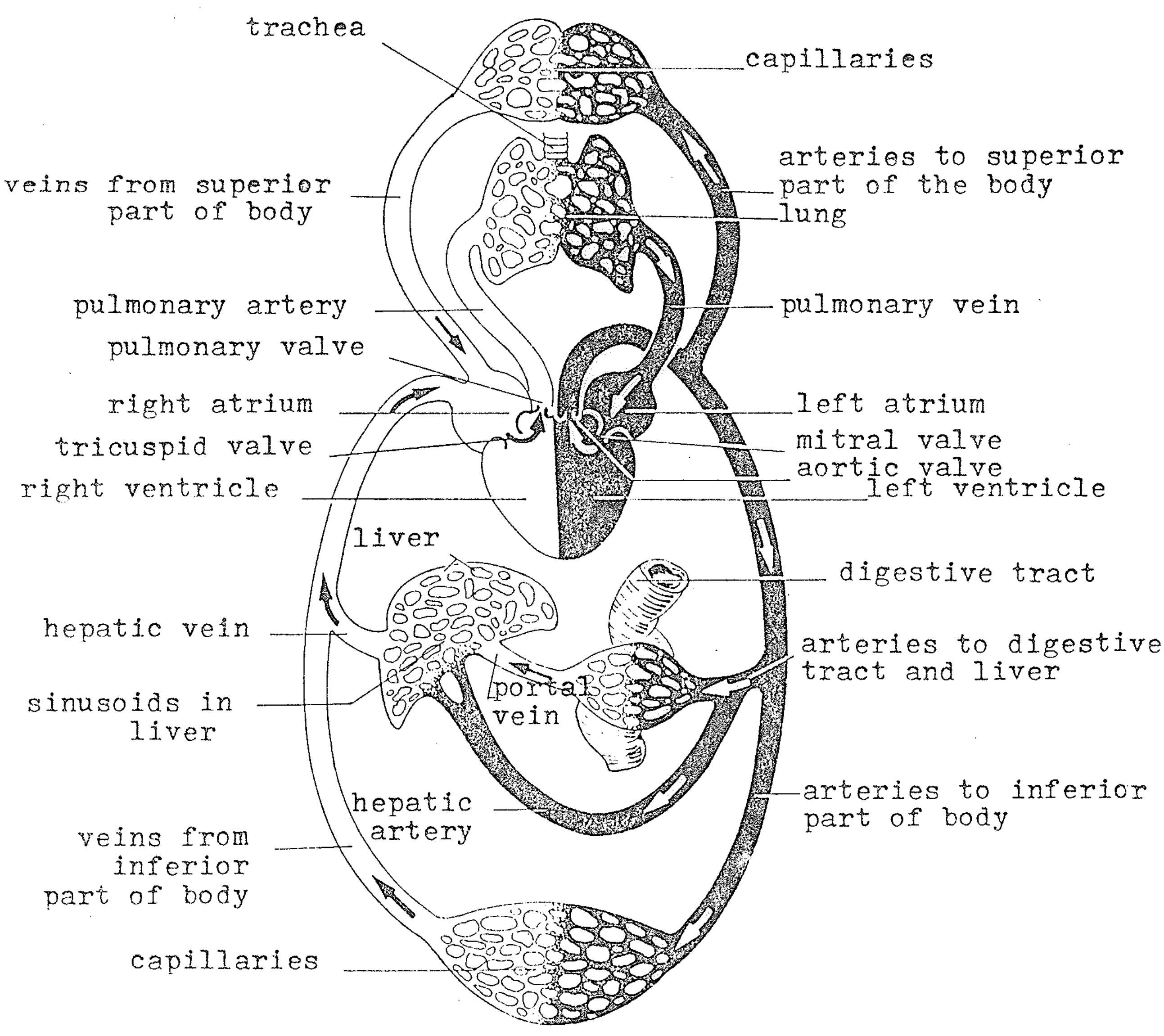

Fig. II.1: Scheme of the double system of circulation. Oxygenated blood is indicated in black, the nonoxygenated in white. Arrows show the direction of the blood flow. (Reproduced from [10]).

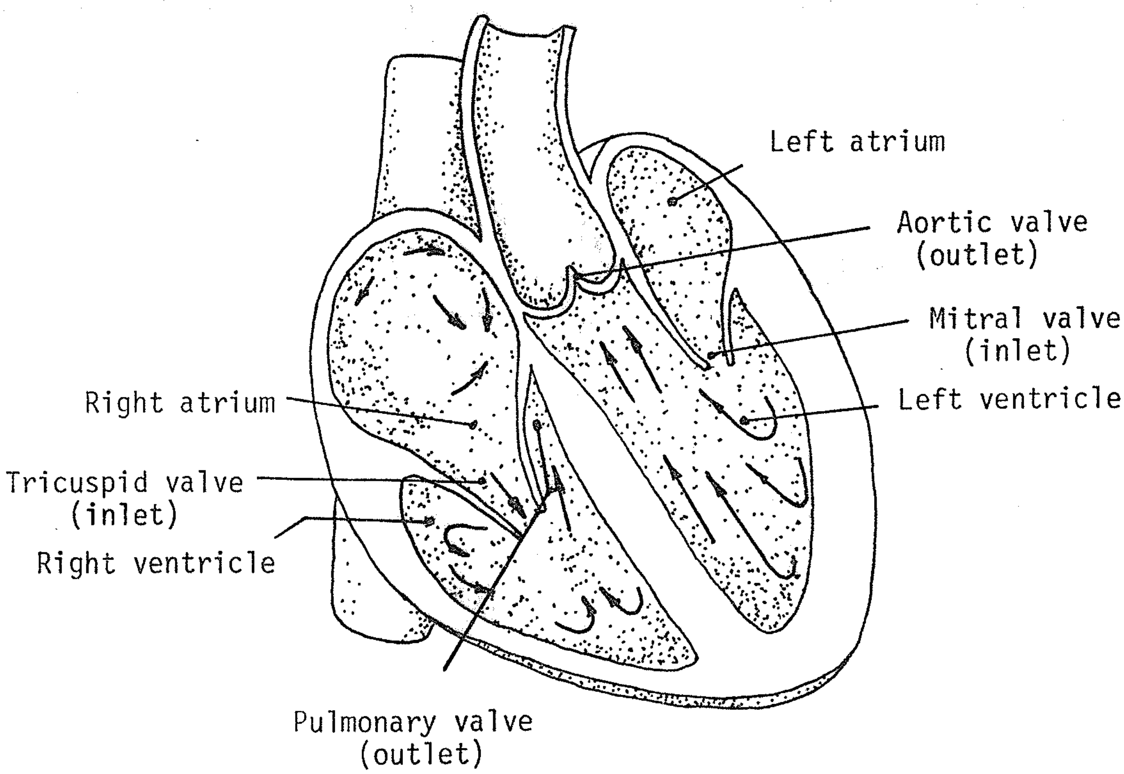

Fig. II.2: Schematic figure of the heart (Reproduced from [26]).

The heart is a pump with four chambers whose function can be visualized with the help of Fig. II.2.

The chambers are classified in accordance with their position: right atrium, right ventricle, left atrium, and left ventricle. The contraction of the heart chambers is called systole and the relaxation is called dyastole. The atria are chambers that have a minor function since they only help filling their respective ventricle. The major pumping action is exerted by the ventricles. The valves control the flow by means of a passive function [26, 29]; they close or open depending on which side the pressure is higher. The blood from the systemic system is received in the right atrium and pumped to the right ventricle where it is, in turn, ejected to the pulmonary system, received by the left atrium, passed to the left ventricle and finally ejected to the systemic circulation. The atria do not have double valves, so when they contract some blood refluxes. Since the ventricles have double valves, the regurgitation is negligible in the healthy heart.

The cardiac function already described can be classified by a separation of five events based on the closed or opened position of the ventricular inlet and outlet valves (see Fig. II.3). The duration and timing of these events are of particular concern in the design of prosthetic heart valves. Notice that the inlet and outlet valves are never opened at the same time [26, 29]. The five events specified in appropriate order for analytical purposes are:

(1) Filling (inlet open, outlet closed)

(2) Atrial Systole (inlet open, outlet closed)

(3) Isovolumetric Contraction (both closed)

(4) Ejection (inlet closed, outlet open)

(5) Isovolumetric Relaxation (both closed)

(1) Filling. The outlet valves have closed before this even starts A rapid increase in the volume of the ventricular chambers produces a fast drop of pressure in these chambers resulting in a rapid rate of filling through the atrioventricular valves. This is followed by a more moderate rate of increase of ventricular volume that produces a reduced rate of filling.

(2) Atrial Systole. Atrial Systole concludes the filling of the ventricular chambers. At the end of this event there is a drop of pressure in the atria that produces the closure of the atrio-ventricular valves.

(3) Isovolumetric Contraction. Inlet and outlet valves of the ventricles are closed when the heart starts its contraction so pressure increases very fast in the ventricles. The ventricular pressure soon reaches and exceeds the arterial pressure which has been decreasing due to the runoff of blood through the peripheral arteries. When the ventricular pressure exceeds the arterial pressure, ventricular outlet valves open, ending the isovolumtric contraction.

(4) Ejection. Initially there is a high rate of ejection due to the strong contraction of the ventricle. The ventricular pressure remains above the aortic pressure, reaches its maximum then drops slightly below the aortic pressure. At this point a more gradual

contraction of the ventricle produces a reduced ejection and the flow continues due to the inertia of the mass of the blood pumped. Finally, the inertial flow is reduced and by the end of the event there is a slight backwards flow that perhaps helps in the closure of the ventricular outlet valves. This closure produces a small secondary peak in the aortic pressure wave, as shown in Fig. II.3.

(5) Isovolumetric Relaxation. Inlet and outlet valves are closed again so the ventricular volumes can not change but the orientation of the musculature does so in order to relax. This relaxation produces a fast pressure drop in the ventricles that soon falls below the atrial pressure and the atrioventricular valves open to start the next cycle.

The sequence of events is similar in both sides of the heart, except that the peak systolic pressure in the left ventricle is about five times higher than that in the right (120 mm Hg left, 24 mm Hg right), and isovolumetric relaxation and isovolumetric contraction are of slightly shorter duration in the right side [26].

Since the aim of this investigation deals with the events in the left heart, the aorta and its main branches, attention is concentrated on this part of the circulatory system. Fig. II.3 is a graph where the events in the left heart and ascending aorta can be visualized in a quantitative way. Instantaneous flow measured in the ascending aorta of dogs and adapted to values expected in man is also shown in Fig. II.3 [29].

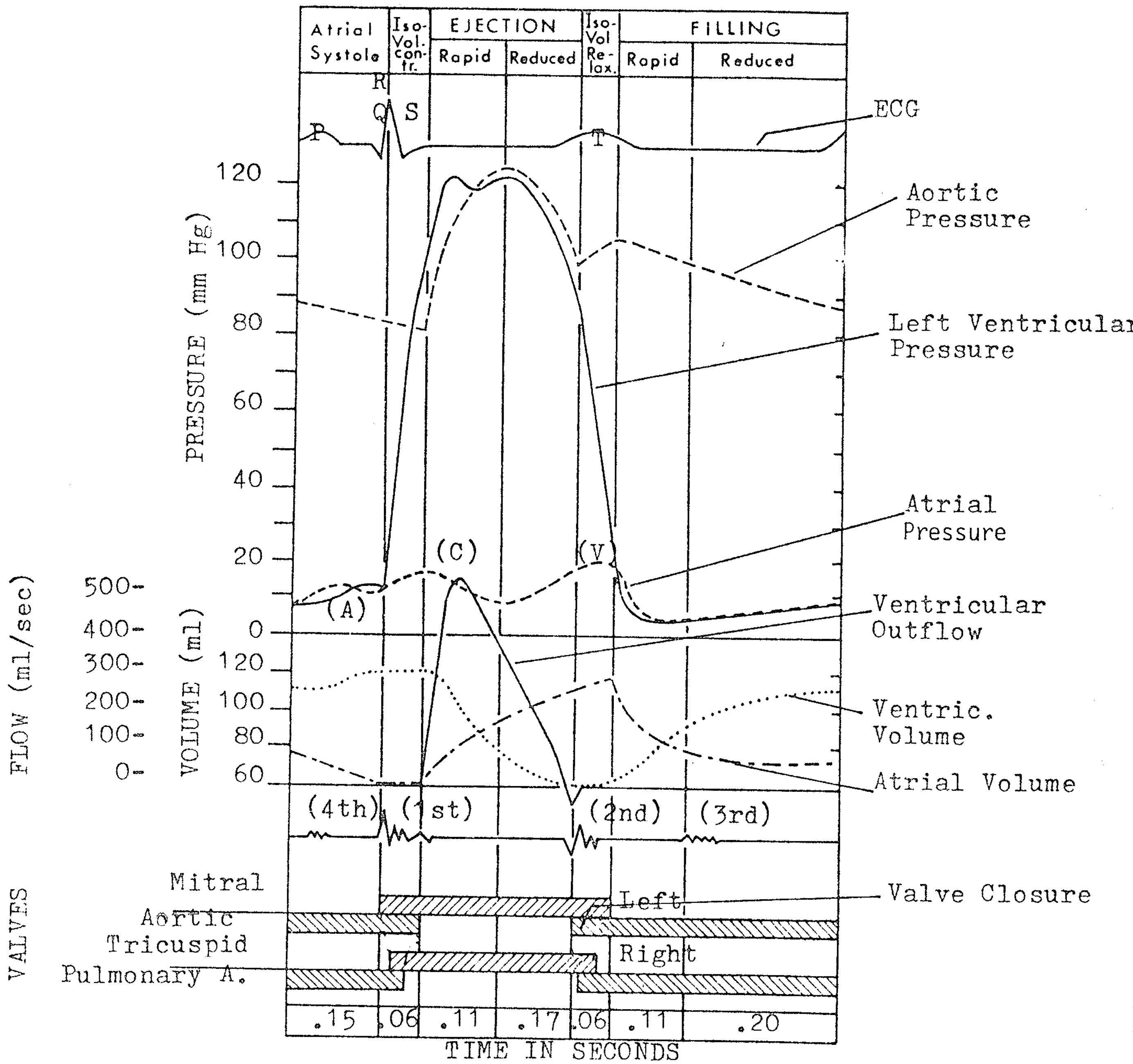

Fig. II.3: Pressure and volume events in the left heart during the cardiac cycle (Reproduced from [29]).

II.2 History of arterial implants

The use of arterial implants is recommended when the arteries have been blocked by emboli (blood clots circulating in the blood), occlusion or severe stenosis (narrowing of the artery), when they have been damaged by trauma (injury by the application of external force or violence), and when they are diseased, such as by advanced arteriosclerosis (narrowing, hardening and loss of elasticity) or aneurism (abnormal dilation).

The first attempts at implantation were done between 1914 and 1947 using rigid materials such as tubes of silver, glass and aluminum; but the success was negligible because the surfaces of these materials are highly thrombogenic (produce blood clots that remain attached to its place of origin) so most grafts were occluded within hours. The first major advances were obtained by Hufnagel in 1947 [21, 22] using tubes made of the thermoplastic polymethyl methacrylate, for implants in the thoracic aorta of dogs.

Homografts and heterografts have been tried also, with different degrees of success but these kinds of implants will not be studied in this work. However, the main problem with artificial grafts was that when the blood came in contact with the surface, spontaneous thrombus (blood clots that remain attached to its place of origin) were produced. The modern design of grafts was initiated by Voorhees et al in 1952 [21, 22]. It was based on the assumption that a porous arterial graft would be sealed with fibrin (fibrous protein formed in the clotting of the blood), thus avoiding leakage and providing an organic layer for the interface between blood and foreign material. It was expected that this organic layer would be less susceptible to thrombosis. The material used for the first experiments was cloth mesh of Vinyon "N" fashioned into tubes. Implanted in the abdominal aorta of dogs and with anticoagulant therapy it remained patent for 153 days [21, 22]. It was found that the porous prosthesis could be preclotted with host blood before implantation thus reducing or avoiding seepage.

The concept of tubes made of porous material has remained as the most suitable concept for arterial substitutes [21, 22]. Fig. II.4 is a cross-section of a prosthesis with the layers that grow after implantation [22].

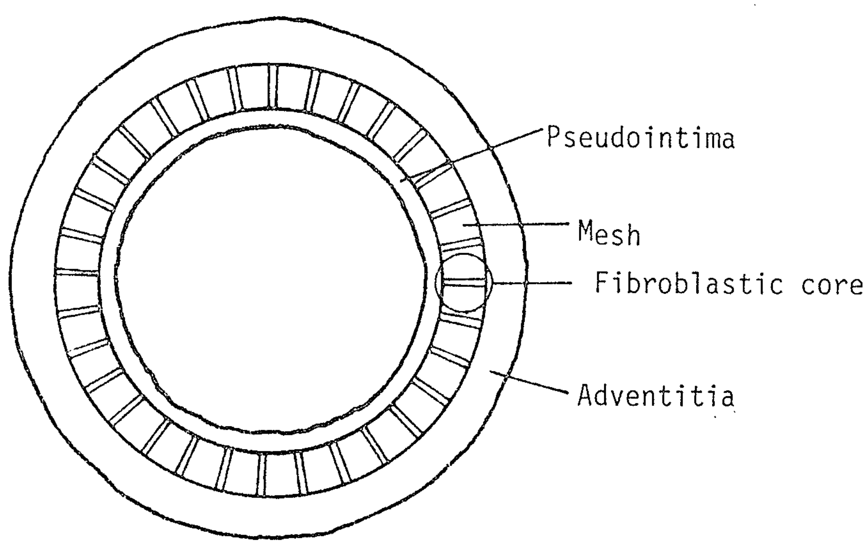

Fig. II.4: Cross-section of a prosthesis with the layers that grow after implantation. (Reproduced from [22]).

After the first work of Voorhees et al, many improvements have been made. Improvements in construction have consisted of refinements which have made the implant more functionally acceptable to the host. Since the pseudointima might thicken as much as 20% of the prosthesis interior diameter, it is convenient to build the graft's internal diameter higher than that of the host vessel. It was found also that a higher porosity would allow a more rapid and better formation of the pseudointima, thus reducing the chances of thrombogenesis. Knitted fabrics have higher porosity and more elasticity than the initial woven ones, (see Fig. II.5) but woven fabrics are difficult to suture since they fray easily. Knitted fabrics do not fray at the suture even if they are cut at different angles. Crimping the prosthesis walls reduces kinking and gives some extensibility which is desirable for prostheses that pass across the joints of the body.

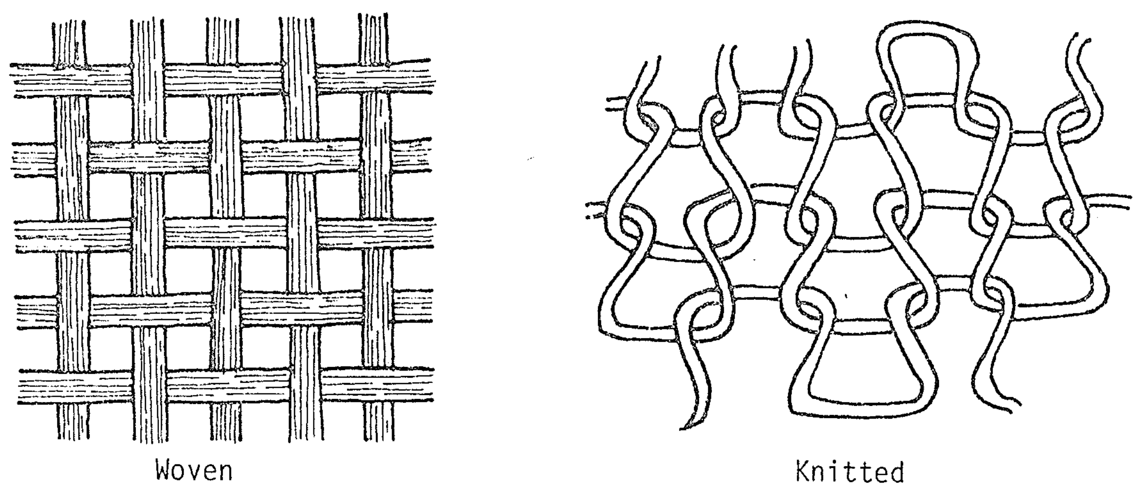

Fig. II.5: Difference between woven and knitted fabrics. (Reproduced from [22]).

Improvements in the biocompatibility of the materials themselves have also been made. Vinyon "N" has a high wettability that produces blood loss through the mesh, even when the material is tightly woven. Inalon sponge, used clinically in aortic grafts in early research, has an increasing brittleness with age and was abandoned. Orlon was found to lose 12% of its strength after six months of implantation, so was abandoned also. Nylon is highly hygroscopic so, after implantation in the human environment the fibers become distorted and lose strength and in some cases there has been reported high thrombogenicity. Invalon was found to be excessively rigid and had a tendency to kink. Teflon, the most inert thermoplastic available, has suitable strength and a suitable endurance limit and thus has been widely used for prostheses but its inertness prohibits proper adherence of the adventitia and pseduointima, thus it is prone to produce thrombosis and anastomotic aneurism (abnormal dilatation at the suture line) [22]. Dacron has become the most commonly used material for valcular prosthesis. Its strength and endurance limits are suitable, it is not as inert as Teflon. Thus the adventitia and pseduointima have better adherence and it does not deteriorate in the organic environment due to water absorption. Most present day arterial implants are thus made of Dacron or similar polyester fiber.

Implants made of copper, silver or gold with imposed negative charges have a minimum of thrombus deposition [23] but, since they are rigid, further understanding of the change of the pulse pressure due to rigid insertions is necessary before these metal insertions can be considered in detail.

From the literature reviewed so far, it is possible to conclude that the requirements for an arterial prosthesis are: (a) to have or produce a thrombus-resistant surface; (b) to have a high degree of conformability; (c) to possess good suturability; (d) to have an outer surface to which surrounding tissue can adhere firmly; (e) to possess an inner surface to which any thrombus that does form can attach firmly to discourage embolization; (f) to have similar elasticity to that of the artery.

No material that fulfills all the requirements has been found [16, 28]. However, most of the actual commercially available grafts today are tubes of woven or knitted construction [15, 17]. The material is Teflon or Dacron. The implants are crimped and their wall thickness is between 1.5 and 0.3 mm. Since they are knitted, they do no fray or unravel under normal working stresses and thus may be sutured close to the end in order to avoid flaps or false aneurism [15, 21, 22]. It is not advisable to use this style of implant for a diameter smaller than 8 mm since thrombosis usually generates in smaller diameters. The diameter of the arterial prosthesis should be larger than that of the host vessel; though how much larger depends on the characteristics of the host vessel. The selection of woven or knitted fabrics depends on the expected and allowable bleeding after implant; less bleeding is expected in a woven prosthesis, and in an aortic implant more dangerous bleeding is expected than that in a small vessel. Fig. A.1 of Appendix A shows a comparison of patency and thrombosis rate of prostheses made of Teflon or Dacron and implanted in the femoral artery of dogs [21]. More characteristics of the arterial prosthesis are given by Appendix A, which is a resumé of the most promising clinical experiments with arterial grafts and the remaining major problems that must be overcome to produce acceptable arterial prostheses.

The commercially available grafts are known to produce changes in the hydrodynamic characteristics of the blood flow [16, 20, 35]. Lee [20] reported that the velocity profile in the Dacron graft is not the same as the velocity profile in the healthy artery, and the velocity profile is important for the adequate distribution of blood to the peripheral vasculature. Gozna [16] proved that the distention of the grafts is only 10% that of major arteries, concluding that this lack of distention produces suture line stress and probably turbulence. The suture line stress produces suture line disruption and the turbulence produces vessel wall damage and thrombosis. Womersley [35] developed a theory for the reflection of the pressure pulse wave that must be generated at rigid inserts in the arterial system. As stated in the Introduction, the main concern regarding arterial prostheses is the magnitude of the increase of the pressure pulse caused by reflected waves as a result of the relative rigidity of the prosthesis. The reflected waves are of concern because they may be added to the incident waves, thus producing higher non-physiological pressure waves that could damage the artery itself or even the heart valves if the insertion is in the aorta, close enough that the reflections are not significantly damped before reaching the heart. It is intended to reproduce this reflected wave phenomenon in a mechanical model described in Chapter III and analyze the phenomenon based on the theory included in Chapter IV.

II.3 The Starr-Edwards and the Bjork-Shiley prosthetic heart valves

The heart valve operation also represents a pressure-flow problem and therefore also merits investigation. Since both the investigation of pressure wave characteristics from arterial implants and the pressure-flow characteristics of the valves require the same instrumentation, the valve measurements were also taken in order to define the difference in mechanical behaviour of the two valves when subjected to a physiological pressure wave.

The Starr-Edwards valve basic design consists of a ball and cage that when open, allows flow around the periphery of the ball because the diameter of the vasculature where the prosthesis is attached is bigger than that of the ball itself, as indicated in Fig. II.6. This type of valve became clinically available in the late 1950's and early 1960's, and it has undergone many improvements in design and materials,therefore only the basic design is discussed. Pictures of a currently employed valve are shown in Fig. II.6 and diagram in Fig. II.8 [31]. The cage is cast in a single piece of stainless steel and the final dimensions are obtained by grinding, then a mirror polishing is achieved by buffing and electro-polishing. Finally the surface is coated with silicon. The knitted Teflon cloth provides a method for fixing the valve to the vasculature by suture. This Teflon cloth is attached to the cage by a

Teflon spreader ring and a braided Teflon thread. The ball is made of Silastic [31].

The Bjork-Shiley valve basic design consists of a free tilting disc that opens or closes when supported between two eccentrically located legs, Fig. II.7. The need for a valve of this type surged from the drawbacks produced by the lack of hydrodynamic compatibility of the precedent models (Starr-Edwards, Cutter-Smeloff, Kay-Shiley, Wada-Cutter). It became clinically available in the late 1960's and, like all other prostheses, has undergone many changes in design and material since then, therefore only the basic design is discussed. Fig. II.7 is a picture of a currently employed valve. The manufacturing procedures and the principle of a knitted Teflon cloth for suture to the vasculature remain the same as for the Starr-Edwards valve. The main feature that improves the Bjork-Shiley valve over the Starr-Edwards valve is that the disc does not overlap the ring so that the flow area of the disc valve can be almost the same as the inner area of the ring, thus diminishing the flow resistance even if the disc does not open 90°. It was found that 60° of opening was enough for minimum pressure drop and for keeping the laminar characteristic of the blood flow. Another improvement of a non-overlaping disc is that it does not hit the ring and therefore the damage to the blood corpuscles is minimized. The ring is colinear with the artery and therefore takes the least possible space. The disc is free to rotate around its own axis, which it does, at an approximate rate of one revolution for every 45 beats; therefore, pressure and wear are evenly distributed around the disc. The weight of the occluder is only about

14% that of the Starr-Edwards ball, therefore the inertial effects for opening and closing are diminished.

Comparison of the mechanical behaviour of the valves is performed on the basis of the principle of pressure energy losses in a fluid passing an obstacle in a horizontal, closed duct. Thus, the valve is considered the obstacle in the arterial duct and the valve that produces smaller pressure energy losses to the flowing fluid has the better mechanical efficiency. The valve performance is also considered on the basis of the pressure wave Fourier components, both upstream and downstream of the valve.

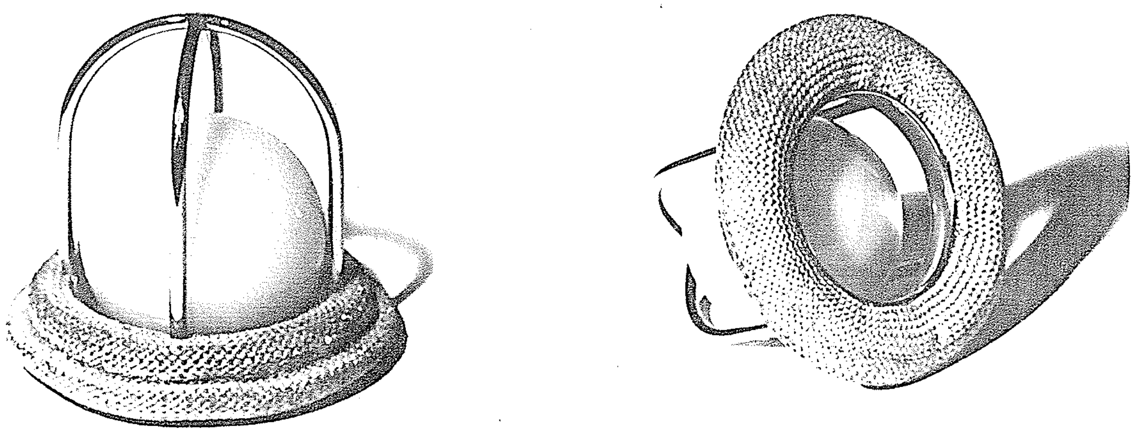

Fig. II.6: The Starr-Edwards ball and cage prosthetic heart valve.

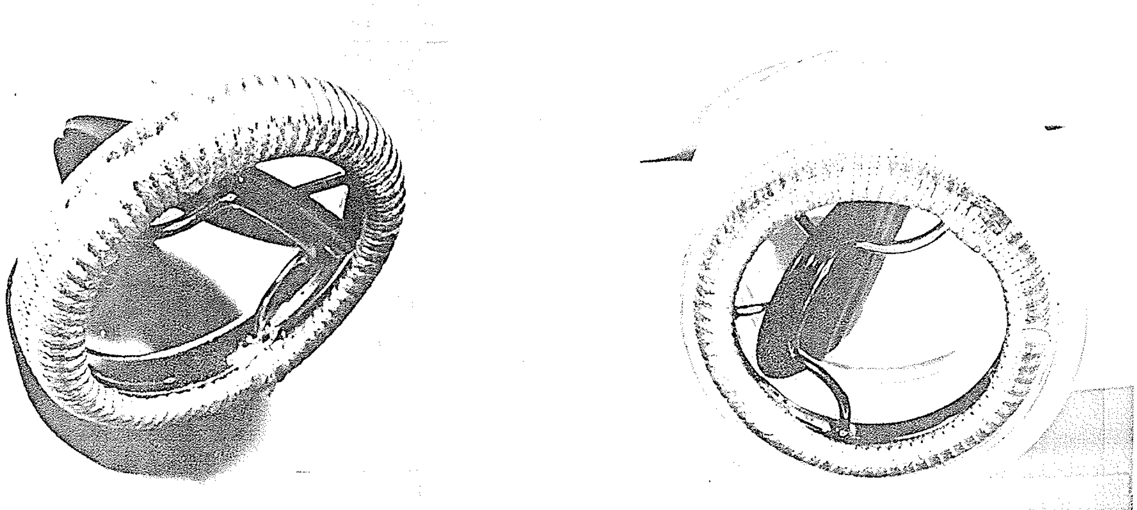

Fig. II.7: The Bjork-Shiley tilting disc prosthetic heart valve.

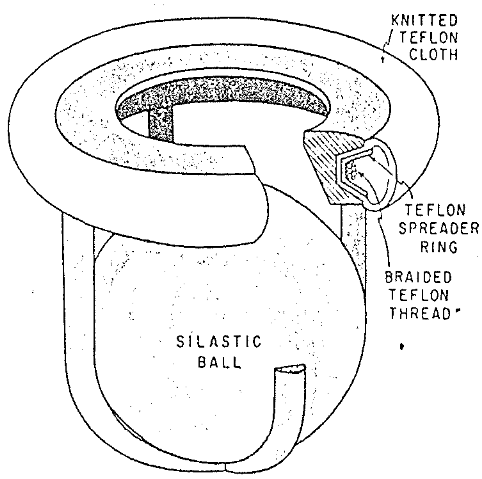

Fig. II.8 Diagram of the construction of a Starr-Edwards valve (Reproduced from [31]).

CHAPTER III DEVELOPMENT OF EQUIPMENT

None of the previous studies have specifically considered the elliptic cross-section as a method for reducing pressure peaks. Since the components of the pressure waves in the aorta and the movement of the heart valves may interact the pressure wave characteristics of the prosthetic heart valves, the Starr-Edwards and the Bjork-Shiley, will also be studied using Fourier Analysis. In order to study the arterial prosthesis and arterial heart valves, a heart-valve-artery model which simulates the behaviour of the cardiovascular system is necessary. Such a system must be developed in accordance with very detailed criteria and specifications in order to ensure that the cardiovascular system is closely simulated. The detailed specifications are shown in Table III.1.

III.1 Specifications

System to be simulated: left ventricle, aortic valve and ascending aorta.

Table III.1 shows the properties of the system that are necessary to be reproduced.

Flow source	Pulsatile with variable range from 50 to 200 beats/minute. Pressure wave is shown in Fig. II.3.
Stroke volume	79 cm^3.
Pressure wave	Physiological pressure wave shape, with maximum 120 mm Hg and minimum 80 mm Hg at 72 beats/minute, see Fig. II.3.
Artery	
Inner radius, a_1.	1 - 1.5 cm
Wall thickness/inner radius relation, k.	0.08 - 0.12
Wall density, ρ.	≈ 1 gr/cm^3
Static modulus of elasticity, E is variable, depending on the inside pressure [35].	
At 80 mm Hg	2 Kg/cm^2
100 mm Hg	4 Kg/cm^2
120 mm Hg	5 Kg/cm^2
160 mm Hg	10 Kg/cm^2
200 mm Hg	15 Kg/cm^2
The anisotropic viscoelastic properties of the artery wall are not well known [35]	
Phase velocity of pressure waves	5 - 6 m/s
Aortic valve	
Opening delay	0.025 s
Closing delay	0.015 s
Regurgitation	Negligible
Circulating Fluid (Blood)	Dynamic viscosity 3 to 4 CP at 36°C. Density 1.01 to 1.1 gr/cm^3 at 36°C.

TABLE III.1 Specifications for Simulated Cardiovascular System

III.2 Apparatus

From the literature review it can be seen that both the arterial implants and the prosthetic heart valves cause disruption of the hydrodynamic characteristics of the blood flow. However, no quantitative values of such disruptions for a physiological pressure wave shape were given for the arterial prostheses. In the case of the prosthetic heart valves, the comparison of the pressure waves both upstream and downstream of the valves was not analysed in terms of the Fourier components. It is the purpose of this investigation to examine the pressure waves using simulated arterial implants and to investigate the performance of the two prosthetic heart valves in a simulated systemic system.

A reciprocating pump was used to simulate the heart and was made of transparent acrylic rod with a conical nozzle at the discharge for producing a gradual change of diameter. The piston was made of P.V.C. rod with Teflon "O" rings for the dynamic sealing. The piston rod was made of aluminum and slid through a Teflon bearing. On the opposite end to the piston, the piston rod had a roller-bearing cam follower. The general assembly with dimensions and list of materials is shown in Fig. B.4 of Appendix B. When forward flow was desired, a cam would drive the piston, see Figs. III.1 and 2. Since it was intended to reproduce the outflow from the heart of an adult man, the appropriate cam was designed by graphical integration from a time velocity graph obtained from the corresponding time-flow graph for the human outflow shown in Fig. II.3. The procedure for obtaining the cam profile by graphical integration is shown in Fig. B.5 of Appendix B and the cam is shown in Fig. B.6 of Appendix B. The cam was coupled to a variable speed motor made by Boston Gear Division, model Ratiotrol, which allowed the pulse rate to be varied between 0 and 100 cycles/minute. To provide a constant and smooth cam movement, a speed reduction of 16:1 between motor and cam and a fly wheel in the transmission were necessary. The contact cam-roller was secured with rubber bands that forced the roller against the cam.

When forward flow was not desired and only the high frequency sinusoidal waves were to be produced, the piston rod was coupled to a vibration exciter which would respond to signals produced by a signal generator. The range of frequencies for this test was 10 - 25 Hz. The list of equipment and assembly diagram for the vibration exciter and its controls are in Table C.2 of Appendix C and Fig. B.2 of Appendix B, respectively.

The outlet valves used were the prosthetic heart valves Starr-Edwards size 1M model 6120 and Bjork-Shiley size 29. Pictures of these valves are in Fig. II.5 and Fig. II.6. The prosthetic heart valves were placed in cases made of acrylic, as shown in Fig. B.7 of Appendix B, the elastic tubes were easy to couple to these cases. The inlet valve was a common plastic poppet valve. The requirements for the valves are small opening and closing delays and minimum regurgitation. Opening delay is defined as the time between the rise of the left ventricular pressure above the aortic pressure and the opening of the valve. Closing delay is defined as the time between the reversal of flow and closure of valve. Regurgitation is defined as backward flow during or after closure of valve. With a pulse duplicator, Olin [27] measured opening delays, closing delays and regurgitation for different prosthetic valves and his results for the Starr-Edwards and Bjork-Shiley valves are shown in Table III.2.

	Starr-Edwards	Bjork-Shiley
Opening delay, in s	0.005 - 0.02	0.0
Closing delay, in s	0.022 - 0.035	0.026 - 0.032
Total regurgitation, in % of forward stroke	2 - 3	9 - 11

TABLE III.2 Opening delays, closing delays and regurgitation for Starr-Edwards and Bjork-Shiley valves [27].

Two elastic tubes of different materials were used to simulate the artery. Tube No. 1 was made of pure latex of inside radius 0.635 cm and tube No. 2 was made of neoprene compound (bicycle inner tube) of inside radius 1.12 cm. Both these were 4 m long. It was desired to use only tubes of pure latex because its dynamic viscoelastic properties had been measured by Klip [19] but, no tubes were available in pure latex with larger radius than that indicated above. The length of the tubes was exaggerated so that the reflected waves from pump and discharge end may be dissipated when reaching the middle part of the tube length, thus at least one section of the tube would satisfy the condition of minimum wave reflection. The necessary physical properties of these two tubes are given in Table V.1.

The circulating fluid used was a mixture of water and glycerine of density 1.05 gr/cm^3 and viscosity 3.8 CP at 20°C. The diastolic pressure of 80 mm Hg was induced by an elevated tank where the liquid would reach a level of 110 cm (80 mm Hg) above the elastic tube. When forward flow was desired a gentle 90° loop in the tube would bring it to the elevated tank and a return line would be coupled between elevated tank and pump see Figs. III.1 and III.2. When high frequency sinusoidal waves without forward flow were required the tube would end in a reservoir partially filled with air for damping the incident waves, see Fig. III.3 (a). Obviously reflected waves from the turn and/or end of the tube were not cancelled but they were reduced using these methods.

The simulated arterial prostheses were produced in two different ways. In the case of tube No. 1, a 15 cm long aluminum sleeve was cut into two half sections such that when fastened together the sections would fit tightly over the elastic tube, immobilizing the section where it had been placed, (see Fig. III.4(b)), and for tube No. 2 a 25 cm long section was replaced by a 2.54 cm I.D. tube of Jayflex^{R}. The reason for using the Jayflex tube was that its modulus of elasticity when working in the physiological pressure range was 165 Kg/cm^2, that is 12 times higher than that of the neoprene compound, therefore Jayflex could be considered as unextensible relative to the neoprene. The round Jayflex was also possible to convert into elliptic tubes in order to replace the round rigid insertion by the elliptic one. In response to the pressure the elliptic insertion would approach a circle, allowing greater flow cross-section, thus reducing the pressure peak. The elliptic insertion placed in the elastic tube is shown in Fig. III.5. The process for producing the elliptic tube consisted of manufacturing a mandrel made of Teflon elliptic sections, see Fig. B.1 of Appendix B. The perimeter of the mandrel was the same as the interior perimeter of the round tube. The round tube of Jayflex was then forced to fit over the mandrel and the assembly was placed in a furnace at 135°C for 30 minutes, to remove the internal stresses of the Jayflex. The reason for using Teflon for the mandrel was that it was easy to machine and the Jayflex would not stick to it.

Electronic equipment was necessary for detecting, measuring and storing or recording the values of the pressure waves generated in the apparatus. Measurement of pressure waves was performed with 2 pressure transducers of the strain-gage type. Pressure transducers were placed at 0.3, 0.5, 1 and 1.5 m from the pump, depending on the experiment to be performed. A picture of one transducer and how it was connected to the main tube is shown in Fig. III.4 and the characteristics of the transducer are given in Table C.1 of Appendix C. Measurement and storage of the signals from the pressure transducers was made using an oscilloscope and measurement and recording were done using an X-Y recorder. Since the signals as obtained from the pressure transducer were of very small amplitude, preamplifiers were used before the oscilloscope and X-Y recorder. Characteristics and connections of the equipment described above are in Table C.3 of Appendix C and Fig. B.3 of Appendix B, respectively.

The performances of the prosthetic heart valves differ slightly from that of the aortic valve, it is a problem that has existed since the prosthetic valves were first initiated. However, the Bjork-Shiley valve is considered as the best available and was used for all the experiments, except for valve comparison when the Starr-Edwards valve was also used.

The viscosity and density of the mixture of water and glycerine as circulating fluid was similar to that of the blood. The peculiar elastic characteristics of the artery wall and its phase velocity for pressure waves were not well reproduced, but since arteries are formed of various anisotropic layers with elastic characteristics that vary along the length of each one [6], it is impossible for a single isotropic material to reproduce the elastic properties of the artery wall. On the other hand a tube with anisotropic wall characteristics would be very difficult to manufacture and analyse.

The modulus of elasticity of the simulated prosthetic insertions was at least 10 times higher than that of the elastic tube, so the simulated round prosthetic insertions would reproduce the effect of inextensibility produced in the cardiovascular system by arterial grafts.

As a result of the design limitations, it is apparent that all desired specifications for the cardiovascular system simulation could not be met. However, the blood could be simulated accurately in both density and viscosity, the arterial properties could be simulated adequately over a reasonable range and the pump could simulate the physiological flow wave. The details of the performance of the equipment are left to Section V, Results and Discussion.

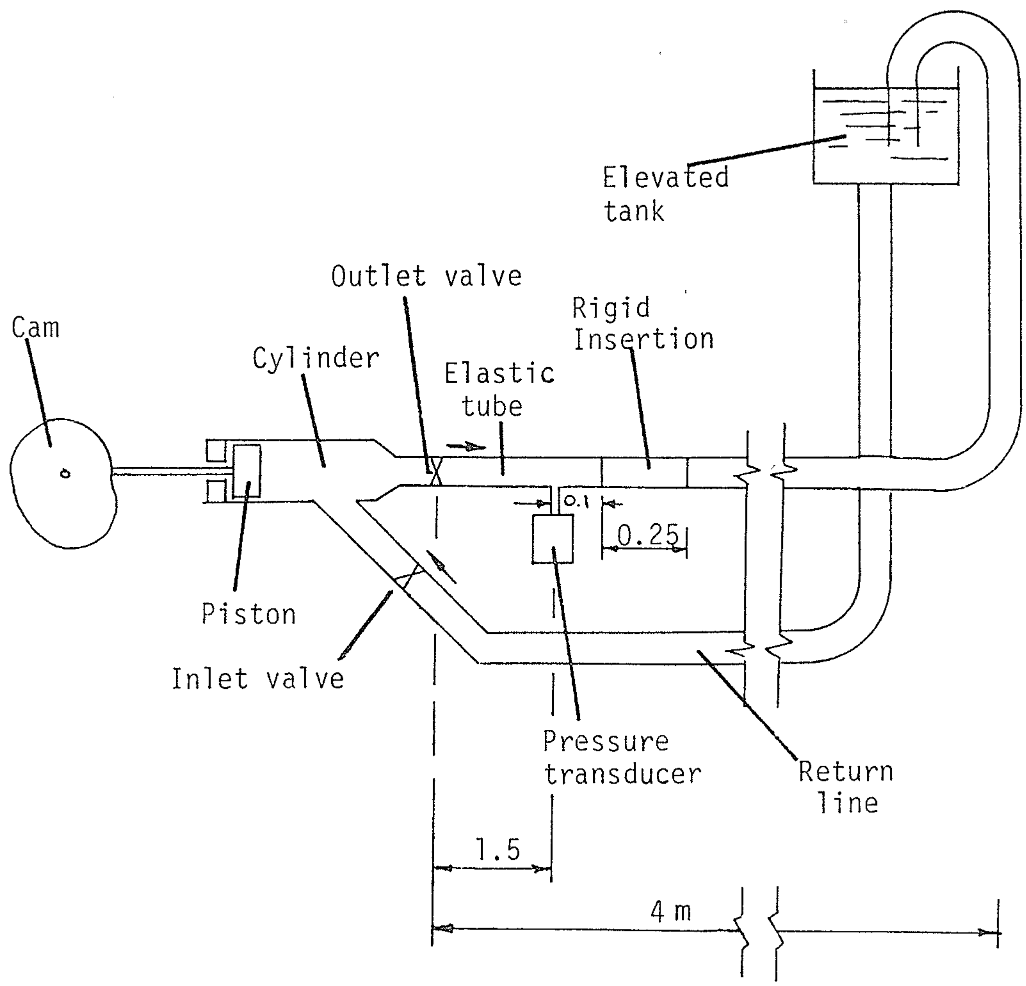

Fig. III.1: Diagram of the model when working with forward flow present. Tube No. 2 and Jayflex insertion were used. Dimensions in meters.

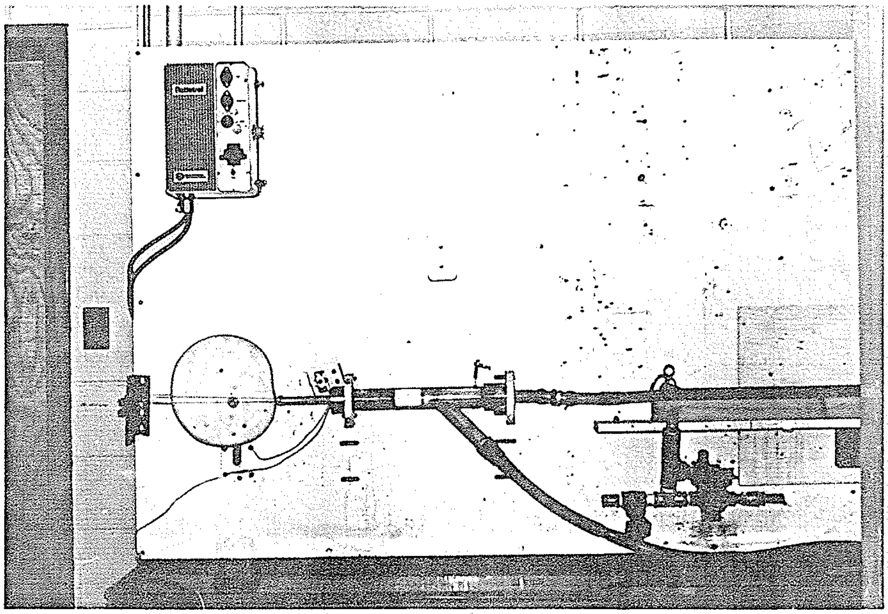

(a)

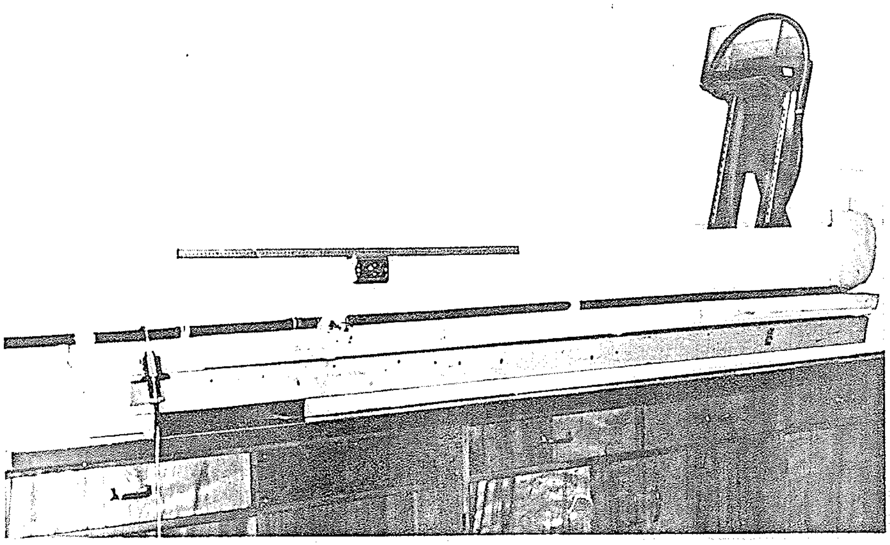

(b)

Fig. III.2: Pictures of the model when working with forward flow present.

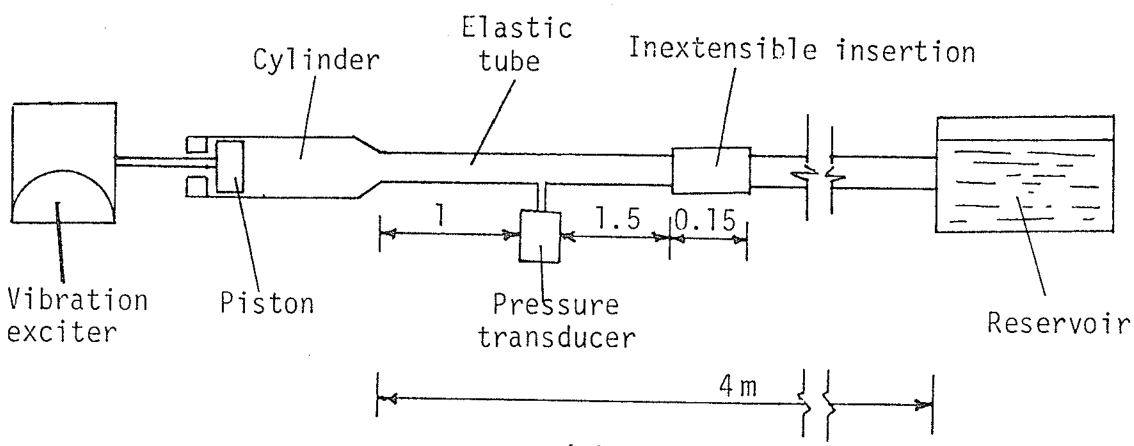

(a)

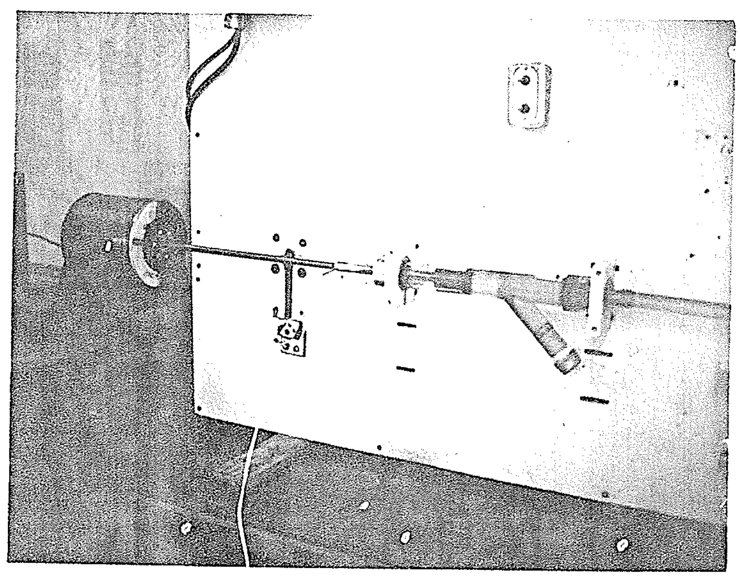

(b)

Fig. III.3: Diagram and picture of the model when working without forward flow. Aluminum inextensible insertion and latex tube were used. Dimensions in meters.

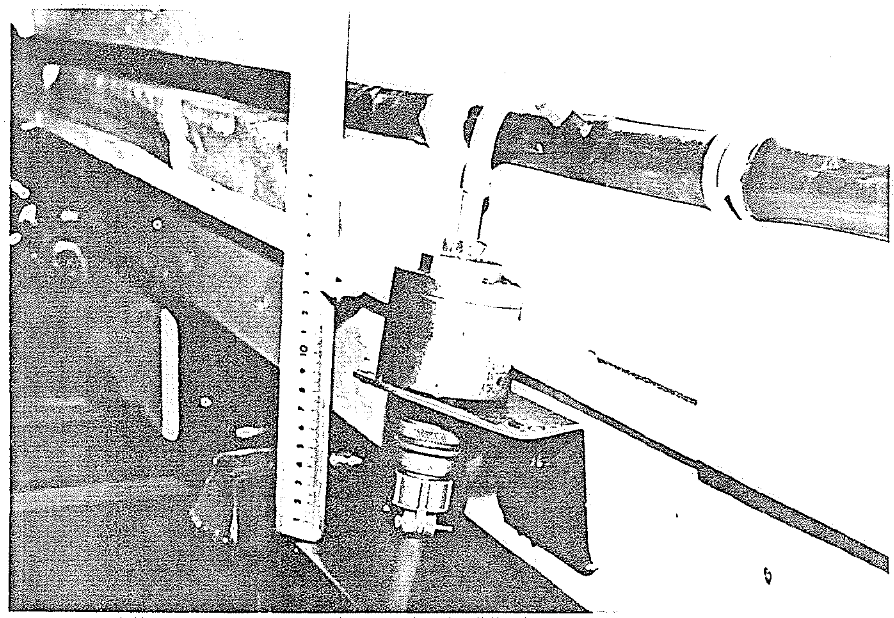

(a)

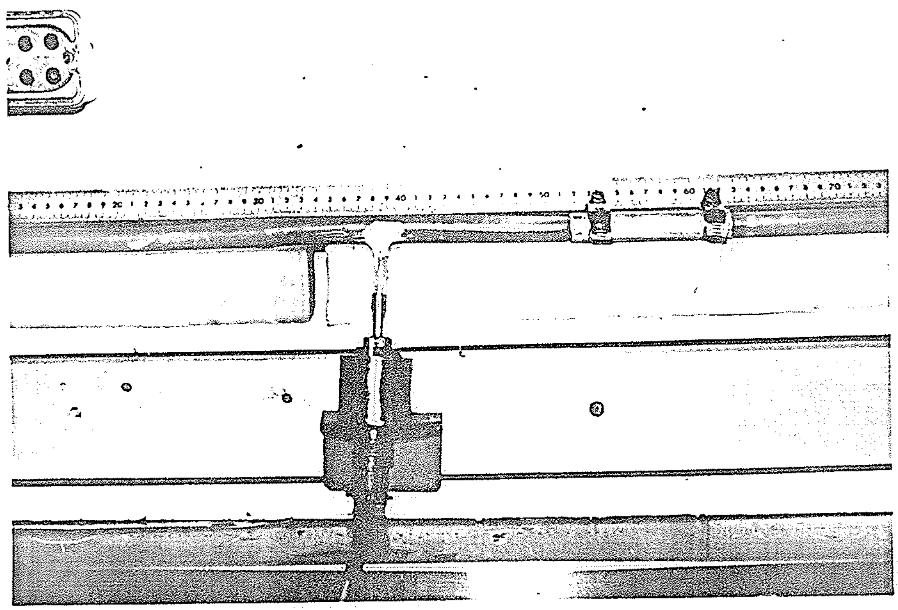

(b)

Fig. III.4: Pictures of the pressure transducer. Picture (b) also shows the aluminum inextensible insertion on the tube No. 1.

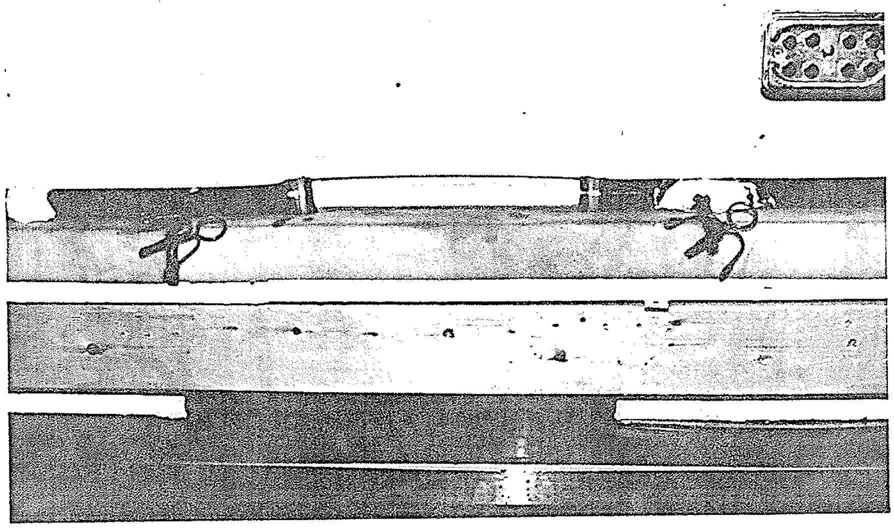

Fig. III.5: Elliptic insertion placed in the elastic tube.

CHAPTER IV. THEORY

When a disturbance is induced in an elastic system it is propagated in the form of waves. When the heart induces blood flow in the cardiovascular system the flow simultaneously induces a pressure disturbance, and both are propagated in the form of flow waves and pressure waves that have a mutual relationship [24]. Furthermore, this wave propagation becomes a characteristic of the cardiovascular system and when a foreign material is implanted (such as the prosthetic arterial implant) this propagation characteristic is modified, perhaps to the extent of being a hazard to the host organism. This is contrary to the beneficial functions that this implant is supposed to perform.

The necessary theory for analysing the pressure wave behaviour was that of pressure wave propagation and pressure wave reflection in elastic tubes filled with viscous fluid. But in order to analyse the data obtained from the pressure events it is necessary to know the relationship between the pressure and the flow events, therefore data analysis is concerned with the relation of pulsatile pressure to flow in elastic tubes filled with viscous fluid.

VI.1 Pressure wave propagation theory

The general equation of the wave travelling at finite velocity is

$$\nabla^2 p - \frac{1}{c_1^2} \frac{\partial^2 p}{\partial t^2} = 0, \qquad \text{(IV.1)}$$

where p is the pressure, c_1 the phase velocity of the wave and t, the time.

In the particular case of a cylindrical vessel where it is assumed that the pressure is uniform across any cross-section, the pressure (and also the flow, as indicated in the next section of this chapter) reduces to a function of position, z, along the vessel and the time, t, therefore, the corresponding simplification of the wave equation becomes:

$$\frac{\partial^2 p}{\partial z^2} = \frac{1}{c_1^2} \frac{\partial^2 p}{\partial t^2} . \qquad \text{(IV.2)}$$

In the presence of friction it is necessary to include the damping term $(L/c_1^2)(\partial p/\partial t)$, where L is the internal damping coefficient of the conducting medium. Thus the equation becomes:

$$\frac{\partial^2 p}{\partial z^2} = \frac{1}{c_1^2} \left(\frac{\partial^2 p}{\partial t^2} + L \frac{\partial p}{\partial t}\right). \qquad \text{(IV.3)}$$

For a tube with walls which have linear mechanical properties, filled with a Newtonian fluid, where laminar flow is induced and subjected to a sinusoidal disturbance, $p_o \sin (nt)$, travelling in the positive direction of the tube z-axis, the solution of the equation with damping becomes:

$$p = p_o e^{-az} \sin (nt - bz) = p_o e^{-az} e^{i (nt - bz)} = p_o e^{int - \gamma z} \qquad \text{(IV.4)}$$

where, since the input is sinusoidal, the coefficient of the cos (nt - bz) term is zero, and where:

p_o = complex-pressure modulus,

n = angular velocity in radians per unit time,

a = F(L) damping constant, a physical property of the tube-fluid conducting medium, where $L = F(\sigma, E, h, \rho, \rho_o, a_1, n, \nu)$,

b = n/c_1, phase constant, a physical property of the tube-fluid conducting medium, where $c_1 = F(L)$,

γ = a + ib = the propagation constant.

For the special case of an ideal inviscid and incompressible fluid in a tube with an ideally elastic thin wall, the damping constant, a, is proportional to the angular velocity, and the phase constant, b, can be evaluated from Young's formula for the phase velocity c_o [16], which is

$$c_o^2 = \frac{Eh}{2\,\rho_o\,a_1} \tag{IV.5}$$

where

E = Modulus of elasticity of the wall,

h = $a_2 - a_1$ = thickness of the wall,

ρ_o = density of the fluid,and

the tube is considered as thin walled for $h/a_1 \leq 0.1$.

When the physical properties of the wall and fluid are not ideal, determining the values of the propagation-constant or the complex-wave-number becomes more difficult. If an elastic tube subjected to pulsatile flow does not have the restriction of zero axial displacement, two modes of wall motion are possible. The first one in the radial direction is associated with the phase velocity of pressure waves, and the second in the longitudinal direction is associated with the longitudinal waves in the tube wall. For the special case of an ideal incompressible fluid in a tube with an ideally elastic thin wall, those modes of vibration reduce, respectively, to

$$\text{Young's formula } c_0 = \{hE/(2a_1\rho_0)\}^{\frac{1}{2}},$$
$$\text{and Lamb's formula } c_1 = \{E/[\rho(1 - \sigma^2)]\}^{\frac{1}{2}}.$$

Therefore they are named Young's mode and Lamb's mode respectively [19, 36].

Klip [19] solved for the complex-wave-number $K = b + ia$ for thick viscoelastic tubes of infinite length and filled with a viscous fluid for two modes, Young's mode and Lamb's mode. He obtained an explicit expression for K^2 that is valid for wall thicknesses up to the size of the inner radius of the tube. His theoretical results for K were compared with those obtained in a pulse generator similar to the model used in this investigation, where harmonic longitudinal waves are generated in the fluid which in turn transmits them to the tube wall made of pure latex. The agreement between his theory and experiments is satisfactory as can be observed in reference [19]. For stating the differential equations for the development of his theory, Klip considered a tube of infinite length, filled with a viscous incompressible fluid and with a homogeneous, isotropic, viscoelastic (Voigt solid) wall. Gravity was neglected, and the surrounding medium was taken to be a gas which was exerting a constant pressure but where density and viscosity could be neglected, thus the complexity of the equations was reduced. Considerations were limited to harmonic longitudinal vibrations about an equilibrium state.

From the displacement vector $\overline{V}$:

$$\overline{V}\ (r,\ z,\ t) = V_r\ i_r + V_z\ i_z \tag{IV.6}$$

Where (i_r) and (i_z) are the unit vectors along the radial and axial axis respectively.

Klip solved linearized differential equations for the wall and the fluid behaviour. Only the solutions of interest for this investigation are given here; i.e., those of the complex-wave-number for Young's Mode.

For Young's mode, general case:

$$K^2 = \frac{\rho_o\ n^2}{(1 + i\ \gamma')E} \left| \frac{N}{I_v - I_o} - \frac{N'}{N} \right|, \tag{IV.7}$$

where
$$N = \frac{(I_v - I_o)\ \rho}{\rho_o} + I_o\ I_v\ (\tau + 1 + \sigma) + \tau(1 - 2\ I_o\sigma)$$

and
$$N' = I_o\ (1 + \sigma)\ (\tau + \frac{I_v\rho}{\rho_o})\ [1 + \tau(1 - \sigma)],$$

where
$$I_o = \frac{i\ Ka_1\ J_o\ (i\ Ka_1)}{J_1(i\ Ka_1)} \approx 2,$$

$$I_v = \frac{(1 - i)\ x'\ J_o\ [(1 - i)\ x']}{J_1\ [(1 - i)\ x']},$$

σ = Poisson's ratio,

J_o ( ) = Bessel function of the zero order,

J_1 ( ) = Bessel function of the first order,

$\tau = \dfrac{2\ a_1/a_2}{a_2/a_1 - a_1/a_2}$ constant that relates inner and outer radius of the tube,

$x' = a_1\ (\rho_o n/2\mu)^{\frac{1}{2}}$, non-dimensional constant that relates some properties of tube and fluid.

I_o is tabulated in Klip [19] for values of x' ranging from 0.1 to 110.

Also

$$\gamma' = \frac{n\ \mu_{vi}}{\mu_s},$$

where μ_{vi} = viscous constant of the wall material (Voigt solid),

μ_s = $E/[2\ (1 + \sigma)]$ Lame's elasticity parameter.

Equation IV.7 was used in this investigation for calculating the damping constant, a, for tube No. 1. The damping constant value was necessary for evaluating the relation between incident and reflected waves (Reflection Factor). This procedure is described in Figs. IV.5 and IV.6 of Section IV.8.0 Experimental Procedure.

IV.2 Pressure wave reflection

It is well known that discontinuities in an elastic medium subjected to vibrations will produce wave reflections [35]. If the medium is an elastic tube filled with viscous fluid where there are waves travelling upstream and downstream as in the case of wave reflection, the resultant pressure is the addition of both waves

$$p = p_1\ e^{int\ -\ \gamma z} + p_2\ e^{int\ +\ \gamma z} \qquad \text{(IV.8)}$$

where p_1 is the modulus of the incident wave and p_2 the modulus of the reflected wave. The sign (-) in $(int - \gamma z)$ means that the wave is travelling in the positive direction of the axial axis and (+) in $(int + \gamma z)$ means that the wave is travelling in the negative direction. If in this tube there is an inextensible insertion of length Δz and the incident wave travels in the positive direction of the z axis, the nature of the harmonic component of the reflection will be as follows (refer to Fig. IV.1):

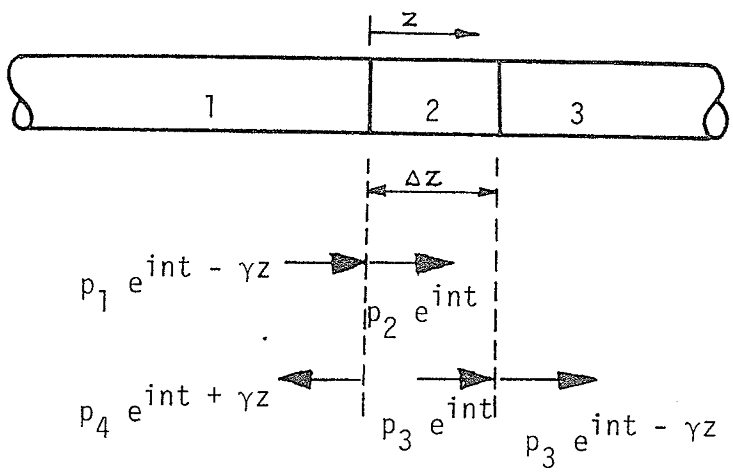

Fig. IV: 1 Inextensible insertion of length Δz in an elastic tube. See text for explanation.

The incident wave is $(p_1\, e^{int - \gamma z})$ and the reflected wave is $(p_4\, e^{int + \gamma z})$. Since the phase velocity in an elastic tube is known to be small compared with that of the inextensible tube [14], and for inextensible insertions which are short compared to the wavelength, it can be assumed that there is not any phase difference of the pressure wave within the inextensible section, only an amplitude drop due to viscous losses (see Fig. IV.4). Therefore the pressure in the upstream end is $(p_2\, e^{int})$, and the pressure in the downstream end is

$(p_3\ e^{int})$. For continuity of pressure, the transmitted wave must be $(p_3\ e^{int\ -\ \gamma z})$ and $(p_1 + p_4 = p_2)$, and for continuity of flow within the rigid tube:

$$\begin{array}{c}\text{Flow at the end}\\ \text{of Section 1}\end{array} = \begin{array}{c}\text{Flow within}\\ \text{Section 2}\end{array} = \begin{array}{c}\text{Fow at the beginning}\\ \text{of Section 3}\end{array} \qquad \text{(IV.9)}$$

The relation between the reflected and incident wave is the Reflection Factor (p_4/p_1) and is solved by consideration of the continuity of pressure and continuity of flow within the rigid section. The development of this relation is in the Sections IV.5.0 Relation of Pulsatile Flow to Pressure and; IV.6.0 The Movement of the Fluid.

IV.3 Short trains of waves

When a source of waves is active continuously in a vessel of a finite length, superposition of reflected waves makes the definition of the fundamental wave very complicated, since the variables are several, such as reflection factors reflection phase and multiple reflections. In such a case it is more convenient to make the analysis in terms of bursts of high frequency sinusoidal waves, such as trains of three to five cycles with a frequency of 10 to 25 Hz. These short trains of waves and their reflections are easy to identify with pressure transducers appropriately located along the vessel because the short train of incident waves is isolated in time from the reflected waves. Fig. IV.2 shows the arrangement of the apparatus for performing the experiment described above.

The principle of the short train of waves could also be used for finding the experimental value of the damping constant for the elastic tubes. From the equation of the damped wave it can be shown that the modulus of the pressure wave measured on the downstream transducer, p_2, with respect to the modulus measured in the upstream transducer, p_1, is ($p_2 = p_1 e^{-a\Delta z}$), thus the damping constant a may be expressed as:

$$a = \frac{1}{\Delta z} \ln \frac{p_1}{p_2} \qquad \text{(IV.10)}$$

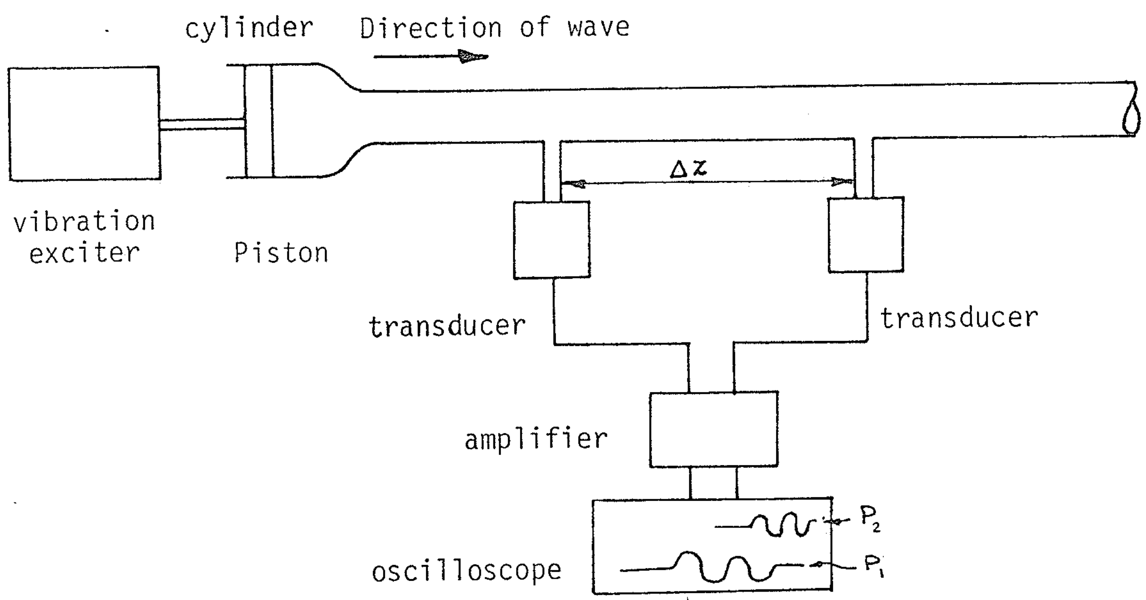

Fig. IV.2: Diagram of the apparatus set-up for detecting short trains of waves.

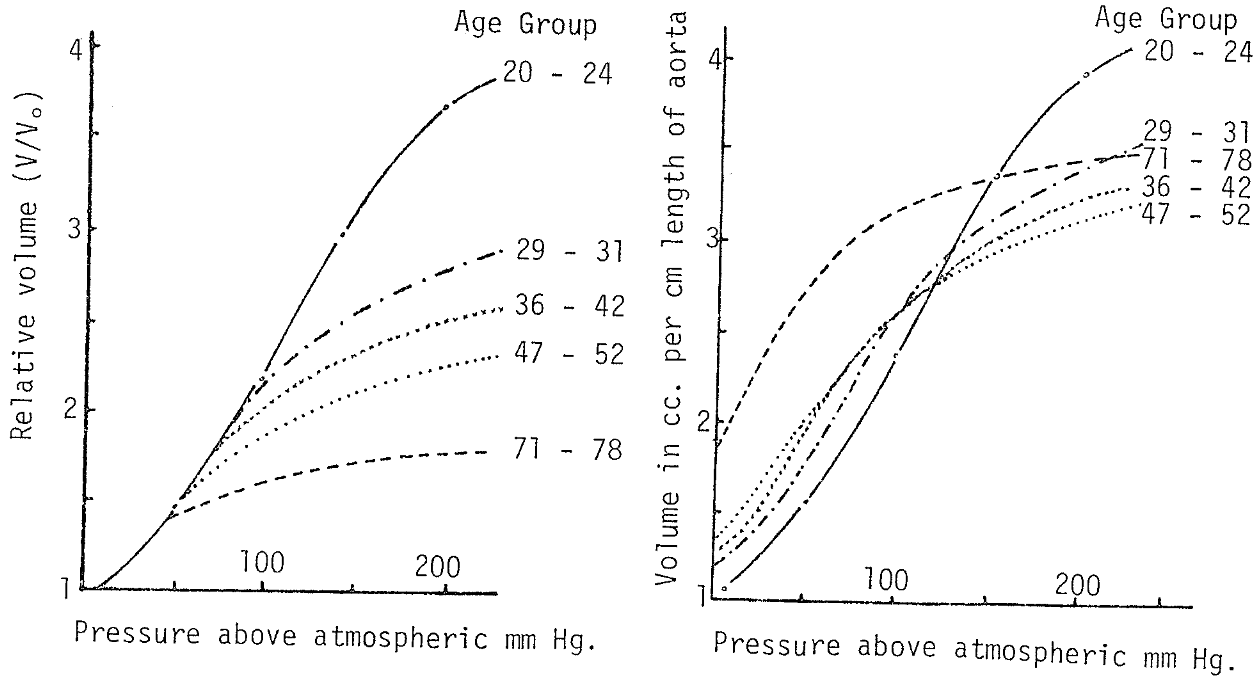

Relative volumes of aortas in five age groups, as a function of applied pressure. The curves are obtained from experimental data by A. L. King.

Curves show Hallock and Benson's observed volumes per unit length of aorta as a function of applied pressure. Each line represents an age group.

Fig. IV.3: Curves of aortic elasticity (Reproduced from [14]).

However, even if the problem of the cross-section distention is solved, the problem of change of continuity of the elastic tube as a source of reflection persists, and for making an appropriate analysis of Caragannis' proposal, appropriate shell theory and pulsatile flow-pressure relationship in elliptic tubes must be developed. Initial experiments with elliptic rigid insertions were performed as part of this investigation.

IV. 4 Elliptic insertion

A solution for diminishing the effect of inextensible insertions has been suggested by A. Caragannis [9]. It is the use of an inextensible thin-walled flexible insertion of elliptic cross-section. When a vessel of this nature is subjected to internal pressure, its eccentricity decreases; thus, the ellipse approaches a circle and small changes of eccentricity produce large changes in area. His design criterion was to provide an ellipse that would deform with pressure changes in such a fashion that the cross-section area would be the same as that of the circular and elastic aorta under the same pressure. The elliptic vessel should become circular at the maximum expected pressure of 200 mm Hg.

Since elasticity of the arteries changes with the age of the person, Caragannis suggested that this variable could be solved using the curves obtained by King and Halloc and Benson [14], relating changes in pressure to changes in cross-section for the aorta of different age groups. See Fig. IV.3.

IV. 5 Relation of pulsatile flow to pressure

As stated at the beginning of this chapter, for analysing the data obtained from the pressure events, it is necessary to know the relation of pulsatile pressure to pulsatile flow in elastic tubes filled with viscous fluid. This is mainly to allow the solution of Equation IV.9 which is required for analysing the data regarding pressure wave reflections and for finding the value of the Reflection Factor.

Pulsatile flow is analysed as a phenomenon of continuum physics, so the corresponding mathematical approach is used, with the necessary simplifications to obtain linear solutions [3, 4, 24, 32, 33, 34, 35]. Womersley's solution [3, 4, 24, 32] for thin-walled tubes is used for most of the analyses. For Womersley's solutions the assumptions are as follows:

i) The flow is laminar.

ii) The fluid is incompressible and has constant viscosity.

Under such conditions the Navier-Stokes equations in cylindrical co-ordinates are simplified to: [3, 4]

$$-\frac{\partial p}{\partial z} = \rho_o \left[\frac{\partial w}{\partial t} + u\frac{\partial w}{\partial r} + w\frac{\partial w}{\partial z}\right] - \mu\left[\frac{\partial^2 w}{\partial r^2} + \frac{1}{r}\frac{\partial w}{\partial r} + \frac{\partial^2 w}{\partial z^2}\right] \qquad \text{(IV.11)}$$

$$-\frac{\partial p}{\partial r} = \rho_o \left[\frac{\partial u}{\partial t} + u\frac{\partial u}{\partial r} + w\frac{\partial u}{\partial z}\right] - \mu\left[\frac{\partial^2 u}{\partial r^2} + \frac{1}{r}\frac{\partial u}{\partial r} + \frac{\partial^2 u}{\partial z^2} - \frac{u}{r^2}\right] \qquad \text{(IV.12)}$$

where: ρ_o = density of the fluid,

w = fluid velocity in the axial direction,

u = fluid velocity in the radial direction,

μ = dynamic coefficient of viscosity of the fluid,

r = radial coordinate,

z = axial coordinate,

and the continuity equation becomes:

$$\frac{\partial u}{\partial r} + \frac{u}{r} + \frac{\partial w}{\partial z} = 0 . \qquad \text{(IV.13)}$$

For the motion of the wall, it is assumed that:

iii) The axial and radial wall displacements ζ and ξ are considered small.

iv) The tube wall material is considered to be an isotropic and homogeneous solid, whose mechanical properties are linear.

v) Wall viscosity is not taken into account.

vi) The tube is considered a thin shell; i.e., $h/a_1 \leq 0.1$.

Incorporating the above assumptions and including the viscous drag at the fluid-wall boundary, the equations of motion for an element in the wall become: [33]

$$\frac{\partial^2 \zeta}{\partial t^2} = - \frac{\rho_o}{\rho} \frac{\nu}{ha_1} \left(\frac{\partial w}{\partial y} + a_1 \frac{\partial u}{\partial z}\right)_{y\,=\,1} + \frac{B}{\rho} \left(\frac{\partial^2 \zeta}{\partial z^2} + \frac{\sigma}{a_1} \frac{\partial \xi}{\partial z}\right) \qquad \text{(IV.14)}$$

$$\frac{\partial^2 \xi}{\partial t^2} = \frac{p}{h\rho} - \frac{B}{\rho} \left(\frac{\sigma \partial \zeta}{a_1 \partial z} + \frac{\xi}{a_1^2}\right) \qquad \text{(IV.15)}$$

where: ζ = inner wall displacement in the axial direction,

ξ = inner wall displacement in the radial direction,

$B = \frac{E}{1 - \sigma^2}$ relation of the elastic constants,

ν = kinematic coefficient of viscosity,

σ = Poisson's ratio,

ρ = density of wall material.

Further assuming that:

vii) Since we deal with motion where the terms u/c, w/c and na_1/c are small, and where u/w will be of the order of na_1/c, the non-linear terms are of the order $1/c$ and we can neglect the inertia terms for the first approximation.

The phenomenon is periodic so the functions can be expressed in terms of their respective Fourier components. Fourier analysis has proved to be a valuable technique for analysing periodic functions, therefore it was used for analysis of the pressure waves.

Before continuing, it is convenient to express the equation for the damped wave (Equation IV.4) in some different way that is suited to the foregoing analysis.

Introducing the dimensionless constants

$$X = \frac{c_o}{c_1} = \frac{b\ c_o}{n}$$

$$Y = \frac{a\ c_o}{n}$$

and

$$c = \frac{c_o}{(X - i\ Y)} \text{ the complex wave velocity}$$

these new expressions lead to the equality

$$int - \gamma z = in(t - \frac{z}{c}).$$

Therefore pressure, fluid velocity components and wall displacement components can be expressed as:

$$p = p_1 \; e^{in(t - \frac{z}{c})}$$

$$u = u_1 \; e^{in(t - \frac{z}{c})}$$

$$w = w_1 \; e^{in(t - \frac{z}{c})}$$

$$\xi = D_1 \; e^{in(t - \frac{z}{c})}$$

$$\xi = E_1 \; e^{in(t - \frac{z}{c})} \quad .$$

Where p_1, u_1, w_1, D_1 and E_1 are each the modulus of the respective complex variable.

As well as the assumptions of an isotropic thin-walled vessel, the following additional assumptions for the wall are necessary for the solution of the differential equations:

viii) ξ, ζ and their derivatives are small.

ix) the tube is cylindrical, uniform and infinitely long.

x) The density of the wall is very close to that of the fluid.

With the conditions and assumptions i) and x), Equations IV.11 to IV.15 are made simultaneous and linearized. The root, R, of these equations becomes: (for detailed procedure see [32] and [33]).

$$R = G \pm \sqrt{G^2 - (1 - \sigma^2)\, H}, \qquad \text{(IV.16)}$$

$$\left(\frac{R}{2}\right)^{\frac{1}{2}} = X - iY = \frac{c_o}{c} , \qquad \text{(IV.17)}$$

where
$$G = \frac{1 + \frac{1}{4} - \sigma}{1 - F_{10}} + \left(\frac{k}{2} + \sigma - \frac{1}{4}\right) ,$$

$$H = \frac{(1 + 2k)}{(1 - F_{10})} - 1 ,$$

$$k = \frac{h\rho}{a_1\ \rho_o} \approx \frac{h}{a_1} ,$$

and
$$F_{10} = \frac{2\ J_1\ (\alpha\ i^{3/2})}{\alpha\ i^{3/2} J_o\ (\alpha\ i^{3/2})} = 1 - M_{10}^{'}\ e^{i\ E_{10}^{'}} ,$$

where

$\alpha = a_1 \left(\frac{n}{\nu}\right)^{\frac{1}{2}}$, non-dimensional parameter that relates some properties of vessel and fluid, this parameter is widely employed throughout the solution of the equations.

and

$J_o\ (Z\ i^{3/2})$ Bessel function of the order zero and complex argument.

$J_1\ (Z\ i^{3/2})$ Bessel function of the order one and complex argument.

The last two expressions are generalized for any real variable, Z.

The expression $(1 - M_{10}^{'}\ e^{i\ E_{10}^{'}})$ is derived from the Bessel functions of complex argument written in terms of modulus and phase [25] as follows:

$$J_o\ (Z\ i^{3/2}) = M_o\ (Z)\ e^{i\theta_o\ (Z)}$$
$$J_1\ (Z\ i^{3/2}) = M_1\ (Z)\ e^{i\theta_o\ (Z)}$$

where (Z) represents (α) in this case. Therefore for in $(1 - M_{10}e^{i\,E'_{10}})$

$$M'_{10} = \sqrt{1 + h_{10}^2 - 2\,h_{10}\cos\sigma_{10}}$$

and

$$E'_{10} = \tan^{-1}\left(\frac{h_{10}\ \sin\ \sigma_{10}}{1 + h_{10}\cos\sigma_{10}}\right)$$

where

$$h_{10} = \frac{2\,M_1}{\alpha\,M_o}$$

and

$$\sigma_{10} = \frac{3\pi}{4} - \theta_1 + \theta_o \quad .$$

Tables for M_o (Z), θ_o (Z), M_1 (Z) and θ_1 (Z) have already been tabulated by McLachlan [25].

For a faster solution of (F_{10}) the second expression $(1 - M'_{10}\,e^{i\,E'_{10}})$ is recommended since M'_{10}/α^2 and E'_{10} have been tabulated by Womersley [32] for values of $\alpha \leq 10$. For values of $\alpha > 10$ the following simple asymptotic expansions can be used:

$$\frac{M'_{10}}{\alpha^2} = \frac{1}{\alpha^2} - \frac{\sqrt{2}}{\alpha^3} + \frac{1}{\alpha^4}$$

$$E'_{10} = \frac{\sqrt{2}}{\alpha} + \frac{1}{\alpha^2} + \frac{19}{24\,\alpha^2\sqrt{2}} \quad .$$

IV. 6 The movement of the fluid

The equation for the oscillatory velocity of the fluid in the axial direction, w, becomes,

$$w = \frac{p_1}{\rho_o c} \left\{ 1 + \eta \frac{J_o (\alpha\, i^{3/2} y)}{J_o (\alpha\, i^{3/2})} \right\} e^{in\,(t - z/c)} \tag{IV.18}$$

where $y = r/a_1$,

$$\eta = \frac{2}{x\,(F_{10} - 2\,\sigma)} - \frac{1 - 2\,\sigma}{F_{10} - 2\,\sigma} ,$$

$$x = \frac{R}{1 - \sigma^2} .$$

By integration, the average axial velocity across the tube, $\bar{w}$, is:

$$\bar{w} = \frac{p_1}{\rho_o c} \{1 + \eta\, F_{10}\}\, e^{in\,(t - z/c)} = \frac{p_1}{\rho_o c} M''_{10}\, e^{i\, E''_{10}}\, e^{in\,(t - z/c)} \tag{IV.19}$$

where: $M''_{10} = |1 + \eta\, F_{10}|$

E''_{10} = phase of $(1 + \eta\, F_{10})$

Values for M''_{10} and E''_{10} have been tabulated by Womersley [36].

For solving the middle term of Equation IV.9, a specific theory was also developed by Womersley [32] in order to find the relation of pulsatile flow in a rigid tube when the pressure gradient is known. This solution is simple since the movements of the tube wall are considered to be zero.

Considering the pressure at the upstream and downstream ends of the inextensible section (Fig. IV.1) as $p_2\ e^{int}$ and $p_3\ e^{int}$ respectively, the sinusoidal pressure gradient can be expressed as:

$$\frac{p_2 - p_3}{\Delta z}\ e^{int} = A'\ e^{int} \qquad \text{(IV.20)}$$

Therefore the Poiseuille equation applied to pulsatile flow can be expressed as:

$$\frac{\partial^2 w}{\partial r^2} + \frac{1}{r}\frac{\partial w}{\partial r} - \frac{1}{\nu}\frac{\partial w}{\partial t} = -\frac{A'}{\mu}\ e^{int} \qquad \text{(IV.21)}$$

the solution for the velocity in the axial direction becomes:

$$w = \frac{A'}{\rho in}\left(1 - \frac{J_o\ (\alpha\ y\ i^{3/2})}{J_o\ (\alpha\ i^{3/2})}\right) e^{int} \qquad \text{(IV.22)}$$

and the average axial velocity

$$\overline{w} = \frac{A'\ a_1^2}{\mu\ \alpha^2}\ M'_{10}\ e^{i\ (nt + E'_{10})} = \frac{p_2 - p_3}{\Delta z\ \ \rho_o}\ M'_{10}\ e^{i\ (nt + E'_{10})} \qquad \text{(IV.23)}$$

At this point it is necessary to make a close observation of the equations of the fluid movement in the elastic and inextensible sections, Equations IV.19 and IV.23. In the case of the elastic tube, Equation IV.19, the velocity is a function of time, radial position and also axial position, therefore at a given instant the velocity profiles are different along the vessel. Regarding the flow in the inextensible section the conditions under which Equation IV.23 was formulated yielded a velocity profile that is a function of time and radial position only but at a given instant the profile is the same all along the inextensible tube; i.e., the phase velocity tends to be infinite. This can be considered as a good approximation for short inextensible sections since in current experiments it was observed that phase velocities in elastic tubes were 4 - 6% of that of the velocities in inextensible tubes. What was previously explained can be visualized better with the help of Fig. IV.4. Equation IV.9 can now be solved.

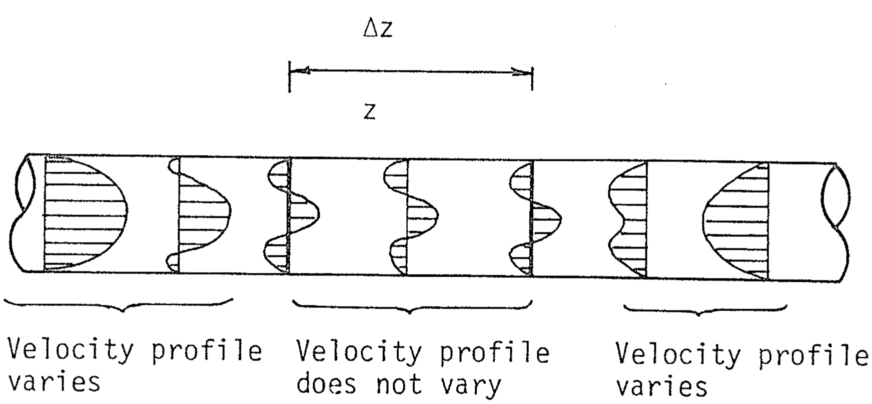

Fig. IV.4: Velocity profile in elastic and inextensible sections of tube at a given time.

IV.6.1 First term of equation IV.9

In this case the flow is in an elastic section and two pressure waves are present, the incident wave ($p_1 e^{in(t - z/c)}$) travelling in the positive direction of z and the reflected wave ($p_4 e^{in(t + z/c)}$) travelling in the negative direction of z, therefore the pressure, p, becomes:

$$p = p_1 e^{in(t - z/c)} + p_4 e^{in(t + z/c)} . \tag{IV.24}$$

Since linearity has been assumed, the flow effects of the retrograde wave are simply added to the forward flow wave. Therefore the average flow, $\bar{w}$, in the left elastic section of the tube shown in Fig. IV.1 becomes:

$$\bar{w} = \frac{p_1}{\rho_0 c}(1 + \eta F_{10}) e^{in(t - z/c)} + \frac{p_4}{\rho_0(-c)}(1 + \eta F_{10}) e^{in(t + z/c)}$$

$$= \frac{p_1 e^{-iz/c} - p_4 e^{iz/c}}{\rho_0 c} M''_{10} e^{i(E''_{10} + nt)} \tag{IV.25}$$

IV.6.2 Second term of equation IV.9

In this case the flow is within an inextensible section, therefore:

$$\bar{w} = \frac{p_2 - p_3}{\Delta z\, \rho_0} M'_{10} e^{i(E'_{10} + nt)} \tag{IV.26}$$

IV.6.3 <u>Third term of equation IV.9</u>

Here the flow is in an elastic section without wave reflection.

$$\bar{w} = \frac{p_3}{\rho_o c} M''_{10} e^{i E''_{10}} e^{in(t - z/c)} \tag{IV.27}$$

Since the tubes are of the same interior diameter (2.5 cm), the value of α is the same for the three sections, and since the phase velocity in the rigid section is very high compared to that in the elastic tube, the flow wave does not suffer appreciable change in phase within the rigid section (see Fig. IV.6), therefore for the flow events it can be considered that $\partial w/\partial z = 0$ within the inextensible section.

Substituting Equations IV.25, IV.26 and IV.27 in Equation IV.9 and for $z = 0$:

$$\frac{p_1 - p_4}{\rho_o c} M''_{10} e^{i E''_{10}} = \frac{p_2 - p_3}{\Delta z \ \rho_o} M'_{10} e^{i E'_{10}} = \frac{p_3}{\rho_o c} M''_{10} e^{i E''_{10}} \tag{IV.28}$$

Since for continuity of pressure $p_1 + p_4 = p_2$ the relation between reflected and incident wave (P_4/P_1) becomes:

$$\frac{p_4}{p_1} = \left\{ 1 + \frac{2c}{in \ \Delta z} \frac{M'_{10}}{M''_{10}} e^{i (E'_{10} - E''_{10})} \right\} \tag{IV.29}$$

Equation IV.29 solves for the pressure wave reflection factor p_4/p_1 when an inextensible insertion of length Δz is placed in a thin-walled elastic tube of infinite length, filled with viscous fluid, when the inner radius of insertion and tube are the same and when the constant $\alpha = a_1 \sqrt{n/\nu}$ and the complex wave velocity $c = c_0/(X - i\ Y)$ are known.

The development of a theory for wave reflection at inextensible insertions in elastic tubes is a very complicated task since the phenomenon is not well known, the variables are numerous and linearization of equations could induce deviations of the results. The above described theory was the only one available and was compared with the experimental results in order to know whether the already available theory would be satisfactory or further development would be necessary. Comparison of such results is done in the corresponding Chapter V Section: Results and Discussion

IV.7 Valve comparison

Comparison of the hydrodynamic efficiency of the Starr-Edwards and Bjork-Shiley prosthetic heart valves is obtained by measuring the pressure energy lost by the stroke volume of fluid when passing through the valves in one systole. The valve that yields the lower losses is obviously the most efficient.

Since the pump and elastic tube are horizontal and closed ducts, the total energy, H_1, of a stroke volume in the tube upstream the valve can be expressed in terms of the Bernoulli's equation

$$H_1 = \frac{\overline{w}_1^{\,2}}{2} m + \frac{\overline{p}_1}{\rho_0} m \ , \qquad \text{(IV.30)}$$

and the total energy, H_2, of the stroke volume in the tube downstream, the valve is

$$H_2 = \frac{\overline{w}_2^{\,2}}{2} m + \frac{\overline{p}_2}{\rho_0} m \, , \tag{IV.31}$$

where $\overline{w}_1$ and $\overline{w}_2$ are the mean velocities of the fluid in the upstream and downstream tubes respectively, $\overline{p}_1$ and $\overline{p}_2$ are the mean pressures of the fluid in the upstream and downstream tubes respectively and, m, is the mass of the stroke volume.

Therefore the expression for the lost energy in the valves, H_{1-2}, becomes:

$$H_{1-2} = H_1 - H_2 \, , \tag{IV.32}$$

thus the lost energy in each valve, Starr-Edwards and Bjork-Shiley can be compared and the results be related to their hydrodynamic efficiency.

IV.8 Experimental procedure

From the objectives for this investigation as stated in the introduction and the nature of the phenomena to be investigated as described in the development of the equipment and the development of the theory, it can be seen that the investigation consists of several distinct experiments designed to give particular information on the experimental system characteristics and the flow characteristics within the system. The measurement of the pressure wave reflection characteristics and the performance of the tube simulating the artery required an experiment to measure the reflection of short trains of waves as well as experiments to measure wave reflections with forward flow. The determination of prosthetic valve performance required the measurement of the pressure wave in the elastic tube at specific locations relative to the valve. And the determination of arterial implant behaviour related to the pressure wave reflections with forward flow required the measurement of the pressure wave at specific locations relative to the simulated arterial prosthesis. The following section describes the experimental procedures in more detail.

IV.8.1 Wave reflection with forward flow

Physiological flow was induced in the apparatus with the cam driving the pump piston and with the elastic tube No. 2, as shown in Fig. III.1 but without an inextensible insertion. Forward flow experiments were not performed in tube No. 1 because the cam was designed for flow in the ascending aorta and diameter of tube No. 1 was too small for such flow. The velocity of the variable speed motor was calibrated with a stop watch and three different flow frequencies were obtained in the pump, 0.83, 1.2 and 1.5 Hz (50, 72 and 90 beats/minute), in order to have data related to the three states of the heart beat, bradycardia, normal at rest and tachycardia. The pressure wave was measured 1.5 m downstream from the valve and recorded on the X-Y recorder. The pressure wave obtained under these circumstances was considered as the "normal", see Figs. V.1, V.2 and V.3. It was expected that the reciprocating pump, due to its rigidity and geometry could be a source of wave reflection as well as the discharge end of the elastic tube, therefore the convenient position for placing the inextensible insertions to be tested was near the midway of the 4 m long elastic tube so the reflected waves from pump and discharge end would be minized by damping before reaching the inextensible insertion. It is known that the high frequency waves are more affected by damping [3] therefore, when it was desired to detect the reflected waves from a rigid insertion, it was considered convenient to place the pressure transducers 10 cm upstream of the inextensible insertion.

For the next experiment, the round rigid insertion of Jayflex was placed in the system by overlaping the elastic tube on the rigid insertion and securing it with rubber bands, see Fig. III.1 and III.5. Their upstream end was located 1.6 m from the valve. Flow was induced for the three frequencies specified above, and the pressure waves that were produced were also recorded on the X-Y recorder and compared with the "normal" wave. A similar procedure was followed using the elliptic Jayflex insert. See Figs. V.1, V.2, and V.3.

IV.8.2 Reflection of short trains of waves

The principle of short trains of waves can be used when it is desired to measure the relation between an incident and a reflected wave (the Reflection Factor) due to a discontinuity in the elastic tube, in this case at an insertion. Fig. IV.5 illustrates the case of the pressure wave which travels downstream in an elastic tube, passes a pressure transducer where it is measured, continues travelling and a partial reflection (with a phase shift of 180°) is generated at an inextensible insertion. The reflected wave travels upstream and is measured as it passes the pressure transducer.

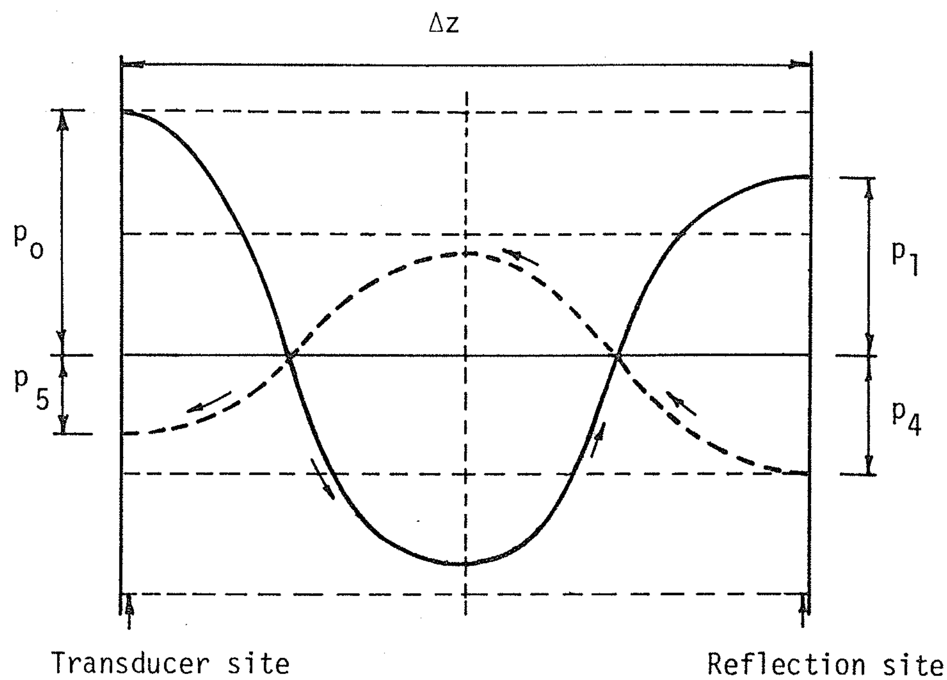

Fig. IV.5: Diagram of the incident wave and the reflected wave.

Fig. IV.6 is a diagram of the arrangement of the apparatus for generating and measuring amplitudes of incident and reflected waves without interference of wave superposition using the principle of the short train of waves and when the damping constant is known. A short train of waves is generated in the pump and travels downstream. If the value of its amplitude at the transducer site is 2 p_o, it is attenuated by the time it gets to the reflection site to an amplitude of 2 p_1 = 2 p_o $e^{-a\Delta z}$. Also, if the amplitude of the reflected wave at the transducer site is 2 p_5 it has been attenuated during its travel from the reflection site where its amplitude was 2 p_4 = 2 p_5 $e^{a\Delta z}$. Therefore the

Reflection Factor is:

$$\frac{p_4}{p_1} = \frac{p_5}{p_o} e^{2\, a \Delta z} \qquad \text{(IV.33)}$$

When physiological flow is induced, the pressure wave is formed by many wave components of different frequencies, amplitudes and phases, as observed in the Fourier analysis. Therefore it is a very complicated task to try to identify the origin and magnitude of the reflected waves. Using the technique of the Short Trains of Waves described in Section IV.3.0, it was possible to determine, at least, approximately, the values of the reflection factor at rigid insertions.

The pump piston was coupled to the electro-magnetic excitor, as shown in Fig. III.3, to produce sinusoidal flow waves that would induce sinusoidal pressure waves in the elastic tube. The test signals had to be of high enough frequency so that they could not overlap each other and at the same time the frequencies should be as close as possible to the physiological frequencies. Under such experimental criteria it was chosen to test with 10, 15, 20 and 25 Hz. These tests would yield a curve with 4 points and such a curve could be extrapolated to the physiological frequency; i.e., 0.8 to 6 Hz. Tube No. 1 was tested first. The first step was to measure the phase velocity, placing 2 pressure transducers in the tube separated by a 2 m section. A short train of waves was produced and the response recorded on the storage oscilloscope. Knowing the distance and the time delay for the signal to travel from one pressure transducer to the other, the phase velocity was deduced. Afterwards the aluminum inextensible insertion and pressure transducer were placed at 2.5 and 1.0 m from the pump respectively. With this spacing the incident and reflected waves were clearly separated when stored in the oscilloscope. Refer to Figs. III.3 and IV.6.

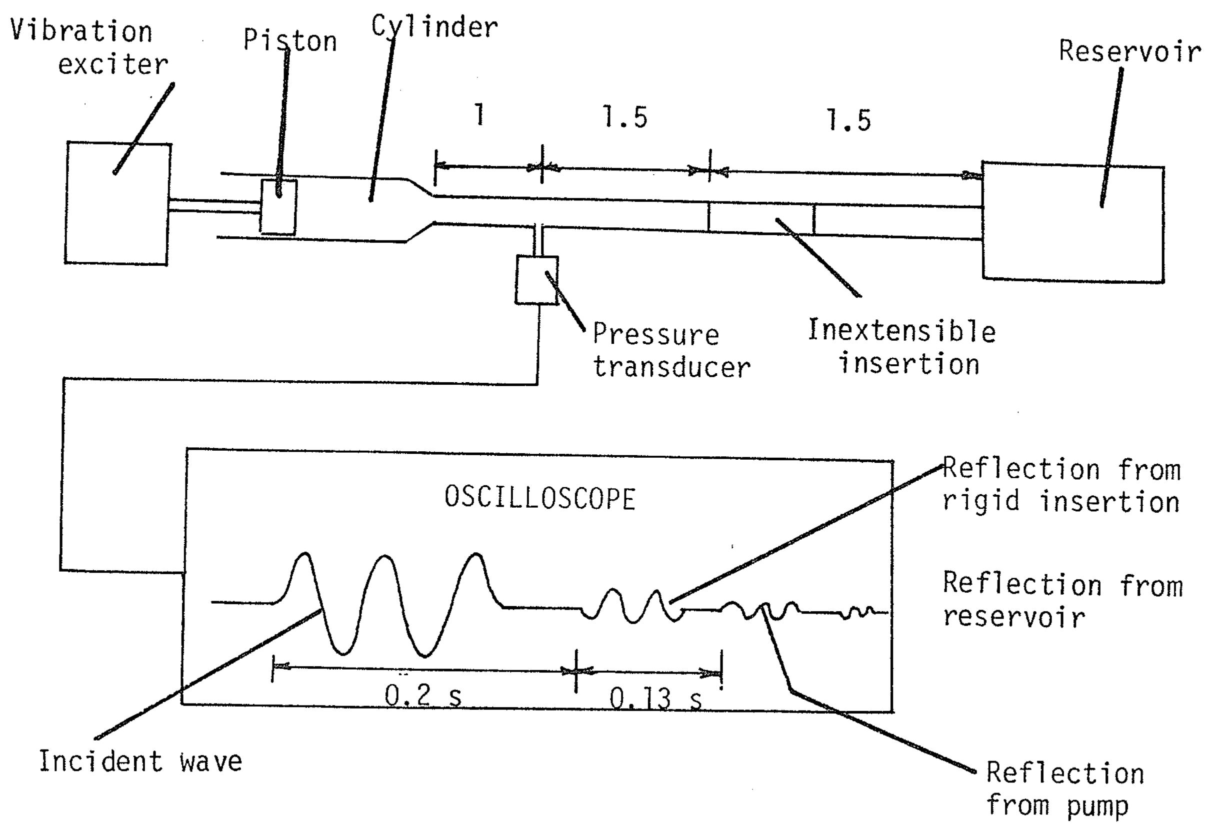

Fig. IV.6: Sample of the oscilloscope reading for a train of 3 sinusoidal waves with phase velocity 15 m/s. Dimensions in meters.

Amplitude of the generated waves was adjusted until a clear signal was obtained and trains of three sinusoidal waves were produced at 10, 15, 20 and 25 Hz. The resultant incident and reflected waves were stored in the oscilloscope and photographed for measuring the corresponding amplitudes.

Using Klip's theory, Equation IV.7, the damping constant for the tube-fluid system was evaluated. Once the values of the damping constant and amplitudes of the incident and reflected waves at the transducer site were known, the Reflection Factor was calculated using Equation IV.33. These experimental values for the Reflection Factor were compared with the theoretical values obtained using Womersley's theory, Equation IV.29. A similar experiment was set up for tube No. 2 (Neoprene compound) but it was not possible to detect clear reflected waves. It was supposed that the reflected waves of such frequencies were so considerably damped by the neoprene compound that after travelling 1 m upstream they had almost totally dissipated.

IV.8.3 Valve comparison

Comparison of the hydrodynamic efficiency and pulse pressure waves produced by the Starr-Edwards and the Bjork-Shiley prosthetic heart valves was performed in order to determine the differences that could be of negative effect for the user. Pressure measurements were taken simultaneously upstream and downstream of the valves in order to evaluate the pressure energy losses in the fluid during systole. Fourier analysis of the resulting pressure waves was employed to determine the effects of the components on each side of the valves.

Since it was not possible to connect a pressure transducer in the pump body, a 40 cm long rigid tube of 2.5 cm of inside diameter was connected as an extension of the pump, as shown in Fig. IV.7. One pressure transducer was connected to the pump extension and the other to the elastic tube.

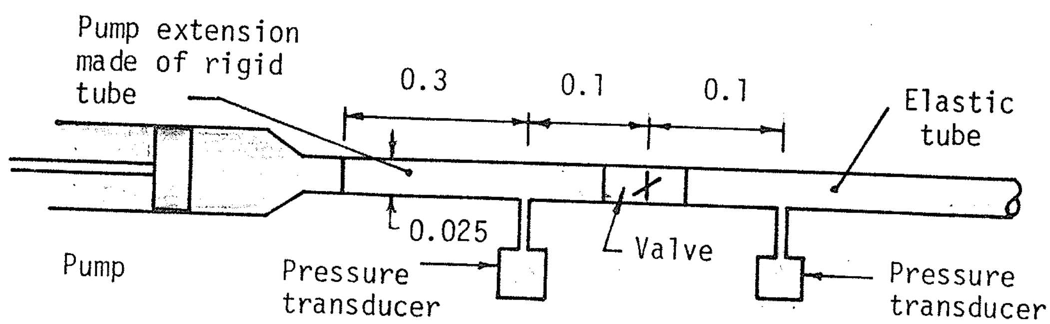

Fig. IV.7: Test for valve efficiency. Dimension in meters.

Both valves were tested with forward flow induced by the pump at 72 beats/minute. Readings of the pressure waves as obtained in the pressure transducers were recorded using the X-Y recorder and are shown in Fig. V.4. Pressure energy losses were calculated using

Equation IV.32 and the Fourier analysis was also obtained for each pressure wave. Finally, comparison of the hydrodynamic efficiency and pressure wave components for each valve were performed. Comments on such results are made in Chapter V.

CHAPTER V RESULTS AND DISCUSSION

The objectives stated in the Introduction regarding the study of negative hydrodynamic effects of the arterial grafts with the possible solution of the elliptic insertion, and the comparison of prosthetic heart valves to determine what hydrodynamic characteristics of the valve that could be helpful or harmful for the host organism have been analysed. A model of circulation was built for in-vitro experimenting with the prosthesis, and the available theory for analysing the phenomena has been studied. Results of the experiments that were performed based on the available theory are included in this section. The usefulness and reliability of such theoretical and experimental results is also discussed.

V.1 Apparatus

V.1.1 Simulated heart system

The function of the variable speed motor was satisfactory. It reproduced the desired speed when the control dial was set to the calibrated positions. The speed reduction of 16:1 between motor and cam plus the flywheel in the transmission were sufficient to avoid jerk. Therefore even though the load on the cam had sudden variations, the rotation of the cam was uniform. The rubber bands provided constant contact between follower and cam for many hours of work. When the rubber band had fatigued and allowed discontinuity of contact, it was immediately made apparent by a hammering sound on the cam. New bands were then installed. Cam wear was hardly detectable even in the areas of maximum pressure.

Pump function was also satisfactory. The piston dynamic sealing provided zero leakage and reduced piston-cylinder friction. The Teflon bearing for the piston rod also produced low friction and the result was a smooth movement of the piston.

The flow pattern achieved in the apparatus was similar to the physiological, but it was only possible to obtain frequencies of 100 beats/minute instead of the maximum desired, specified as 200 beats/minute in Table III.1 because the cam would produce exaggerated vibration beyond 100 beats/minute.

The artificial heart valves used for the pump outlet were the ideal parts for the experimental purposes, because they have been specifically designed to work intermittently. When first experimenting it was thought that the pump inlet valve should also be a prosthetic valve, but after testing with the ordinary one-way poppet valve, it proved to have very short closing and opening delays (in the same range as the prosthetic valves) and since the inlet flow was not the object of investigation, the poppet valve was considered sufficient.

V.1.2 Simulated aorta

Working with the elastic tube No. 1 (pure latex) was very convenient because the viscoelastic properties of the latex are well known. Unfortunately it was not possible to obtain latex tubes in the diameter required for tube No. 2. The neoprene compound tube was used as tube No. 2 but the viscoelastic properties of the wall were not known. It was therefore not possible to fully understand why high frequency wave reflections from the rigid insertion were not detected at 1.5 m upstream from the reflection site. Due to lack of space, the horizontal length of both tubes had to be 4 m which was not long enough to completely damp the unwanted reflected waves from the pump and discharge end at the middle length of the tube.

Thus when experimenting with the elastic tubes, wave reflection from pump and discharge end were present in all sections of the tubes, therefore the condition of no wave reflection was not satisfied and the analysis of the flow-pressure events became very complicated. Under the conditions above described the resultant pressure wave with physiological flow, as measured 1.5 m downstream the valve in tube No. 2 and for the frequencies 52, 72 and 90 beats/minute is shown in Figs. V.1, V.2 and V.3. Comparison may be made with the physiological pressure wave at 72 beats/minute shown in Fig. II.3. The detailed characteristics of the two tubes used to simulate the aorta are given in Table V.1.

	No. 1 Pure Latex	No. 2 Neoprene Compound
Inside radius, a_1	0.635 cm	1.12 cm
Outside radius, a_2	0.875 cm	1.22 cm
Thickness, h	0.24 cm	0.10 cm
Length, ℓ	4 m	4 m
Wall density, ρ	0.92 gr/cm^3	0.90 gr/cm^3
$\gamma' = n\ \mu_{vi}/\mu_s$	≈ 0.02	-
Lame's elasticity parameters		
$\mu_s = E/\{2\ (1 + \sigma)\}$	5.5×10^6 dyn/cm^2	-
$\lambda_s = E\ \sigma/\{(1 + \sigma)\ (1 - 2\sigma)\}$	$124\ \mu_s$	-
where n = angular velocity E = modulus of elasticity σ = Poisson's ratio.		
Phase velocity, c_1, when filled with a mixture of water and glycerine of density 1.05 gr/cm^3 and viscosity 3.8 CP at 22°C.	1400 cm/s	1500 cm/s
Modulus of elasticity, E, in the physiological pressure range.	16 - 17 Kg/cm^2	11 - 14 Kg/cm^2

Table V.1: Physical properties of the elastic tubes.

The inextensible inserts displayed the behaviour expected of them. The aluminum sleeve for tube No. 1 did not give any problems. The round Jayflex insertion for tube No. 2 did not present appreciable distension when forward flow was induced, therefore it behaved as rigid. The elliptic Jayflex insertion showed a clear change in eccentricity during systole, increasing its cross-section area and thus allowing larger flow area. Deformation of the major and minor axis of the elliptic insertion when subjected to static pressure is shown in Fig. B.8 of Appendix B.

The elevated tank provided a reliable hydrostatic pressure in the tubes, equivalent to the diastolic aortic pressure. Since the tank altitude was variable, it also worked as a reference for calibrating pressure transducers and electronic equipment.

V.1.3 Electronic equipment

The performance of the pressure transducers was satisfactory, but their pressure range, 0 - 3.5 Kg/cm^2, was rather large compared with the working range 1 - 1.27 Kg/cm^2, therefore the output signal variation range was quite small and the output required amplification to match the X-Y recorder and oscilloscope sensitivities. Also the X-Y recorder and oscilloscope picked up noise when working at their maximum sensitivities therefore, in order to obtain satisfactory performance a preamplifier with noise filtering was necessary. The vibration exciter proved to be a good device to produce short trains of pressure waves in the elastic tubes for frequencies between 10 and 25 Hz. The pressure waves initiated by the exciter, called waves, were distorted to some extent, see Figs. B.10

and B.11. The lack of uniformity in the pressure waves produced by the exciter was due to the lack of appropriate rigidity of the frames that supported the exciter and the pump.

V.2 Wave reflection with forward flow

V.2.1 Elastic tube without insertions

For the reasons stated in Section IV.8.1, the pressure transducer was placed 1.5 m downstream from the valve. At this point the diastolic pressure would fall below the 80 mm Hg hydrostatic pressure, because when the piston starts its backward displacement the pressure in the pump drops below atmospheric pressure (see Fig. V.4) but the fluid in the elastic tube still has the forward momentum transfered by the piston therefore there is a tendency to "empty" the elastic tube thus, the pressure in the elastic tube drops below the 80 mm Hg hydrostatic pressure. The time-pressure curve obtained under the above described conditions is quoted as the "normal" and for the three experimental rates 50, 72 and 90 beats/minute is shown in Figs. V.1, V.2 and V.3 where they are also compared with the curves obtained when the insertions were placed. The pressure wave peaks obtained when the inextensible insertions were placed were 13 - 28% higher than the pressure peak of the "normal" curve which was obtained without insertions.

V.2.2 Inextensible insertions

The round inextensible insertion proved to modify the pressure pattern with higher systolic peaks than the "normal" in all frequencies. When testing with the elliptic insertion the systolic pressure peaks were between 7 and 8% (based on the "normal" value) lower than with the round insertion when working at 72 and 90 beats/minute but it did not show significant effect at 50 beats/minute. The elliptic insertion did not reduce the systolic peak to the "normal" value.

The above described quantitative effects with the elliptic insertion agree with what was expected. In response to the pressure the elliptic insertion approached a circular configuration allowing greater flow cross-section that reduced the pressure peak but the discontinuity of material represented by the insertion material could not be overcome. Thus the expected effect in this respect was experimentally satisfied, but not enough theory of pulsatile flow and wave reflection in elliptic tubes has been developed to make possible theoretical evaluation of the experiment.

Comparison of the pressure waves for the three cases, "normal", round insertion and elliptic insertion, and for the three beat rates are shown in Figs. V.1, V.2 and V.3. Table V.2 gives numerical comparison of systolic pressure peaks due to the insertions compared to the normal wave.

	Overpressure respect to the "normal" when the inextensible insertions were placed, expressed in percent and for the three beat rates $$o/o = \frac{p_A - p_B}{p_B} \times 100$$ p_A = maximum pressure above diastolic with inextensible insertions p_B = maximum pressure above diastolic "normal"		
Insertion	52 beats/min	72 beats/min	90 beats/min
Round	19%	28%	21%
Elliptic	19%	21%	13%

Table V.2: Comparison of systolic pressure peaks.

V.3 Fourier analysis of pressure waves with forward flow

In order to be able to determine the individual role of the components of the pressure waves and recognize those components that take part in the rise of the pressure peaks when inextensible insertions are installed in the elastic tube, Fourier analysis of the pressure waves was performed for the three cases; "normal", with round insert and with elliptic insert. Each were tested at the three frequencies 52, 72 and 90 beats/minute. Values of the Fourier components for all the cases above specified in terms of the mean components, real parts and imaginary parts are shown in Tables C.4, C.5 and C.6 of Appendix C. The same components in terms of magnitude and phase in the complex plane are shown in Figs. B.12, B.13 and B.14 of Appendix B. The reconstruction of the pressure waves from their sinusoidal components oscillating on the mean term, for the "normal" round and elliptic insertion at 72 beats/minute are shown in Figs. B.15, B.16 and B.17 of Appendix B. From Figs. B.12, B.13 and B.14 it is observed that the insertions induced changes in magnitude and phase. At 52 beats/minute the changes of magnitude and phase are similar for both insertions, at 72 beats/minute the changes in phase still are similar but the round insertion shows larger magnitudes for the first and second harmonics. At 90 beats/minute the phase change due to the inextensible insertions is more noticeable and for the first harmonic the magnitudes are smaller than the "normal" one but for the second harmonic of the wave, the magnitudes for the inextensible insertions are significantly larger than those for the "normal" case. All the changes described are the result of the change of impedence that the inextensible insertions produce in the elastic tube. The reader interested in values of such changes is referred to the Figs. B.12, B.13 and B.14.

From the reconstruction of the pressure waves at 72 beats/minute shown in Figs. B.15, B.16 and B.17, it is observed that the increase of the pressure peaks with the insertions is mostly due to the large amplitudes of the first and second harmonics of such pressure waves. It is thus possible to quantify the effects of the extensible oval insertion relative to the inextensible insertions, noting that the oval insertion is 7 - 8% better (based on the "normal" value) than the inextensible insertions and that for higher pulse rates the percentage of improvement increases.

V.4 Wave reflection of short trains of waves

Experimental values of the reflection factor at rigid insertions were obtained in tube No. 1 using the aluminum sleeve as a rigid insertion. Using the technique of the short trains of sinusoidal pressure waves, the reflection factor was calculated for 4 frequencies: 10, 15, 20 and 25 Hz and a Frequency-Reflection Factor curve, Fig. B.9 of Appendix B, was obtained. This curve may be extrapolated to the physiological frequencies; i.e., 0.8 - 6 Hz as shown in the same Fig. B.9.

The pressure waves obtained were not perfectly sinusoidal (see Figs. B.10 and B.11 of Appendix B) mostly due to lack of rigidity of the frames that supported the electromagnetic exciter. Another source of pressure wave distortion was the geometry of the pump. Particular difficulty was faced when testing with 10 Hz because generation of more than one wave at this frequency would produce wave superposition of incident and reflected waves, therefore a single wave had to be produced. However, the average of the amplitudes of each train of pressure waves, as detected by the pressure transducer and stored in the oscilloscope, was used for calculation of the reflection factor at the rigid insertion. Figs. B.10 and B.11 show the shape of the incident and reflected pressure waves in the elastic tube at the transducer site. These figures also show the oscilloscope sensitivities in mV/cm for the amplitudes and in ms/cm for the sweep velocity. The oscilloscope was calibrated with the elevated tank to give 720 mV/100 cm H_2O for the pressure values. With the information above described, the amplitudes of the incident and reflected waves were evaluated by direct measurement from the Figs. B.10 and B.11.

The damping constant, that was frequency dependent, was evaluated using Equation IV.7,

$$K^2 = \frac{\rho_o \, n^2}{(1 + i \, \gamma')E} \left(\frac{N}{I_v - I_o} - \frac{N'}{N}\right) \tag{IV.7}$$

and the experimental values of the Reflection Factor were calculated using Equation IV.33,

$$\frac{P_4}{P_1} = \frac{P_5}{P_o} \, e^{2 \, a \Delta z} \quad . \tag{IV.33}$$

Table V.3 summarizes the experimental values of the Reflection Factor and the information that was previously necessary and has been described above.

Frequency (Hz)	Damping Constant, a. (cm^{-1})	Amplitude of incident wave, p_0. (cm H_2O)	Amplitude of reflected wave, p_5. (cm H_2O)	Reflection Factor $\frac{p_4}{p_1}$
10	-0.00155	236	56	0.38
15	-0.00180	79	20	0.43
20	-0.00210	66	15	0.43
25	-0.00179	72	20	0.46

Table V.3: Experimental results of the Reflection Factor for the tube No. 1 with the 15 cm long inextensible sleeve.

Theoretical results for the Reflection Factor p_4/p_1 were also calculated using Equation IV.29,

$$\frac{p_4}{p_1} = \left\{ 1 + \frac{2\ c}{in\ \Delta z} \frac{M'_{10}}{M''_{10}} e^{i\ (E'_{10} - E''_{10})} \right\}^{-1} \qquad \text{(IV.29)}$$

The theoretical and experimental results for the Reflection Factor in tube No. 1 are compared in Fig. B.9 of Appendix B. There is an obvious disagreement between experimental and theoretical results. This divergence may arise from the fact that Womersley's theory was developed for thin tubes with a relation of $h/a_1 \leq 0.1$ and tube No. 1

has a relation $h/a_1 = 0.38$. The theory does not account for viscous components of the tube wall, but it seems to be of minor consequences [4]. Unfortunately no other theory related to wave reflection at rigid insertions was available.

V.5 Prosthetic heart valves

Comparison of the hydrodynamic efficiency of the Starr-Edwards and Bjork-Shiley prosthetic heart valves was performed on the basis of the comparison of the energy lost by the stroke volume during one ejection period (Equation IV.32) while testing each valve separately at a frequency of 72 beats/minute. The analysis of the Fourier components of the pressure waves generated by each valve was also performed.

From the pressure waves obtained (see Figs. IV.7 and V.4) at 2 points along the tube, one 10 cm upstream the valve and the other 10 cm downstream the valve, graphical integration methods yielded the mean pressure difference between the 2 points during the ejection period, $P_1 - P_2$, for the Starr-Edwards valve.

$$P_1 - P_2 = 8910 \text{ dyn/cm}^2 \text{ (6.68 mm Hg)},$$

and for the Bjork-Shiley valve,

$$P_1 - P_2 = 4210 \text{ dyn/cm}^2 \text{ (3.16 mm Hg)}.$$

The diameter of the elastic tube (2.24 cm), when under the physiological pressure, would become the same as that of the pump extension (2.5 cm), see Fig. IV.7. Therefore the mean fluid velocity before and after the valve, could be considered the same and Equation IV.32 reduces to

$$H_{1-2} = \frac{p_1 - p_2}{\rho_0} m = (p_1 - p_2) \forall$$

where $\forall$ is the stroke volume of the pump, 79 cm^3, and the lost energy in each valve during ejection was, for the Starr-Edwards valve

$$H_{1-2} = 704000 \text{ dyn.cm}$$

and for the Bjork-Shiley

$$H_{1-2} = 333000 \text{ dyn.cm} \quad .$$

Higher energy losses in the fluid passing through the valve mean higher shear stress and possibly turbulence. Shear stresses in the blood in the order of 40000 dyn/cm^2 produce hemolysis (trauma to the blood cells) [12]. Turbulence in the blood flow induces embolization [16]. Determination of whether the shear stresses in the fluid exceed the critical value when passing through the prosthetic valves is beyond the scope of this investigation, but comparative results of the amount of damage to the blood cells and the survival of the patients using one valve or the other indicates that the hydrodynamic design of the Bjork-Shiley valve is more acceptable to the host organism than that of the

Starr-Edwards [11, 12, 13, 18, 27]. Bjork [8], testing prosthetic heart valves in a pulse duplicator proved that turbulence was fully developed in the circulating fluid when passing by a Starr-Edwards valve, and that most of the flow was laminar when passing by a Bjork-Shiley valve. Hemolysis and embolization have a negative effect on the recovery of the valve user and therefore are contrary to the purpose of the valve implantation. The reader interested in a detailed description of the negative effects of hemolysis and embolization is referred to Fernandez [11], Ferry [12], Fraser [13] and Kastor [18].

The Fourier components of the pressure waves from Fig. V.4 are shown in Table C.7 of Appendix C, where the most significant components are included in terms of their mean part, harmonic number and real and imaginary parts. The inertial forces induced by the larger mass of the Starr-Edwards valve occluder (the mass of the Bjork-Shiley occluder is 14% of that of the Starr-Edwards occluder) and the wave reflection that takes place at the obstacle represented by the ball occluder are indicated by the changes in magnitude and phase observed in the Fourier components of the Starr-Edwards valve.

From the evaluation of the energy losses and from the changes in the phase and magnitude of the pressure wave components, it is clear that mechanically the Bjork-Shiley valve is superior to the Starr-Edwards. Although the wave shapes 'in vivo' could be quite different from those of the simulation system used here, the relative effects of the respective valves on pressure-wave components and flow will remain in the order of those measured here.

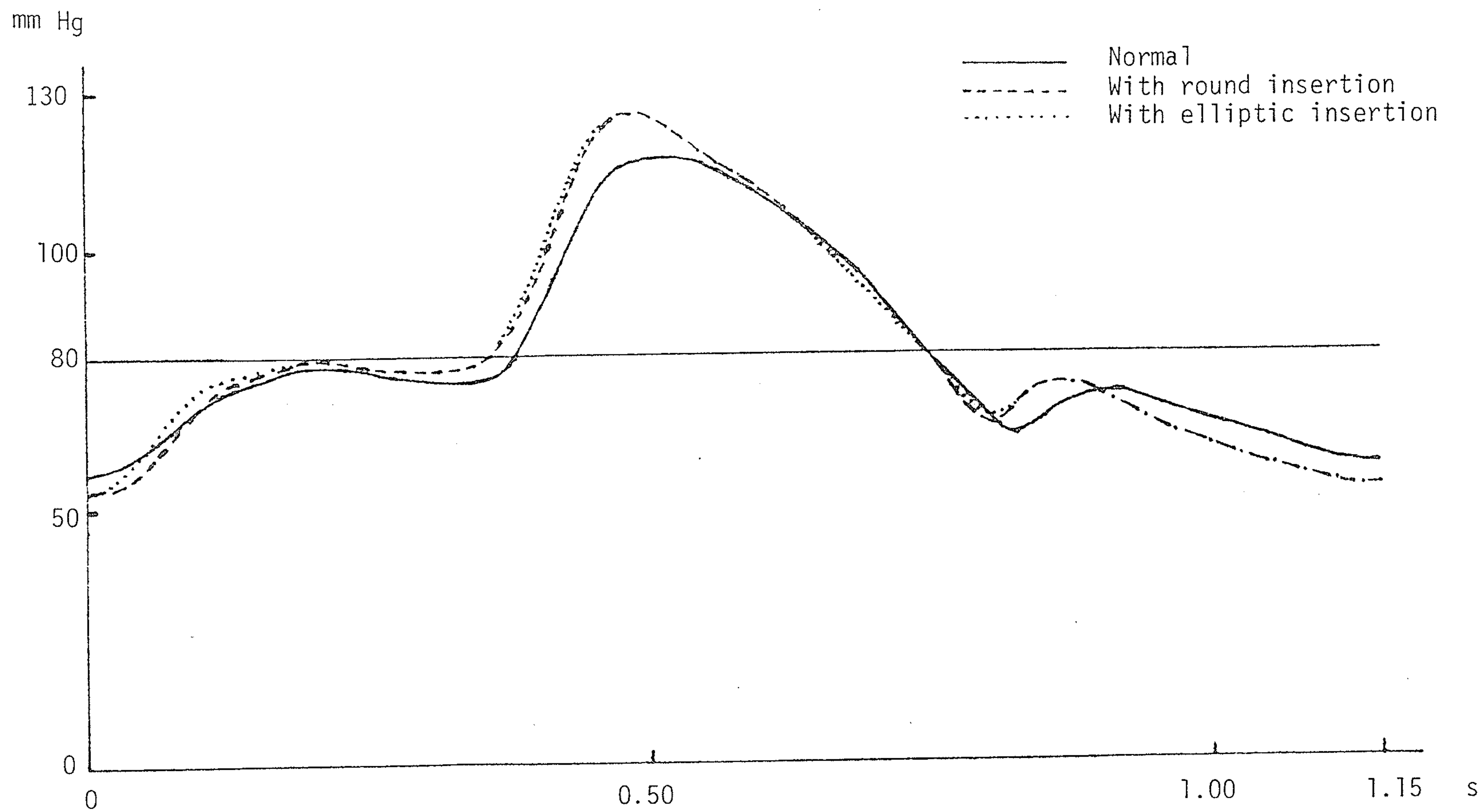

Fig. V.1: Comparison of the pressure waves obtained with forward flow at 52 beats/minute in tube No. 2.

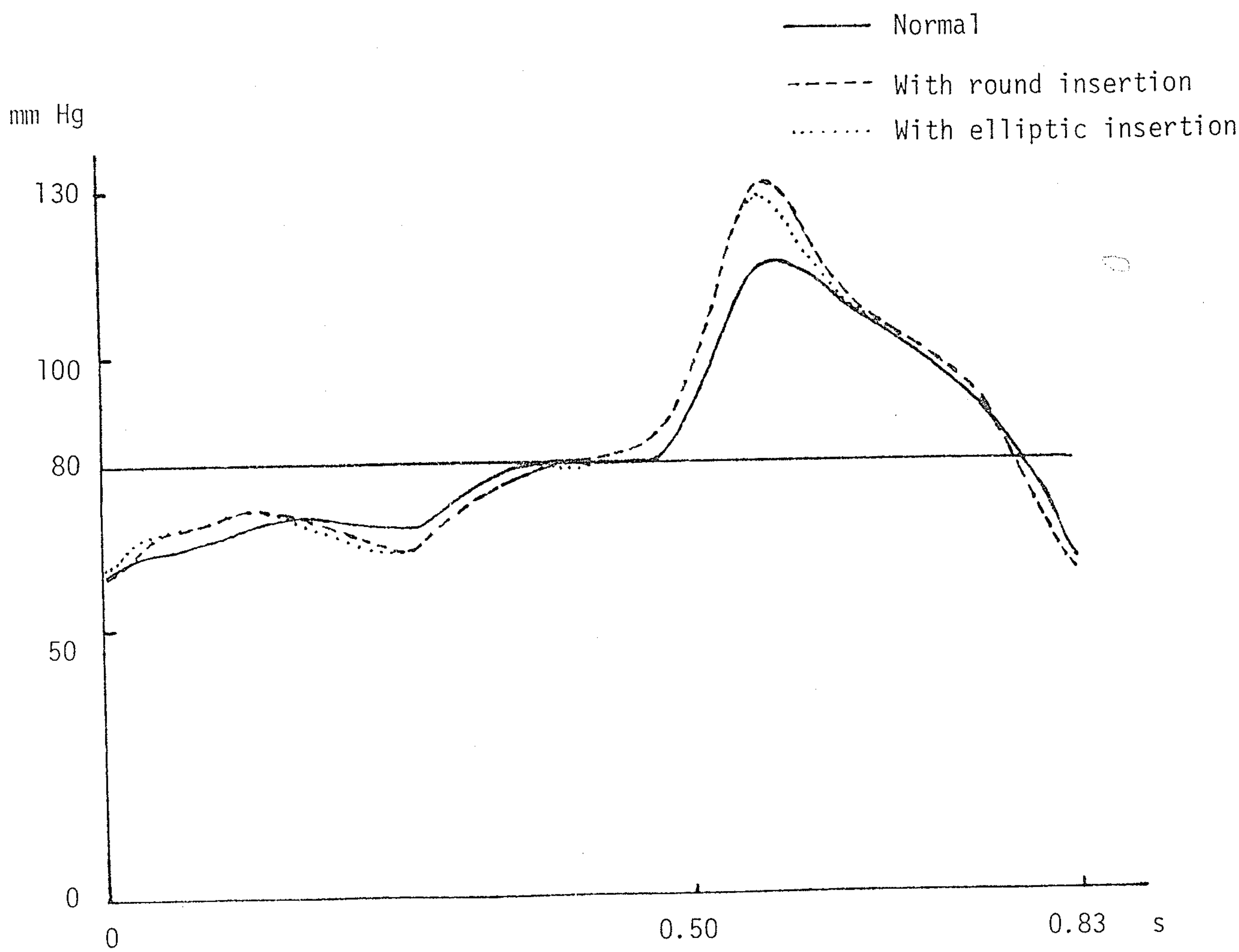

Fig. V.2: Comparison of the pressure wave obtained with forward flow at 72 beats/minute in tube No. 2.

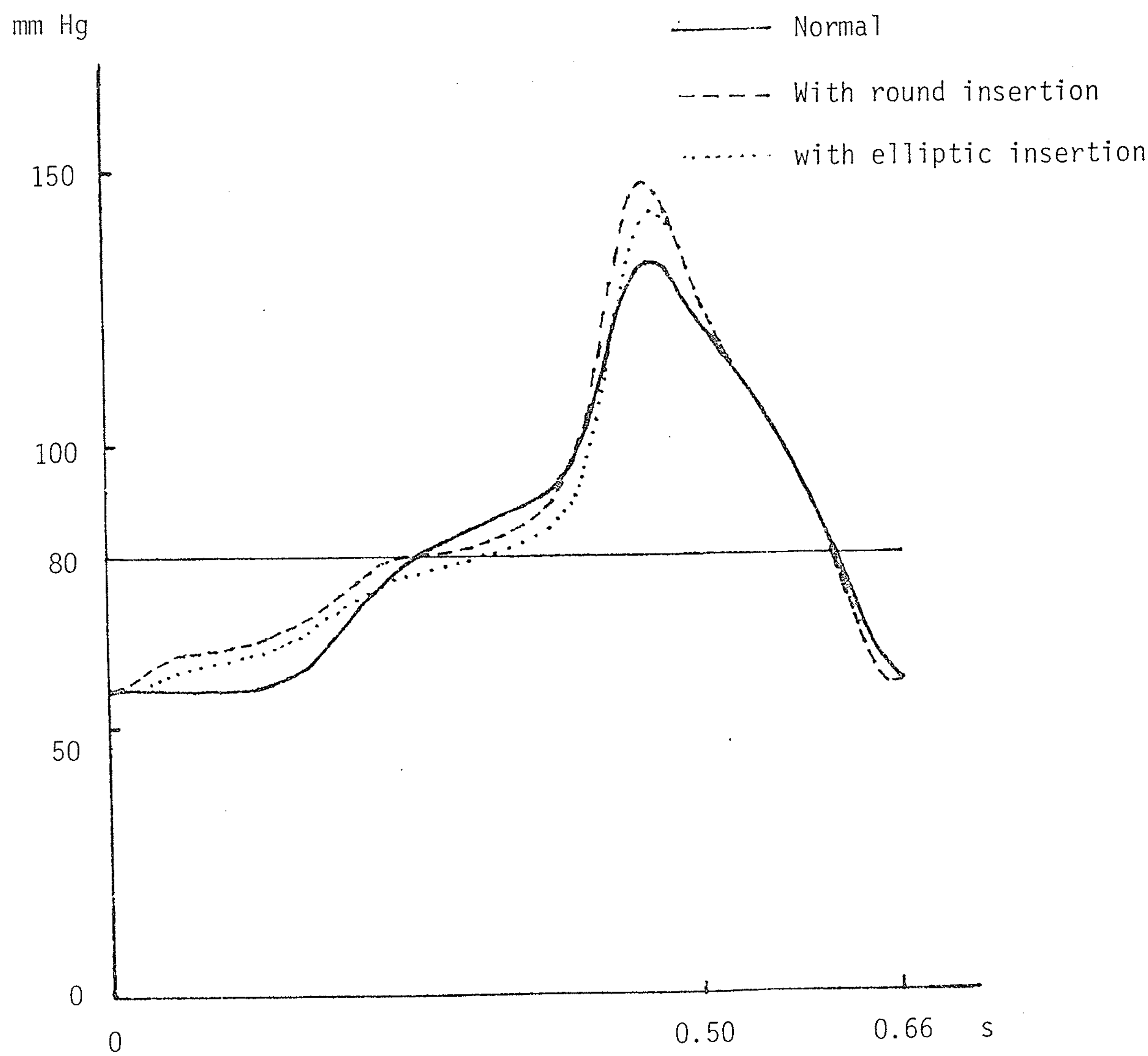

Fig. V.3: Comparison of the pressure waves obtained with forward flow at 90 beats/minute in tube No. 2.

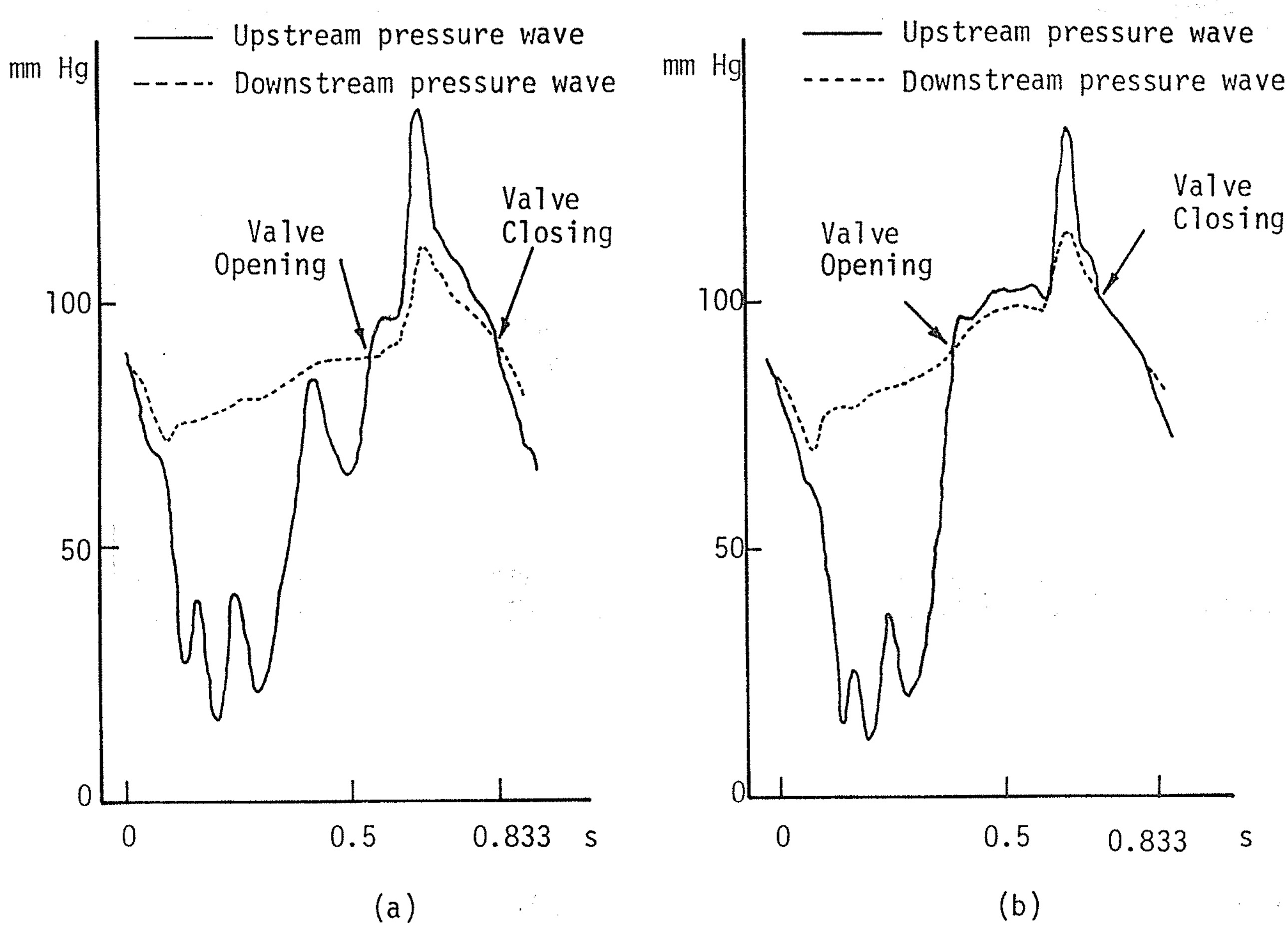

Fig. V.4: Prosthetic heart valve comparison (a) Starr-Edwards,
(b) Bjork-Shiley.

CHAPTER VI CONCLUSIONS

No material for arterial prosthesis has been found that fulfils all the requirements for working properly. The actual commercially available grafts made of woven or knitted Teflon or Dacron are known to produce changes in the hydrodynamic characteristics of the blood flow, producing reflected pressure waves as a result of their relative inextensibility. The reflected waves may be added to the incident ones thus producing higher non-physiological pressure waves that could damage the artery itself or even the heart valves. Changes in the hydrodynamic characteristics of the blood flow such as turbulence and high shear stresses can produce hemolysis and embolization, therefore prosthetic heart valves should have such hydrodynamic design that avoids turbulence and high shear stresses to the blood.

A mechanical model that simulated the human circulation in the left ventricle and ascending aorta was built for reproducing and measuring the reflected wave phenomenon at round inextensible insertions and for evaluation of the possible solution with an elliptic inextensible insertion that increased the flow area when subjected to moderate increases in pressure. The model was also used for performing and evaluating studies of physiological flow through Bjork-Shiley and Starr-Edwards prosthetic heart valves. As a result of the design limitations it was apparent that all desired specifications for the cardiovascular system could not be met. However, the blood could be simulated adequately over a reasonable range, the pump could simulate the physiological pressure wave, the simulated round prosthetic insertion reproduced the effect of inextensibility and the simulated elliptic insertion behaved as deformable, but inextensible because at the same time that it was susceptible to changes of cross-section under moderate pressure variations thus allowing higher flow area during ejection, its perimeter did not significantly elongate. The prosthetic heart valves were used as part of the mechanical model and also comparison of their hydrodynamic efficiency was performed. It was possible to quantify the effects of the deformable but inextensible oval insertion relative to the inextensible round insertion noting that the pressure peak in the round insertion was 7 - 8% higher than the elliptic insertion. It was not possible to make a theoretical evaluation of the experiment with the elliptic insertion because not enough theory of pulsatile flow and wave reflection in elliptic tubes has been developed.

The development of a theory for wave reflection at inextensible insertions in elastic tubes is a very complicated task since the phenomenon is not well known, the variables are numerous and linearization of equations could lead to deviation in the results. The described theory was the only one available and when compared with the experimental results it was found that further development was necessary because the theoretical and experimental results for the reflection in tube No. 1 are in disagreement. The divergence may arise from the fact that Womersley's theory was developed for thin tubes with relation of $h/a_1 \leq 0.1$ and the tube No. 1 has a relation $h/a_1 = 0.38$. The theory does not account for viscous components of the tube wall but it seems to be of minor consequences. Also it is noticed that the theory was developed considering that incident and reflected waves were in phase, but in experimentation it was observed that there is a phase shift between incident and reflected waves.

Quantization of energy losses of flow when passing an obstacle in a round tube, represented by a prosthetic heart valve in this case, using Bernoulli's equation when the mean flow and mean pressure drop are known has long been proved as a reliable procedure. From the evaluation of the energy losses and from the changes in magnitude and phase of the pressure wave components, it was clear that the Bjork-Shiley valve is hydrodynamically superior to the Starr-Edwards. Although the wave shapes "in vivo" could be quite different from those of the simulation system used here, the relative effects of the respective valves on pressure wave components and flow will remain in the order of those measured here.

Fourier techniques proved to be a valuable and indispensable tool for analysing pressure pulse waves because it would not be possible to fully understand such a complicated phenomenon only from the resultant waves.

The magnitude of reflected waves due to rigid insertions obtained in both cases, without and with forward flow, is significant and makes us believe that if a similar effect is produced by insertions in arteries, these nonphysiological pressure waves will damage the host organism. The only way to verify if similar phenomena as observed in this model occur in organisms is by "in vivo" experimentation. This last procedure is very costly in terms of money and time and complicated as well, therefore it is done only when it is estimated to be worth while. From the results obtained in our model it appears that experimentation with animals is worthwhile since if similar effects are found precautions should be taken when implanting artificial arteries, specially if they are implanted near the heart where the overpressure could damage the heart valves. Specific effects and difficulties have been identified from experimentation with this model that also provides an inexpensive guide to what variables should be recorded and controlled when working with animals.

APPENDIX A SOME CHARACTERISTICS OF ARTERIAL GRAFTS

The following clinical experiments with arterial grafts are the most promising ones:

Velour grafts: Complete endothelialization of pseudointima in artificial grafts does not occur in man, even though it happens in some animals, so Sauvage et al [28] have suggested that a velour surface would help the ingrow of perigraft tissue. These initial results in a small group of patients are promising.

Collagenized grafts: This technique consists of the subcutaneous implant of a coarse Dacron mesh with a silicon mandrill inside. After six to eight weeks the Dacron mesh is invaded by connective tissue and collagenized; then the mandrill is removed, leaving a tube ready for implantation [22].

Impervious prosthesis: An impervious prosthesis of synthetic, thrombus-resistant surface would not need healing time before working properly. Therefore, it would have even more advantages than a previous prosthesis that develops complete endothelialization, which needs time to form. The known requirements for an arterial prosthesis to work are: a) thrombus resistant surface; b) high degree of conformability; c) ease of suturability; d) outer surface to which surrounding tissue can adhere firmly; e) inner surface to which any thrombus that does form can attach securely to avoid embolization; and, f) similar elasticity to that of the artery: no impervious material has been found that fulfils all of them. One of the most perfect, Gore-tex (expanded polytetra-fluorethylene), satisfies conditions b) to e) but does not satisfy the important conditions a) and f) [28].

Negative charge: Implants made of copper, silver or gold with imposed negative charge have a minimum of thrombus deposition [23] but, their rigidity could be very inconvenient.

The following tables define the remaining major problems that must be overcome to produce acceptable arterial prostheses.

THROMBOGENICITY

Reason	Causes	Attempted solution
Thrombotic plaque deposits at the suture line.	Turbulence, high shear and boundary layer separation; conditions that may occur at the anastomosis between a rigid graft and an extensible vessel.	Production of a graft with similar elasticity than that of the host vessel at the suture line [16]
Pseudointimal distraction.	Insufficient adherence of the pseudointima to the prosthesis wall.	Velour, collagenized, and thrombus-resistant surface prosthesis [22, 28].
Pseudointimal thickening.	The initial thrombus layer on the interface graft blood is thrombogenetic itself, so there is a wall thickening that under normal conditions stops when the blood reaches a certain velocity. In many cases, the thickening continues until the graft is occluded.	Same as previous solution and grafts made of silver, copper, or gold with imposed negative charge. These have shown a minimum of thrombus deposition, but their rigidity is very inconvenient [23].

ANASTOMOTIC ANEURISMS

Reason	Causes	Attempted solution
Suture line disruption.	Implant fatigue or fraying of woven grafts due to excessive stress at implantation or excessive stress as a result of the different expansion between graft and vessel.	Production of a graft with similar elasticity as that of the host vessel at the suture line. Improvements of suture techniques [16, 21].
Vessel wall damage.	Turbulence produces vessel weakening and dilatation. The difference in distension between host vessel and graft is reported as a possible cause of turbulence.	Graft with similar distension as vessel [16].

Bowel erosion: Due to friction between the intestine and the arterial prosthesis, and Prosthesis infection are other problems that will not be discussed in this work.

Change in hemodynamic characteristics: There is not much investigation done regarding the changes of hemodynamic characteristics induced by a prosthesis, even though it is well known that such characteristics are important [16]. The velocity profile plays an important role in the appropriate distribution of blood through the peripheral vasculature, and it has been reported by Lee et al [20] that: "The Dacron bypass graft does not reflect reverse flow components...." And it is obvious that the original pressure wave and flow would be distorted by wave reflections originating at a rigid insertion, thus with possibilities of overloading the heart valves. Gozna et al [16] proved that distention due to pressure variation in major arteries was of the order of ten percent, and only one percent in the prosthesis. They also concluded that the difference in extensibility between host vessel and prosthesis causes suture line stress and probably turbulence; the first produces suture line disruption, and the second vessel wall damage and thrombosis.

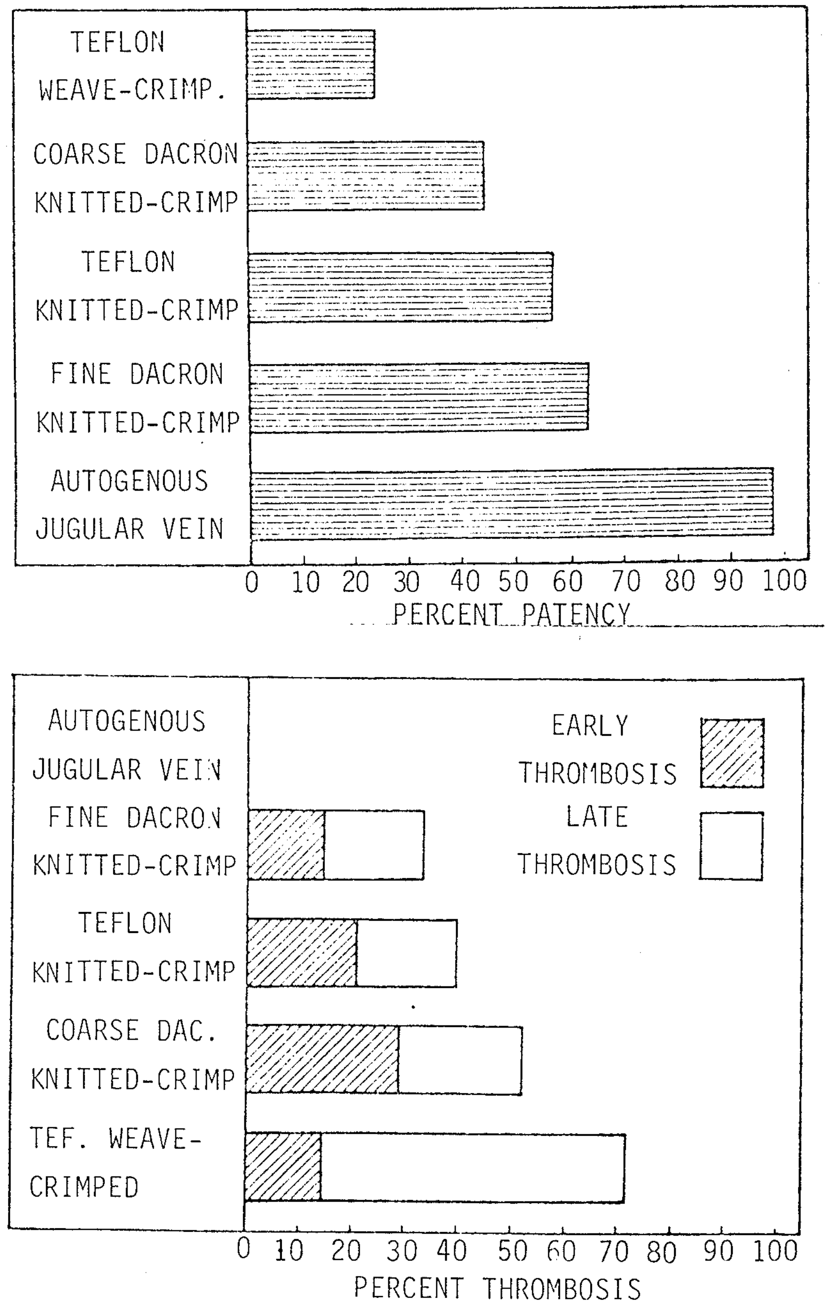

FIG. A.I.: Patency and thrombosis rate of prosthesis made - in teflon or dacron and implanted in the femoral artery of dogs (Reproduced from [21]).

APPENDIX B. FIGURES

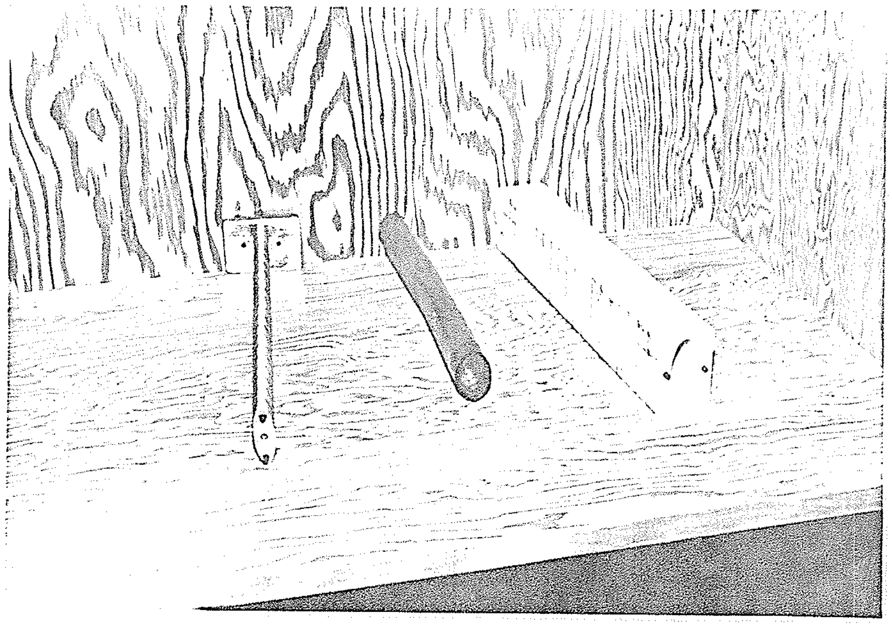

(a)

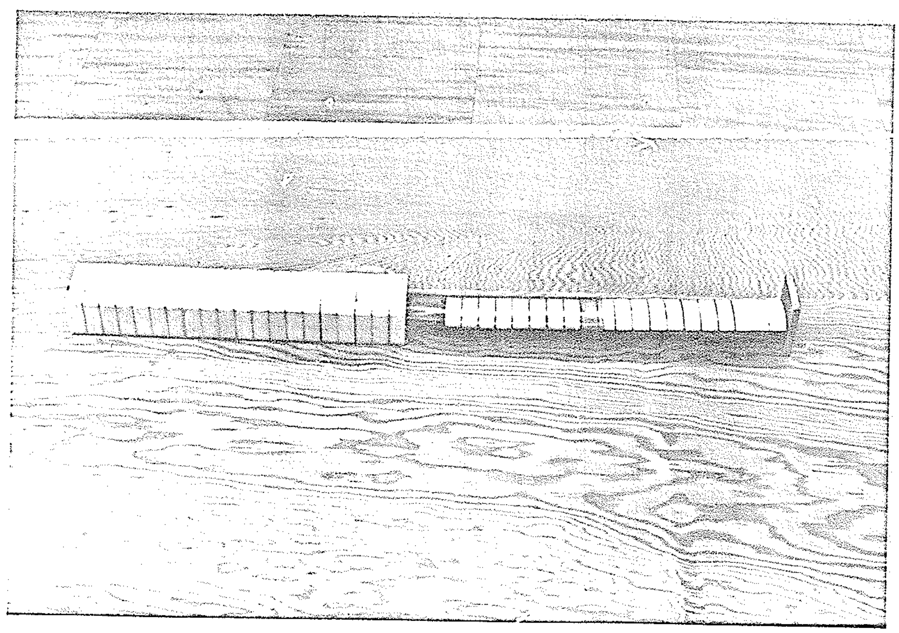

(b)

Fig. B.1

Pictures of the elliptic tube and its mold.

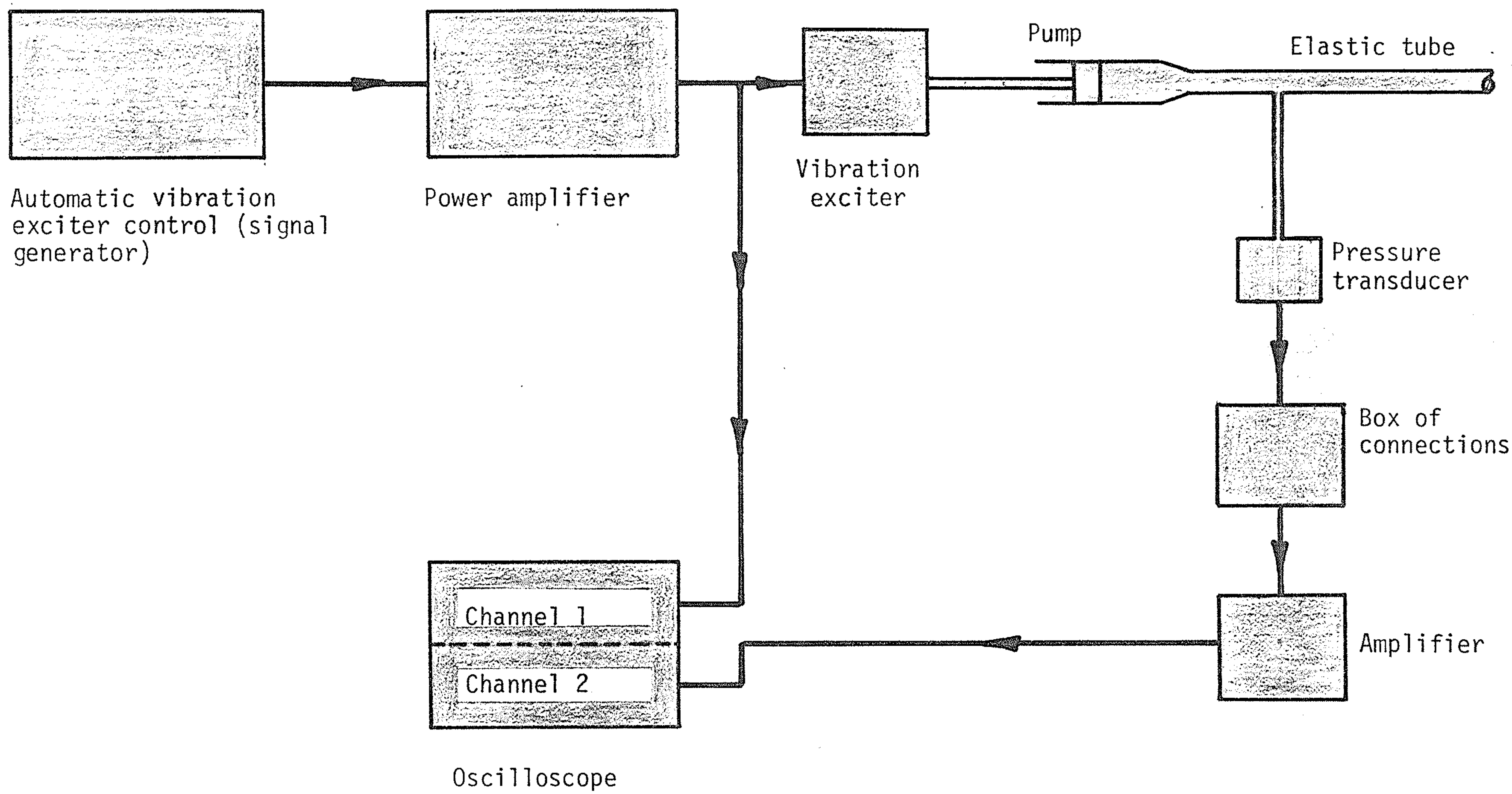

Fig. B.2: Assembly diagram of the equipment required for producing, detecting and storing signals from short trains of pressure waves.

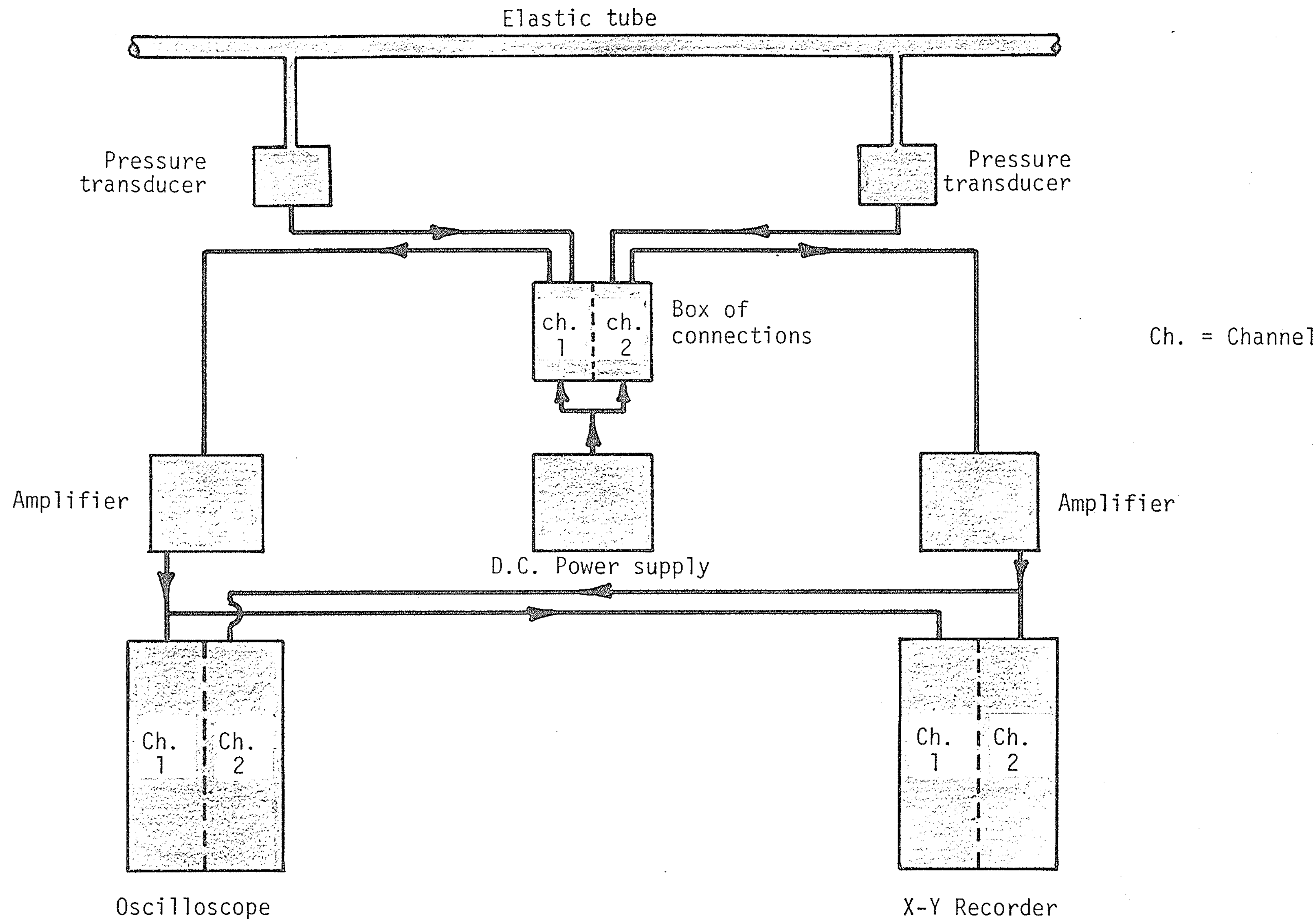

Fig. B.3: Assembly diagram of the equipment required for detecting and storing or recording signals from pressure waves when forward flow was produced.

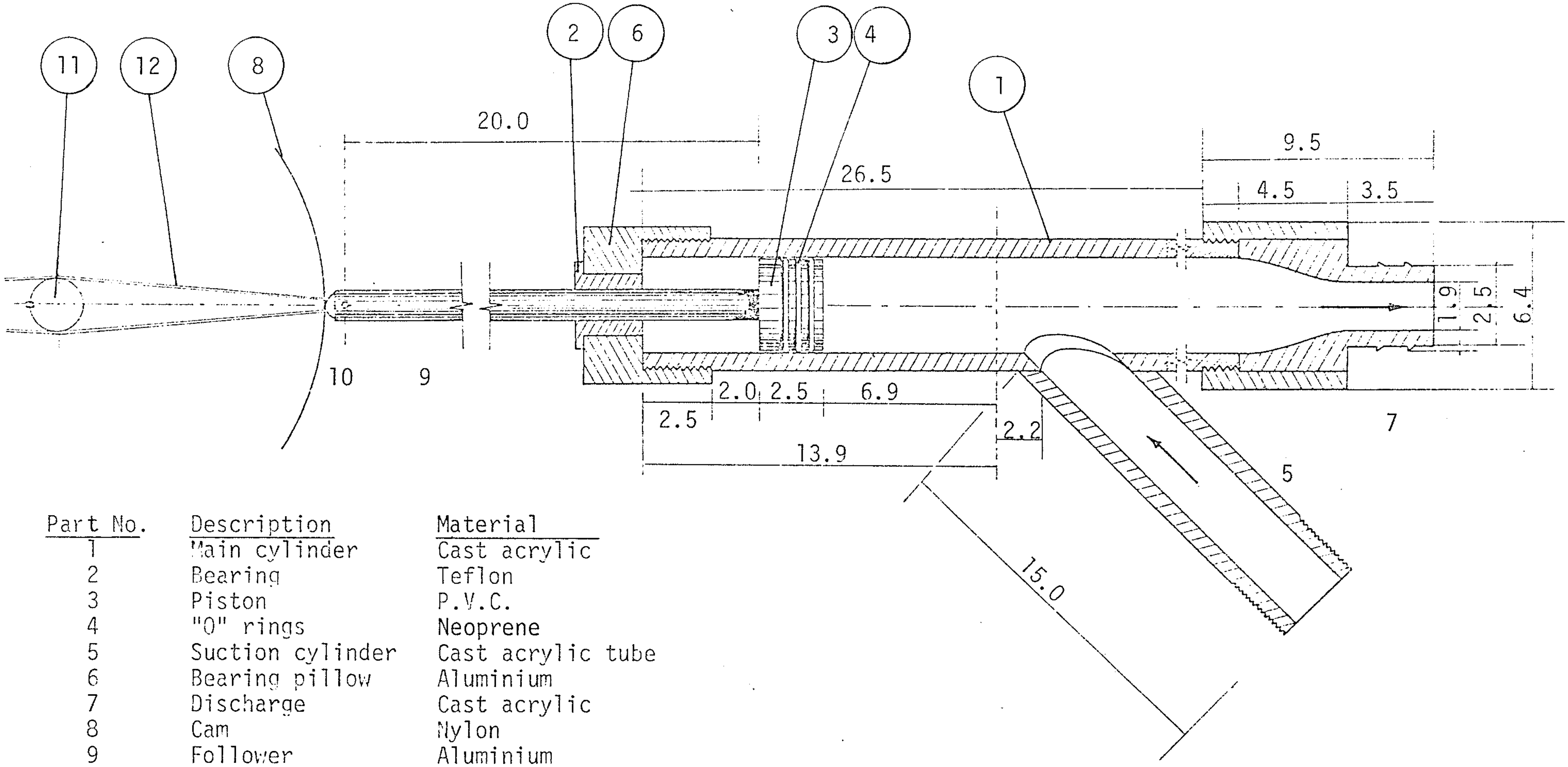

Part No.	Description	Material
1	Main cylinder	Cast acrylic
2	Bearing	Teflon
3	Piston	P.V.C.
4	"O" rings	Neoprene
5	Suction cylinder	Cast acrylic tube
6	Bearing pillow	Aluminium
7	Discharge	Cast acrylic
8	Cam	Nylon
9	Follower	Aluminium
10	Roller	Brass on a roller bearing
11	Cam shaft	Cold rolled steel
12	Rubber bands	Latex

Dimensions in cm

Fig. B-4

Reciprocating pump for reproducing the human ventricular outflow.

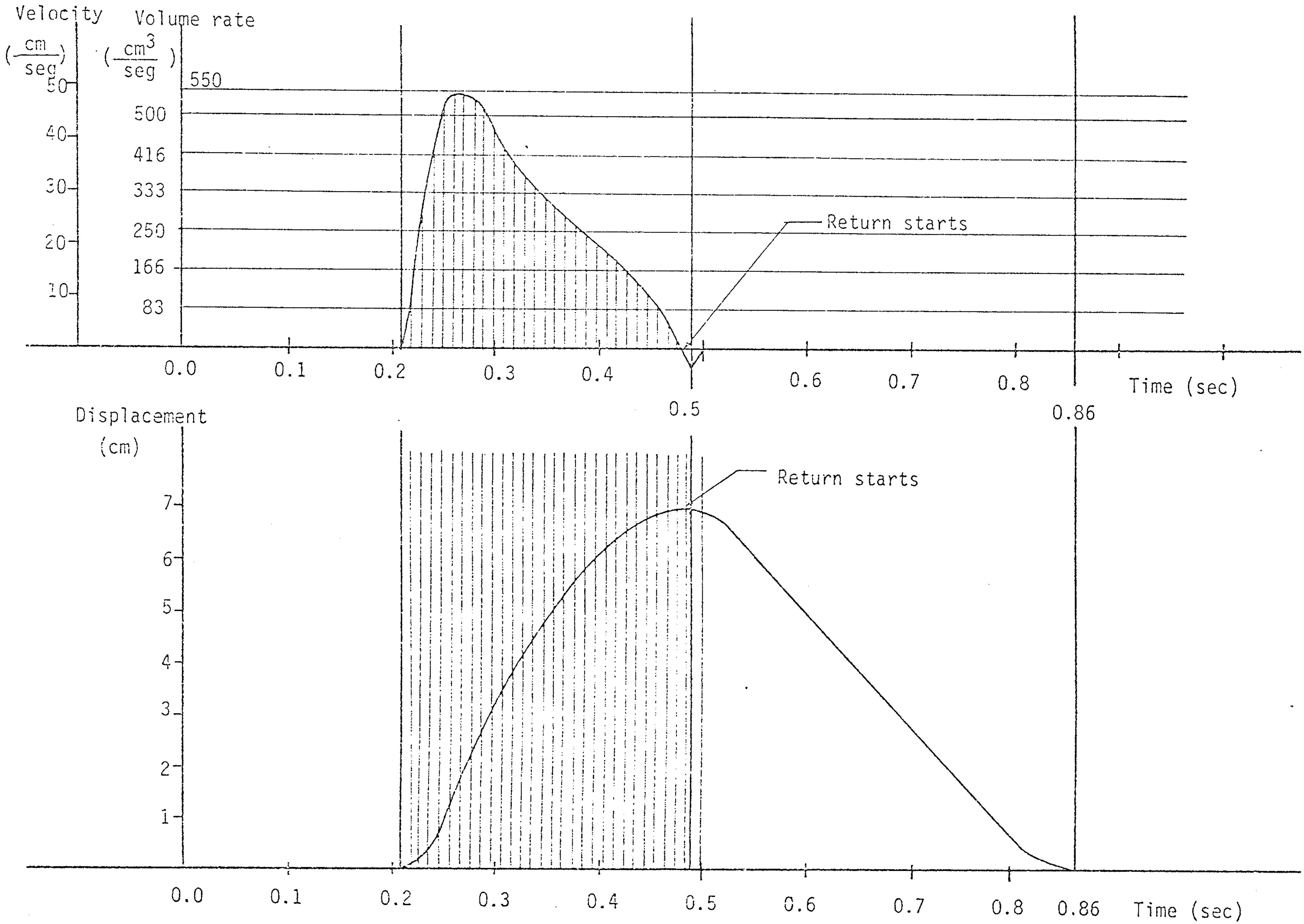

Fig. B-5. Graphical integration for the cam profile.

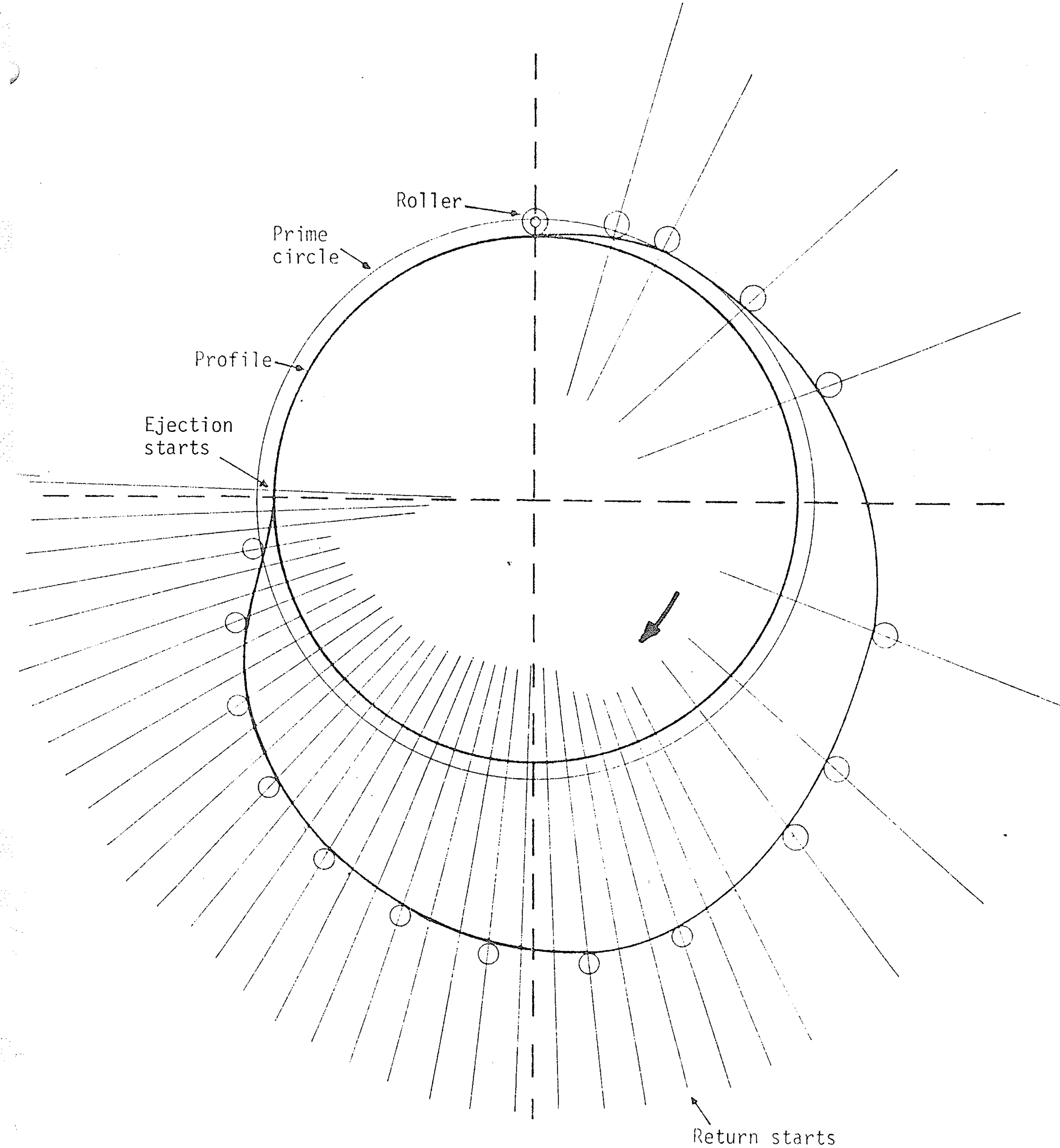

Fig. B.6: Cam profile. Scale 1:2.

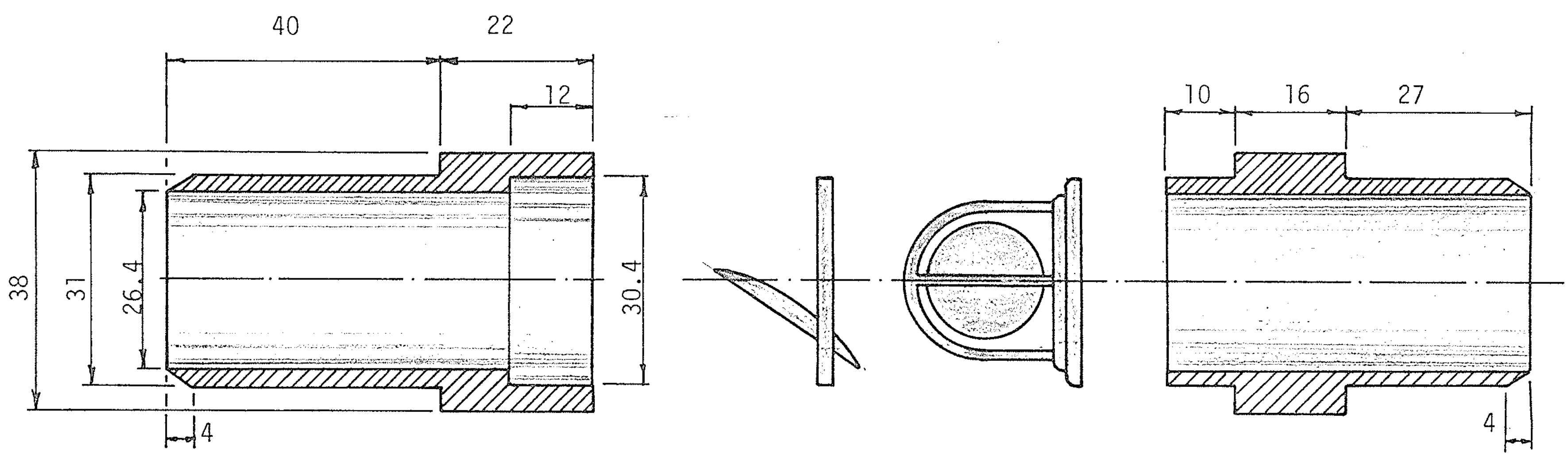

Fig. B.7: Diagram of the valve case made of acrylic. Case consists of two parts; right and left drawings. The Bjork-Shiley valve or the Starr-Edwards valve, center drawings, could be placed. The two half cases were manufactured with a pressure fit. Dimensions in millimeters.

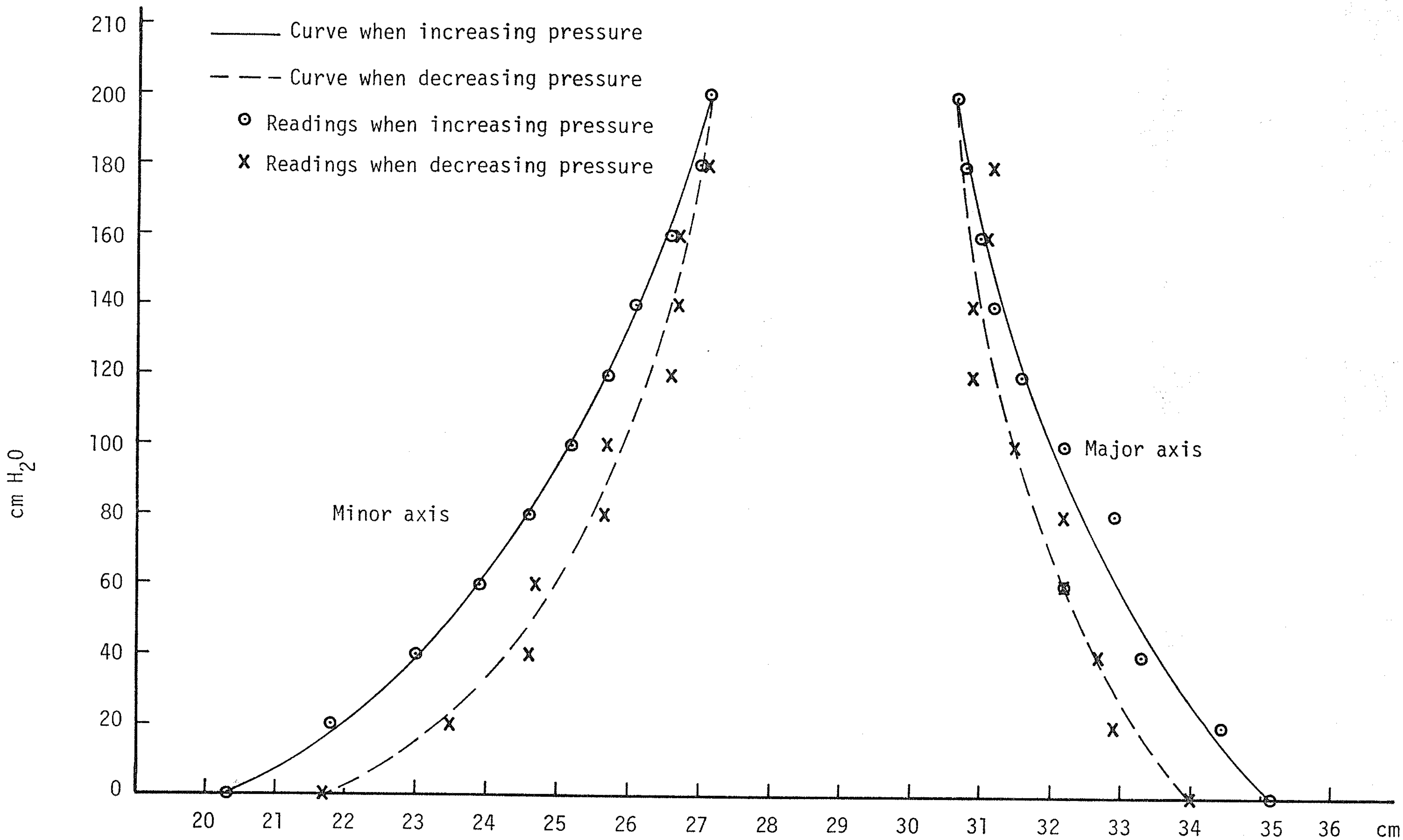

Fig. B.8: Deformation of the major and minor axis of the Jayflex elliptic tube when subjected to hydrostatic pressure.

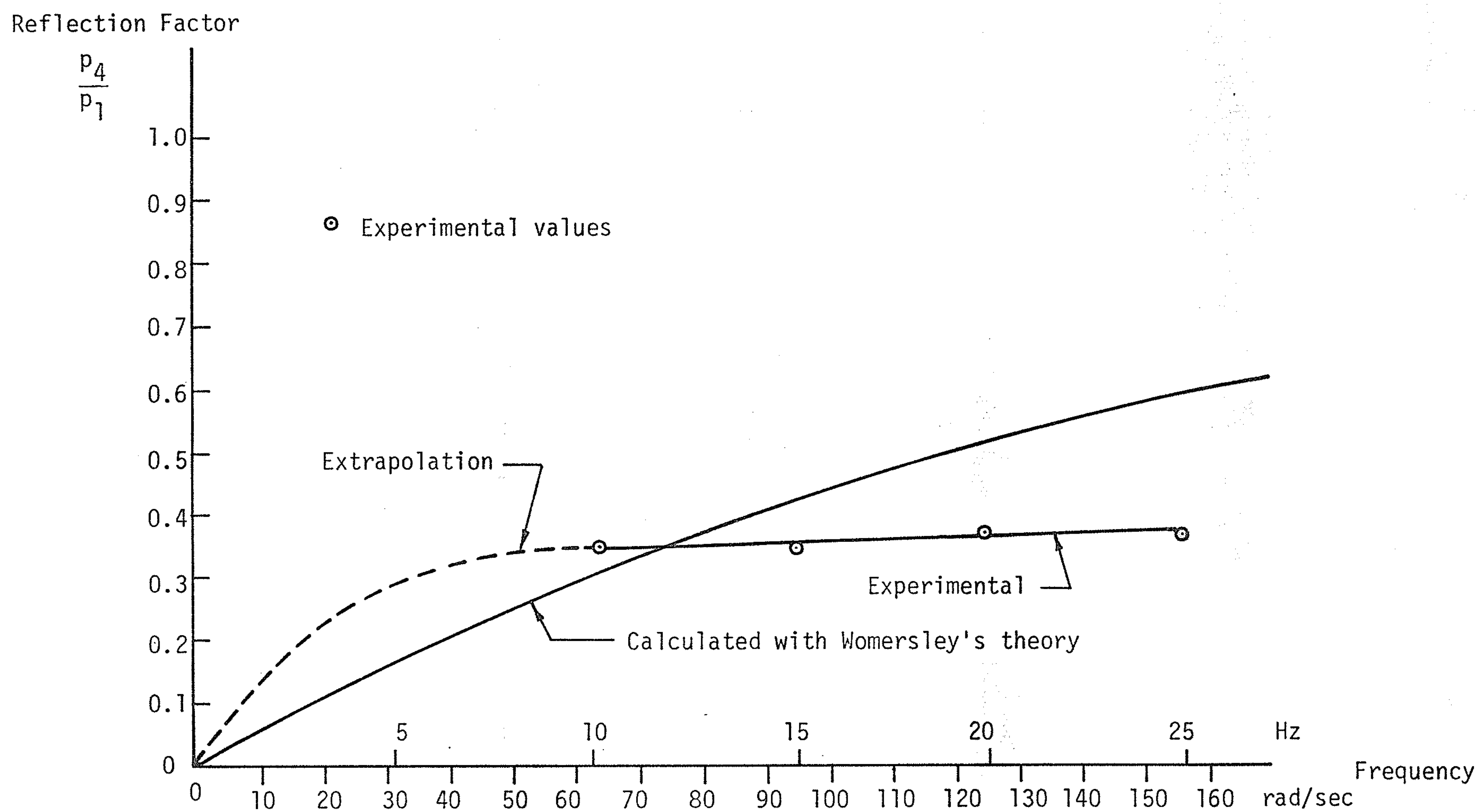

Fig. B.9: Values of the Reflection Factor for tube No. 1 with the 15 cm long inextensible sleeve for frequencies between 10 to 25 Hz and extrapolation to zero frequency. Comparison with theoretical results obtained with Womersley's theory is also shown.

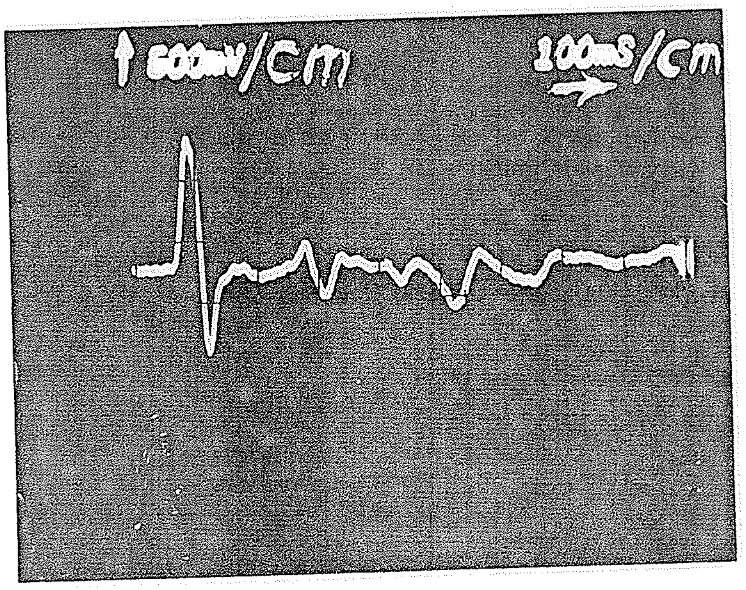

(a)

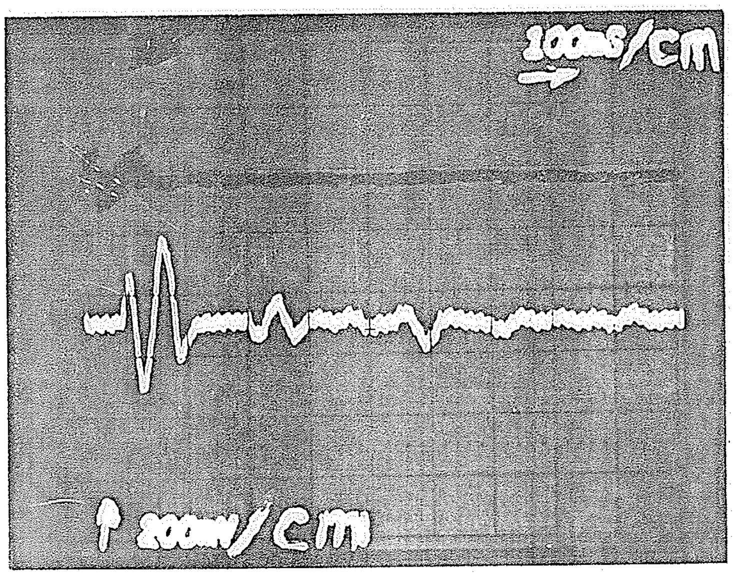

(b)

Fig. B.10: Photographs of the oscilloscope storage for short trains of pressure waves. X axis reads sweep velocity in ms/cm and Y axis reads pressure in mV/cm. Pressure calibration was 720 mV/100 cm H_2O and each screen division is 1 cm. (a) Pressure wave at 10 Hz. (b) Pressure wave at 15 Hz.

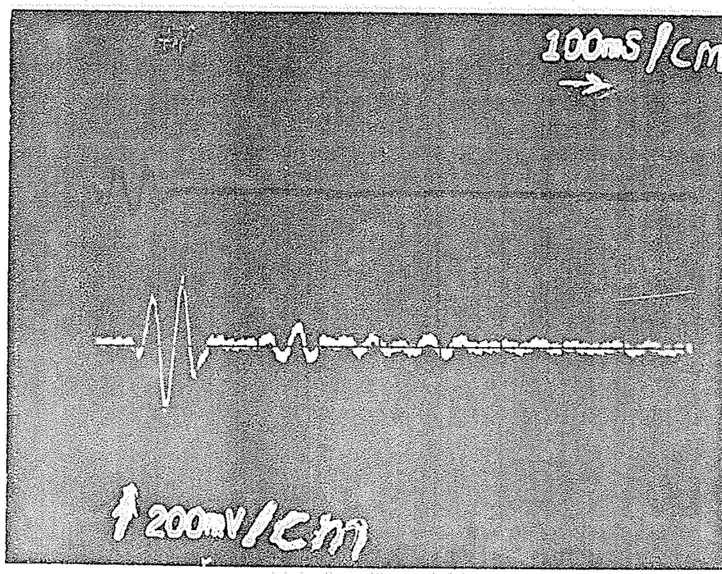

(a)

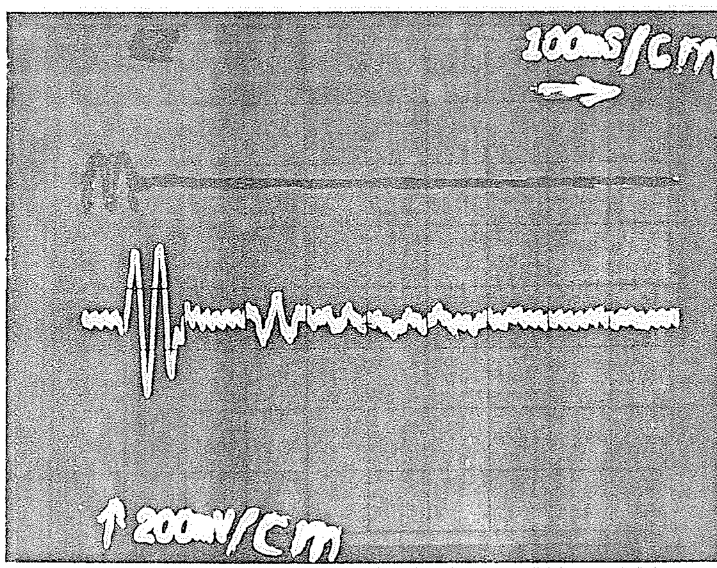

(b)

Fig. B.11: Photographs for the oscilloscope storage for short trains of pressure waves. X axis reads sweep velocity in ms/cm and Y axis reads pressure in mV/cm. Pressure calibration was 720 mV/100 cm H_2O and each screen division is 1 cm. (a) Pressure wave at 20 Hz. (b) Pressure wave at 25 Hz.

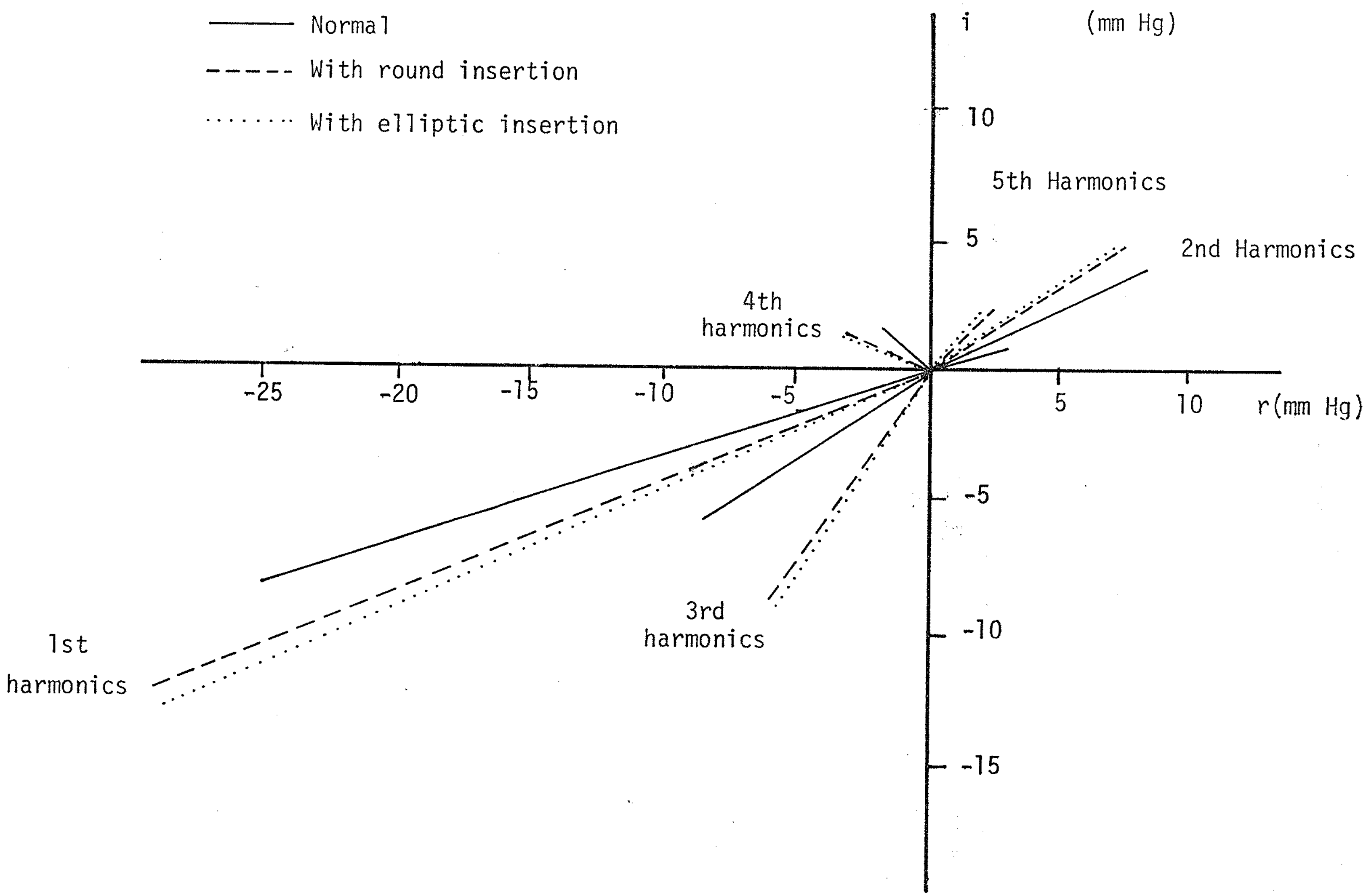

Fig. B.12: Fourier components of the pressure wave in terms of magnitude and phase on the complex plane, obtained with forward flow at 52 beats/minute in tube No. 2.

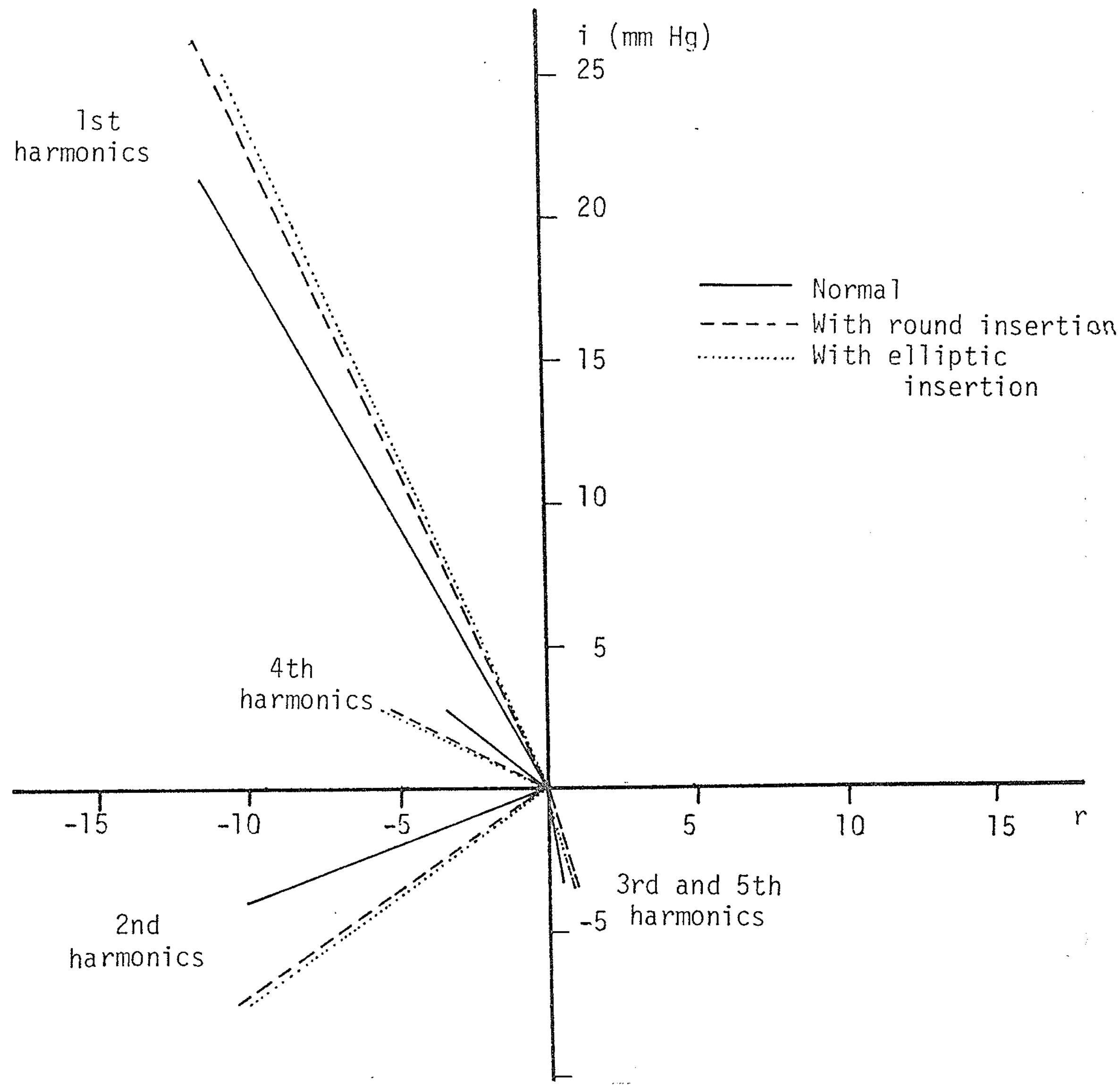

Fig. B.13: Fourier components of the pressure wave in terms of magnitude and phase on the complex plane, obtained with forward flow at 72 beats/minute in tube No. 2.

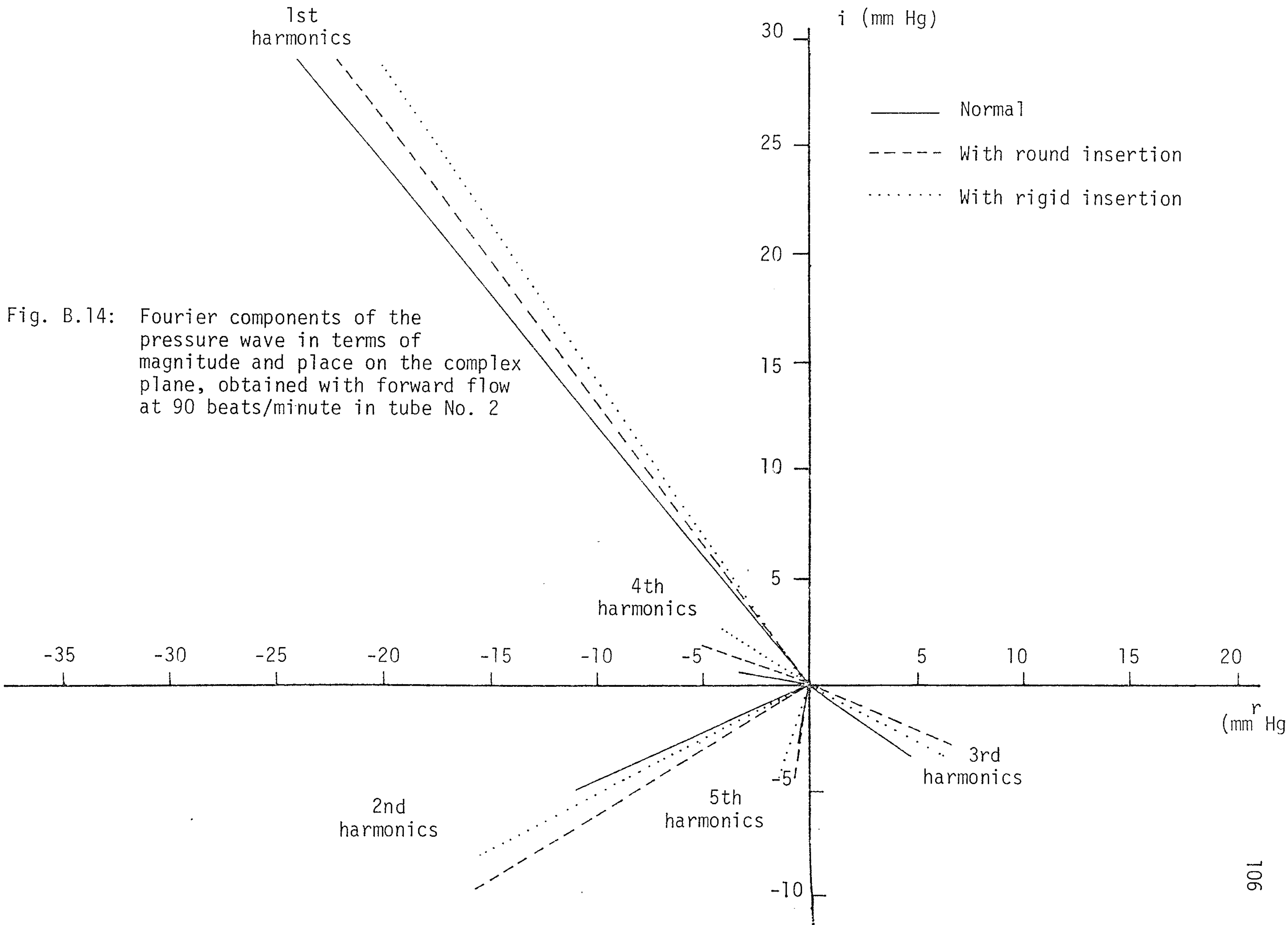

Fig. B.14: Fourier components of the pressure wave in terms of magnitude and place on the complex plane, obtained with forward flow at 90 beats/minute in tube No. 2

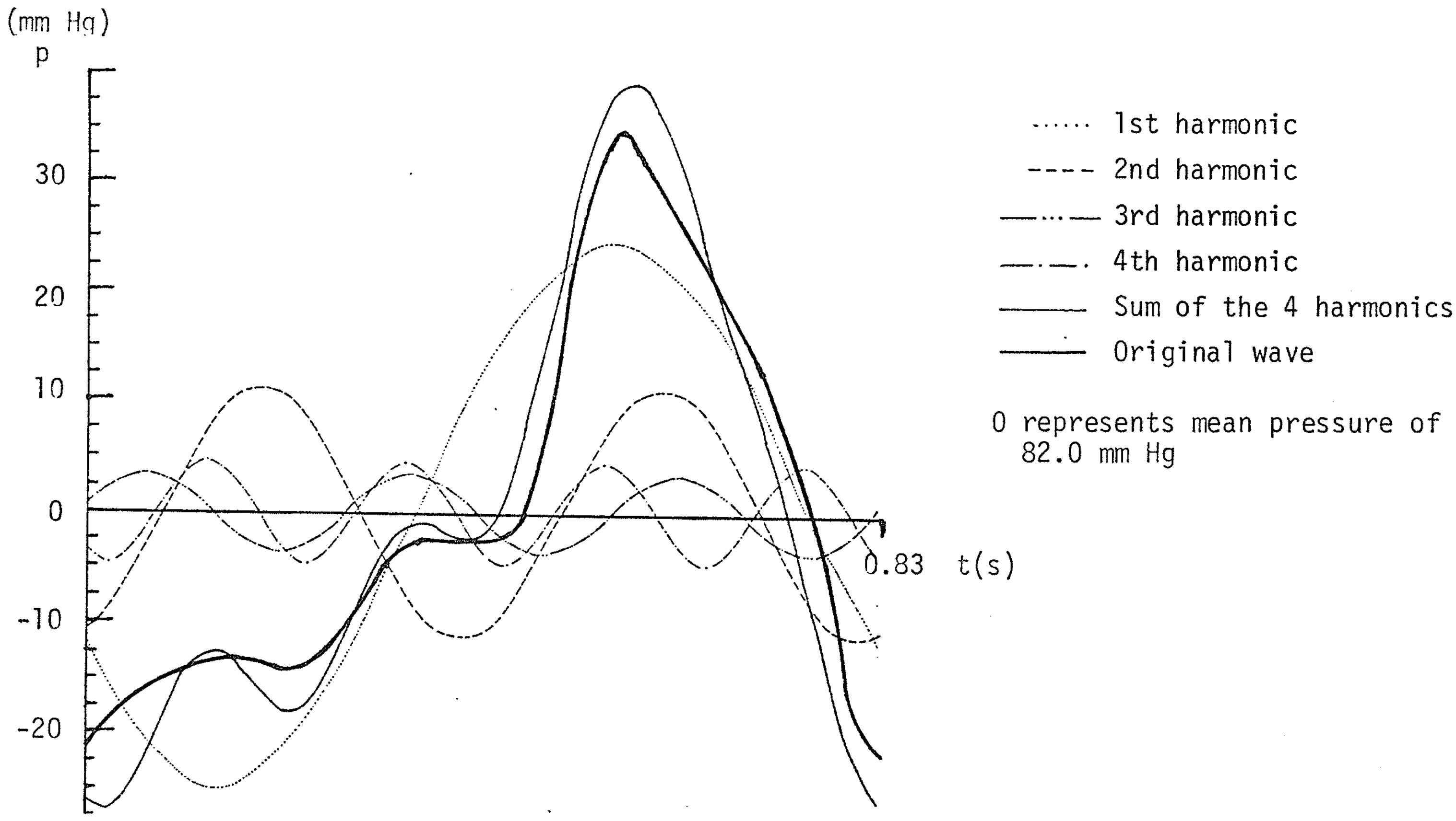

Fig. B.15: Reconstruction of the "normal" pressure wave from the first 4 harmonics oscillating on the mean term. Frequency 72 beats/minute.

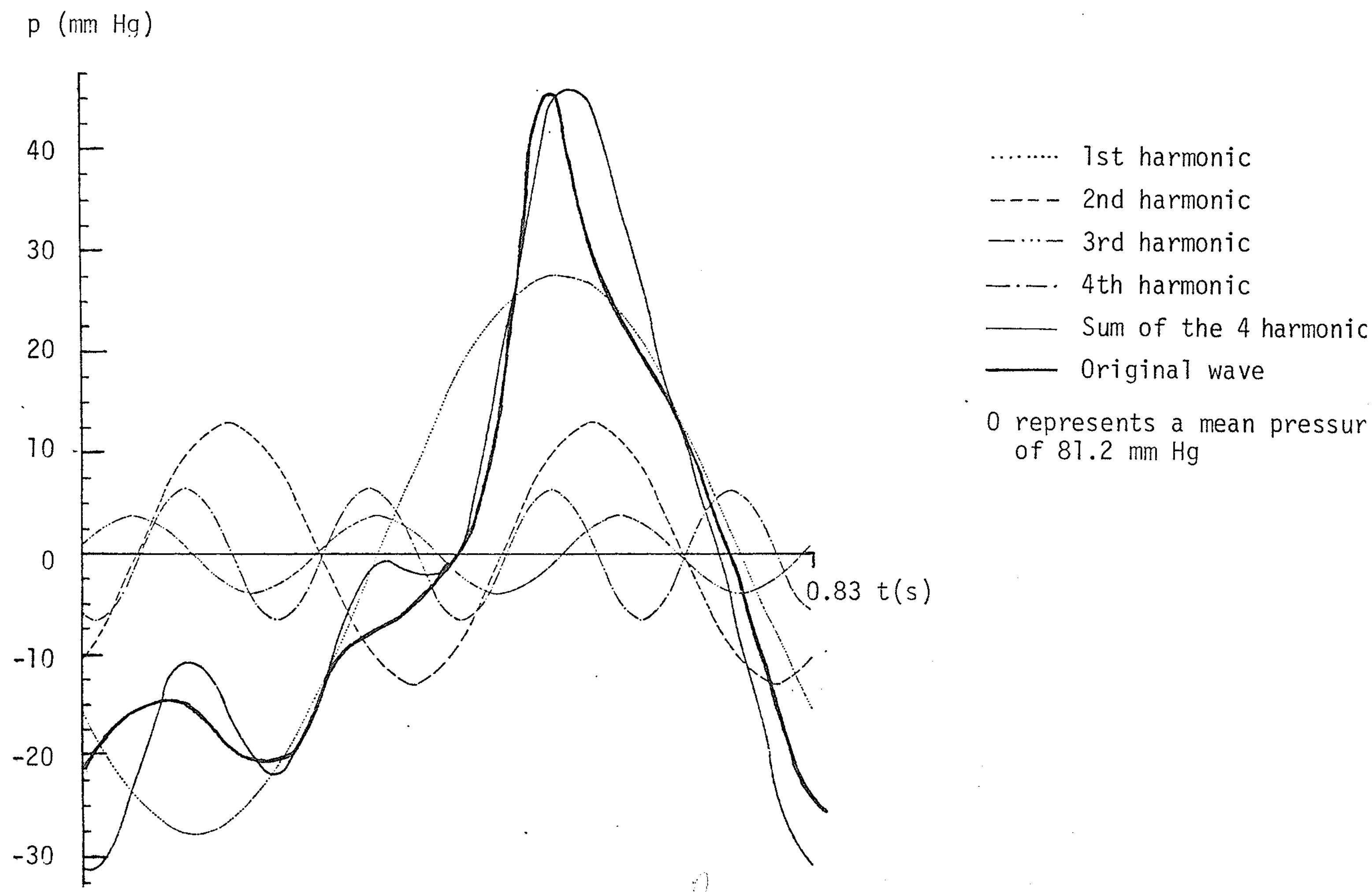

Fig. B.16: Reconstruction of the pressure wave with elliptic insertion from the first 4 harmonics oscillating on the mean term. Frequency 72 beats/minute.

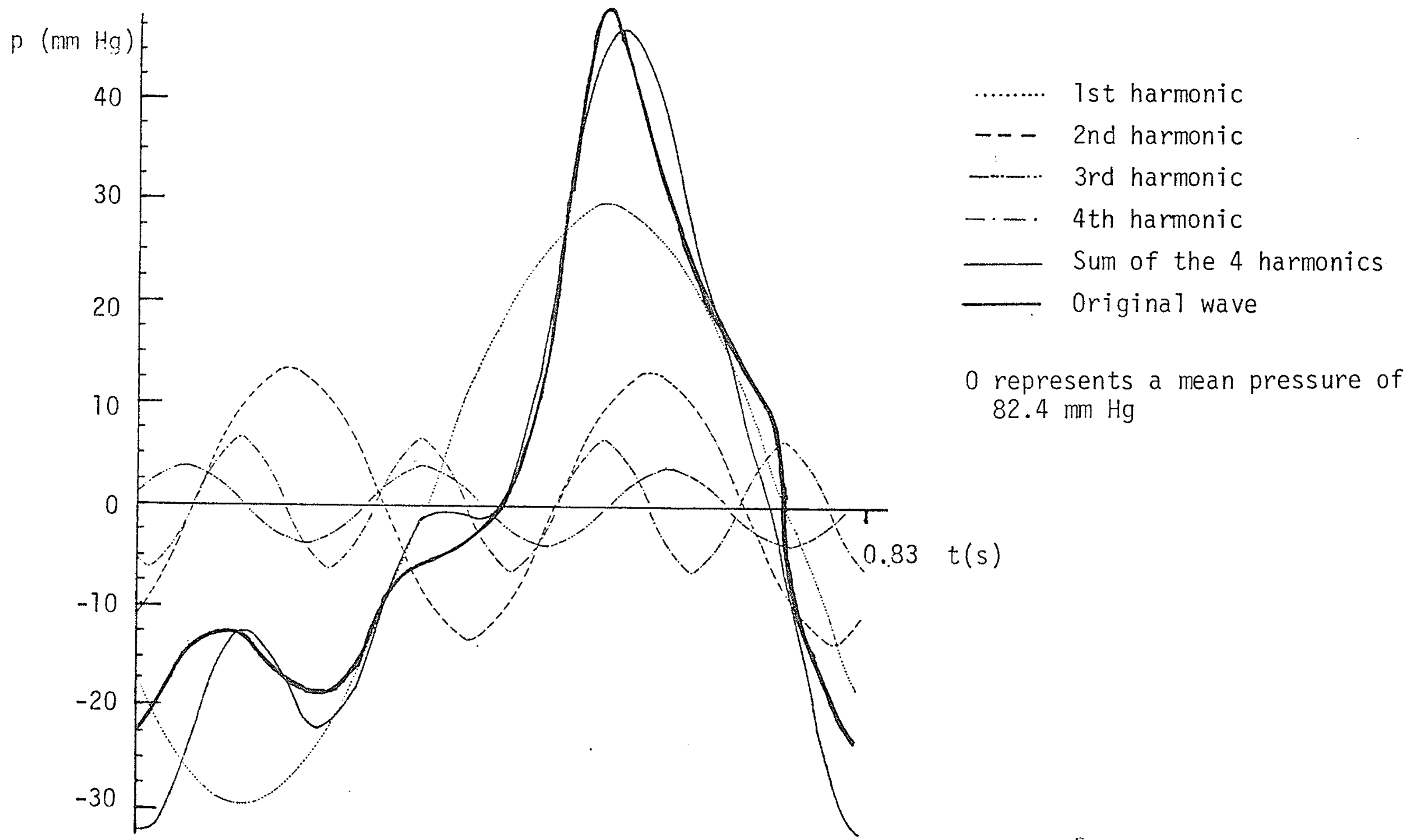

Fig. B.17: Reconstruction of the pressure wave with round insertion from the first 4 harmonics oscillating on the mean term. Frequency 72 beats/minute

APPENDIX C. TABLES

Make: Data Sensor

Model: SPS923A

Transducer No. 1 has the serial Number 902

Transducer No. 2 Number 904

Bridge resistance: 350Ω

Working range: 0 - 3.5 Kg/cm^2 (0 - 50 psi) absolute

Excitation, maximum D.C.: 10V

Accuracy when working at 25 Hz (maximum frequency in our experiments); 99%

Calibration Table:
Excitation for calibration: 5V
Test temperature: 25°C

Pressure in % of maximum	Output in V No. 1	Output in V No. 2
0	0.00006	0.00005
20	0.00290	0.00292
40	0.00581	0.00575
60	0.00880	0.00870
80	0.01181	0.01160
100	0.01470	0.01450

Table C.1: Characteristics of the pressure transducers.

Part Name	Make	Model	Serial
Amplifier	Hewlett-Packard	2470A	818-01544
Automatic vibration exciter control (signal generator)	MB Electronics	N685/N685	587
Box of connections			
Oscilloscope	Tektronix	7313	PN386-2199-00
Power amplifier	MB Electronics	2250 MB	261
Pressure transducer	Data Sensor	SPS923A	902
Vibration exciter	MB Electronics	PM-50	719

Table C.2: List of equipment of the assembly required for producing, detecting and storing signals from short trains of pressure waves.

Part Name	Make	Model	Serial
Amplifiers (2 pieces)	Hewlett-Packard	2470A	818-01544 & 818-01546
Box of connections			
D.C. Power supply	Hewlett-Packard	6289A	6B0573
Oscilloscope	Tektronix	7313	PN386-2199-00
Pressure transducers (2 pieces)	Data Sensor	SPS923A	902 & 903
X-Y Recorder	Hewlett-Packard	7046A	1503A01866

Table C.3: List of equipment of the assembly required for producing, detecting and storing signals from pressure waves when forward flow was produced.

52 cycles / minute

Coefficient	Real (mm Hg)	Imaginary (mm Hg)
Mean term	- 1.35	
1	- 25.15	- 8.21
2	8.32	3.91
3	- 8.52	- 5.71
4	- 1.71	1.54
5	2.93	0.91

72 cycles / minute

Coefficient	Real (mm Hg)	Imaginary (mm Hg)
Mean term	2.05	
1	- 11.53	20.63
2	- 10.40	- 3.79
3	0.47	- 3.107
4	- 3.52	2.566
5	0.04	- 3.04

90 cycles / minute

Coefficient	Real (mm Hg)	Imaginary (mm Hg)
Mean term	2.19	
1	- 22.97	28.60
2	- 10.52	- 4.80
3	4.559	- 3.269
4	- 3.12	0.577
5	- 0.528	- 2.64

Table C.4: Fourier components of the pulse waves generated in the elastic tube No. 2 without rigid insertion.

52 cycles / minute

Coefficient	Real (mm Hg)	Imaginary (mm Hg)
Mean term	1.421	
1	- 28.63	12.91
2	6.87	4.615
3	- 5.726	- 8.92
4	- 3.34	1.215
5	1.835	2.17

72 cycles / minute

Coefficient	Real (mm Hg)	Imaginary (mm Hg)
Mean term	1.16	
1	- 10.89	24.52
2	- 10.33	- 7.457
3	1.011	- 3.109
4	- 5.636	2.76
5	- 0.125	- 4.25

90 cycles / minute

Coefficient	Real (mm Hg)	Imaginary (mm Hg)
Mean term	1.91	
1	- 19.13	28.25
2	- 14.94	- 7.749
3	5.938	- 3.24
4	- 3.95	2.61
5	- 1.449	- 4.34

Table C.5: Fourier components of the pulse waves generated when the elliptic insertion was placed on the elastic tube No. 2.

52 cycles / minute

Coefficient	Real (mm Hg)	Imaginary (mm Hg)
Mean term	1.94	
1	- 29.11	- 12.22
2	7.238	4.947
3	- 5.98	- 8.64
4	- 3.13	1.38
5	2.386	2.436

72 cycles / minute

Coefficient	Real (mm Hg)	Imaginary (mm Hg)
Mean term	2.359	
1	- 11.63	25.28
2	10.67	- 7.467
3	0.906	- 3.004
4	- 5.46	2.78
5	- 0.152	- 4.167

90 cycles / minute

Coefficient	Real (mm Hg)	Imaginary (mm Hg)
Mean term	2.40	
1	- 21.14	28.34
2	- 15.16	- 9.35
3	6.309	- 2.849
4	- 4.79	1.88
5	- 0.756	- 4.325

Table C.6: Fourier components of the pulse waves generated when the round insertion was placed on the elastic tube No. 2

Disc valve, upstream

Coefficient	Real (mm Hg)	Imaginary (mm Hg)
Mean term	8.29	
1	1.11	- 46.56
2	- 9.93	0.848
3	3.55	3.74
4	- 6.305	5.239
5	2.008	0.646

Disc valve, downstream

Coefficient	Real (mm Hg)	Imaginary (mm Hg)
Mean term	- 8.806	
1	6.96	- 11.70
2	3.90	- 0.637
3	1.33	1.189
4	- 1.86	- 0.810
5	0.766	- 1.663

Ball valve, upstream

Coefficient	Real (mm Hg)	Imaginary (mm Hg)
Mean term	9.03	
1	- 2.449	- 42.81
2	- 1.245	- 5.09
3	- 0.618	7.711
4	- 5.813	- 4.50
5	0.686	4.105

Ball valve, downstream

Coefficient	Real (mm Hg)	Imaginary (mm Hg)
Mean term	- 7.26	
1	4.445	- 10.61
2	4.68	- 1.305
3	0.0139	1.826
4	- 0.396	- 1.861
5	1.449	0.107

Table C.7: Fourier components of the pressure waves shown in Fig. V.4 for valve comparison. (72 cycles/min.)

REFERENCES

1. AKLONIS, J.J., MacKNIGHT, W.J., and SHEN M., Introduction to Polymer Viscoelasticity, Wiley Interscience, 1972.

2. ANLIKER, Max, "Toward a Nontraumatic study of the Circulatory System", Biomechanics, its Foundations and Objectives, V.C. Fung (Editor), Prentice-Hall Inc., 1970.

3. ATTINGER, E.O., "Elements of Theoretical Hydrodynamics", in Pulsatile Blood Flow, E.O. Attinger (Editor),McGraw-Hill Book Co., 1964.

4. ATTINGER, E.O., "The Mathematical Approach to Hemodynamics, with Particular Reference to Womersley's Theory" in Pulsatile Blood Flow, E.O. Attinger (Editor), McGraw-Hill Book Co., 1964.

5. BASMAJIAN, J.V., Primary Anatomy, The Williams & Wilkins Co., Baltimore, 1970.

6. BERGEL, D.H., "Arterial Viscoelasticity" in Pulsatile Blood Flow, E.O. Attinger (Editor), McGraw-Hill Book Co., 1964.

7. BJORK, V.O., "A New Tilting Disc Valve", Scandinavian Journal of Thoracic and Cardiovascular Surgery 3, p. 1, 1969.

8. BJORK, V.O. and OLIN C., "A Hydrodynamic Comparison Between the New Tilting Disc Aortic Valve Prosthesis and the Corresponding Prosthesis of Starr-Edwards, Kay-Shiley, Smeloff-Cutter and Wada-Cutter in the Pulse Duplicator", Scan. Journal Thor. Cardiovasc. Surg. 4, 31, 1970.

9. CARAGANNIS, G., B.Sc. Flow in Distensible Elliptical Tubes (Mechanical Engineering) Thesis, 1975, The University of Manitoba, Wpg., Manitoba.

10. CROUCH, James E., Functional Anatomy, Lea & Febiger, Philadelphia, 1972.

11. FERNANDEZ, J., MARANHAO, V., GOOCH, A.S., MORSE, D., and NICHOLS, H.T., "The Bjork-Shiley Prosthesis. A Significant Advance in Aortic Valve Replacement", the Annals of Thoracic Surgery, Vol.14, No. 5, Nov., 1972.

12. FERRY, L.B., "Mechanical Hemolysis in Flowing Blood" in Biomechanics, its Foundations and Objectives, Y.C. Fung (Editor), Prentice-Hall Inc., 1970.

13. FRASER, R.S. and WADDELL, J. "Systemic Embolization After Aortic Valve Replacement", J. Thorac. Cardiovasc. Surg., 54:81, 1967.

14. GANONG, W.F., Review of Medical Physiology,11th ed., Lange Medical Publications, Los. Altos, Calif., 1975.

15. GUIDOIN, R.G., and AWAD, J.A., "Preclotting and Thrombosis of a Dacron Prosthesis, A Scanning Electron Microscope Study", Biomaterials, Medical Devices and Artificial Organs, Vol. 3, No. 3., p. 365, 1975.

16. GOZNA, E.R., MASON, W.F., MARBLE, A.E., WINTER, D.A., and DOLAN, F.G., "Necessity for Elastic Properties in Synthetic Arterial Grafts", The Canadian Journal of Surgery, Vol. 17, p. 176, May, 1974.

17. GUIDOIN, R.G. and AWAD, J.A., "Preclotting and Thrombosis of a Dacron Prosthesis. A Scanning Electron Microscope Study", Biomaterials Medical Devices and Artificial Organs, Vol. 3, No. 3, p. 365-382, 1975.

18. KASTOR, J.A., AKBARIAN M., BUCKLEY,M.J., DINSMORE, R.E., SANDERS,C.A., SCANNELL,J.G., and ASTEN,W.G., "Paravalvular Leaks and Hemolitic Anemia Following Insertion of Starr-Edwards Aortic and Mitral Valves", J. Thorac. Cardiovasc. Surg. 56:279, 1968.

19. KLIP, W., VAN-LOON, P., and KLIP, D.A., "Formulae for the Phase Velocity and Damping of Longitudinal Waves in Thick-Walled Visco-elastics Tubes", Journal of Applied Physics, V l. 38, No. 9, p. 3745-55, August, 1967.

20. LEE, B.Y., TRAINOR, F.S., and MADDEN, J.L., "Significance of Pulsatile Blood Flow Patterns in Various Graft Materials", Bulletin de la Société Internationale de Chirurgie, No. 4, p. 326, 1974.

21. LEE, H. and NEVILLE, K., Handbook of Biomedical Plastics, Chapter 5, Pasadena Technology Press, 443 Orange Grove Circle, Pasadena, Cal. 91105, 1971.

22. LORD, R.S.A., "The Search for a Local Arterial Substitute", Australian New Zealand Journal of Surgery, Vol. 44, No. 4, Nov., 1974.

23. LUCAS,T.R., STANCZEWSKI,B., RAMASAMY, N., SRINIVASAN, S., KAMMLOTT,G.W., and SAWYER, P.N., "Nonthrombogenic A.C. Polarized Copper Prosthesis", Biomaterials, Medical Devices and Artificial Organs, Vol. 3, No. 2, 1975.

24. McDONALD, D.A., "The Relation of Pulsatile Pressure to Flow in Arteries", Journal of Physiology, Vol. 127, p. 533-552, 1955.

25. McLACHLAN, N.W., Bessel Functions for Engineers, Oxford University Press, 1941.

26. MYERS, G.H. & PARSONET, V., Engineering in the Heart and Blood Vessels, Willey Interscience, New York, 1969.

27. OLIN, C., "Pulsatile Flow Studies of Prosthetic Aortic Valves", Scandinavian Journal of Thoracic and Cardiovasc Surg. 5:1-12, 1971.

28. SAUVAGE, L.R., BERGER, K.E., MANSFIELD, P.B., WOOD, S.J., SMITH, J.C., and OVERTON, J.B., "Future Directions in the Development of Arterial Prosthesis for Small and Medium Caliber Arteries", Surgical Clinics of North America, Vol. 54, No. 1, p. 213, Feb., 1974.

29. SELKURT, E.E., Physiology, Little, Brown & Co., Boston, 1971.

30. SKALAK, R., "Wave Propagation in Blood Flow", Symposium on Biomechanics (Nov., 1966), Y.C. Fung (Chairman), ASME Applied Mechanics Division, New York.

31. STARR, A. and EDWARDS, M.L., "Mitral Replacement: Clinical Experience with a Ball-Valve Prosthesis", Annals of Surgery, 154, p. 726, Oct., 1961.

32. WOMERSLEY, J.R., "Method for the Calculation of Velocity, Rate of Flow and Viscous Drag in Arteries when the Pressure Gradient is Known", Journal of Physiology, Vol. 127, p. 553-563, 1955.

33. WOMERSLEY, J.R., "Oscillatory Motion of a Viscous Liquid in a Thin Walled Elastic Tube I. The Linear Approximation for Long Waves", Philosophical Magazine, Vol. 46, p. 199-221, 1955.

34. WOMERSLEY, J. R., "Oscillatory Flow in Arteries: The Constrained Elastic Tube as a Model of Arterial Flow and Pulse Transmission", Physics in Medicine and Biology, Vol. 2, No. 2, October, 1957.

35. WOMERSLEY, J.R., "Oscillatory Flow in Arteries II. The Reflection of the Pulse Wave at Junctions and Rigid Inserts in the Arterial System", Physics in Medicine and Biology, Vol. 2, No. 4, April, 1958.

36. WOMERSLEY, J.R., "An Elastic Tube Theory of Pulse Transmission and Oscillatory Flow in Mammalian Arteries", Wright Air Develop. Center Tech. Rep. WADC-TR, 56-614, 1957.